

Doctoral Dissertation (Shinshu University)

**Research study on the reuse of textile waste
selvage for high-performance mechanical
properties: stab-proof and buffering applications**

March 2020

CHUANG YU CHUN

CONTENTS

CONTENTS.....	I
List of Figures	IV
List of Tables.....	VII
CHAPTER 1	1
1.1 Current status of textile waste.....	2
1.1.1 High performance textile waste	4
1.1.2 The selvage of high modulus woven fabrics.....	6
1.2 Reusing methods and current status of other high modulus fibrous materials	9
1.2.1 Heat recovery and chemical recycling.....	10
1.2.2 Mechanical recycling.....	11
1.3 Non-woven technology and mechanism.....	12
1.4 Personal protective equipment (PPE)	16
1.4.1 Stab-resistance materials.....	17
1.4.2 Buffer resistance materials.....	20
1.5 Constitution of this dissertation	22
Reference	25
CHAPTER 2	31
2.1 Introduction.....	32
2.2 Experimental	33
2.2.1 Materials	33
2.2.2 Preparation of recycled staple fibers.....	34
2.2.3 Preparation of recycled fabric.....	35
2.2.4 Test methods and standards.....	36
2.3 Results and discussion	37
2.3.1 Areal density and air permeability	37
2.3.2 Tensile strength	39
2.3.3 Tearing test.....	41
2.3.4 Bursting strength test	43
2.4 Conclusions.....	45
References.....	45
CHAPTER 3	48
3.1 Introduction.....	49
3.2 Experimental	51
3.2.1 Materials	51
3.2.2 Preparation of aramid composite matrices.....	52

3.2.3	Preparation of hybrid-fiber-reinforced composite boards.....	53
3.2.4	Test methods and standards.....	54
3.3	Results and discussion	55
3.3.1	Effect of hot pressing on tensile strength of aramid composite matrices	55
3.3.2	Effect of hot pressing on tearing strength of aramid composite matrices	57
3.3.3	Tensile and tearing strengths of hybrid-fiber-reinforced composite boards.....	58
3.3.4	Air permeability of aramid composite matrices and hybrid-fiber-reinforced composite boards	60
3.3.5	Bursting strength of aramid composite matrices and hybrid-fiber-reinforced composite boards	61
3.3.6	Static puncture resistance of aramid composite matrices and hybrid-fiber-reinforced composite boards	63
3.4	Conclusions.....	65
	References.....	65
CHAPTER 4	69
4.1	Introduction.....	70
4.2	Materials and methods	72
4.2.1	Materials	72
4.2.2	Method.....	73
4.2.3	Test methods and standards.....	75
4.3	Results.....	77
4.3.1	Mechanical property of recycle high strength pet matrices	77
4.3.2	Tensile strength of hybrid-fabric fibrous planks	78
4.3.3	Tearing strength of hybrid-fabric fibrous planks	80
4.3.4	Bursting strength of hybrid-fabric fibrous planks.....	82
4.3.5	Static stab-resistance of hybrid-fabric fibrous planks.....	83
4.4	Conclusions.....	84
	References.....	85
CHAPTER 5	89
5.1	Introduction.....	90
5.2	Materials and methods	92
5.2.1	Materials	92
5.2.2	Preparation of filament/woven-reinforced fabric composites.....	93
5.2.3	Test methods and standards.....	95
5.3	Results.....	96

5.3.1 Tearing strength.....	96
5.3.2 Static puncture strength.....	98
5.3.3 Dynamic puncture strength	99
5.3.4 Summary of comparison	100
5.4 Conclusions.....	101
References.....	102
CHAPTER 6	106
6.1 Introduction.....	107
6.2 Experimental	109
6.2.1 Materials	109
6.2.2 Preparation of PET/TPU buffering sandwiches.....	109
6.2.3 Test methods and standards.....	111
6.3 results and discussion.....	112
6.3.1 Effects of basic weight of nonwoven cover sheets on bursting strength of PET/TPU buffering sandwiches	112
6.3.2 Effects of basic weight and number of nonwoven cover sheets on air permeability of PET/TPU buffering sandwiches	114
6.3.3 Effects of basic weight and number of nonwoven cover sheets on resilience rate of PET/TPU buffering sandwiches.....	116
6.3.4 Effects of basic weight and number of nonwoven cover sheets on drop-weight impact test of PET/TPU buffering sandwiches	118
6.4 Conclusions.....	121
References.....	121
CHAPTER 7	126
List of publications	131
Scientific presentation.....	132
Acknowledgement	133

List of Figures

Figure 1.1 World's Major Textile Exporters in 2017[1].....	3
Figure 1.2 high-performance textile wastes and reuse/recycle process [12]	6
Figure 1.3 Recycle of the waste Kevlar® (p-aramid) woven selvages.....	6
Figure 1.4 High-modulus Kevlar® woven fabrics (photo of the rapier loom is from PANTER, Italy).....	7
Figure 1.5 Synthetic molecular reaction formula of Kevlar®, benzene ring and the hydrogen bonding [16].....	9
Figure 1.6 Structure of Kevlar® selvage	9
Figure 1.7 The process of recycled fabric.....	14
Figure 1.8 Needle-bonding process	15
Figure 1.9 Recycled selvage and staple fibers.....	15
Figure 1.10 Schematic diagram of the waste selvage recycling process	16
Figure 1.11. Schematic of puncture process	19
Figure 1.12 Penetrate model of the penetrate process	20
Figure 1.13 Drop-weight impact test arrangement	21
Figure 2.1 Recycled selvage and staple fibers.....	34
Figure 2.2 Areal density of recycled fabrics.....	38
Figure 2.3 Air permeability of recycled fabrics.....	38
Figure 2.4 Tensile force along the CD and MD of recycled fabric.....	40
Figure 2.5 The tensile strength of recycled fabric	40
Figure 2.6 SEM images of thermal-bonding points in the recycled fabric.....	41
Figure 2.7 Force-displacement curve of recycled Kevlar® fabric-CD (a) without heat treatment (b) with heat treatment (c) data comparison of K9	41
Figure 2.8 The tearing force of along the CD and MD of the recycled fabrics as related to the employment of hot pressing.....	42
Figure 2.9 Bursting force of recycled fabrics that are processed (a) with or (b) without the heat treatment.....	44
Figure 2.10 Bursting strength of recycled fabrics. “NH” means no heat treatment (i.e. the control group) and “H” means hot pressed samples	44
Figure 3.1 Images of the a) aramid selvage, b) aramid staple fibers, c) aramid composite matrix and d) aramid woven fabrics.....	52
Figure 3.2 Schematic diagrams of aramid composite matrix and hybrid-fiber-reinforced.....	53
Figure 3.3 Tensile strength of recycled aramid composite matrices as related to the employment of hot pressing.....	56

Figure 3.4 SEM images and schematic diagrams of the drawing mechanism of tensile strength.....	57
Figure 3.5 Tearing strength along the CD and MD of aramid composite matrices as related to the employment of hot pressing.	58
Figure 3.6 (a) tensile strength and (b) force-displacement curve of hybrid-fiber-reinforced composite boards.	59
Figure 3.7 Tearing strength of hybrid-fiber-reinforced composite boards.....	60
Figure 3.8 Air permeability of aramid composite matrices and hybrid-fiber-reinforced composite boards.	61
Figure 3.9 Bursting strength of aramid composite matrices and hybrid-fiber-reinforced composite boards.	62
Figure 3.10 Static puncture resistance of aramid composite matrices and hybrid-fiber-reinforced composite boards.	64
Figure 3.11 Static puncture resistance-displacement curves of a) non hot-pressed and b) hot-pressed aramid composite matrices.....	64
Figure 3.12 Static puncture resistance-displacement curves of aramid composite matrices and hybrid-fiber-reinforced composite boards as related to the employment of hot pressing.	64
Figure 4.1 Images of recycled high strength PET selvages.	73
Figure 4.2 Images of (a) basalt, (b) carbon-fiber, and (c) aramid plain woven fabrics. .	73
Figure 4.3 Manufacturing process of hybrid-fabric fibrous planks.	74
Figure 4.4 The equipment and puncture needle of static puncture resistance test.....	76
Figure 4.5 a) Tensile load, b) tensile strength of hybrid-fabric fibrous planks as related to fiber blending ratios and c) force-displacement curve.....	79
Figure 4.6 Damage level of (a) basalt, (b) carbon-fiber, and (c) aramid woven fabrics after tensile tests.....	80
Figure 4.7 Elongation of hybrid-fabric fibrous planks as related to fiber blending ratios.....	80
Figure 4.8 Tear strength of hybrid-fabric fibrous planks as related to fiber blending ratios.....	81
Figure 4.9 Elongation of hybrid-fabric fibrous planks as related to fiber blending ratios.....	81
Figure 4.10 Bursting strength of hybrid-fabric fibrous planks as related to fiber blending ratios.....	82
Figure 4.11 Static puncture resistance of hybrid-fabric fibrous planks as related to fiber blending ratios.	84
Figure 4.12 Static puncture resistance-displacement curve of hybrid-fabric fibrous planks of HP9 and HP9K.....	84

Figure 5.1 Schematic diagrams of the manufacture of fabric composites.	94
Figure 5.2 Schematic diagrams of the tearing test fabric composites. (a) Test schematic of the tearing strength test; (b) Cross Machine Direction (CD); (c) Machine Direction (MD).	95
Figure 5.3 The equipment and puncture needle of dynamic puncture resistance test. ...	96
Figure 5.4 Tearing strength of filament/woven-reinforced fabric composites without heat treatment.	97
Figure 5.5 Tearing strength of filament/woven-reinforced composites fabrics that have been thermally treated.	97
Figure 5.6 Static puncture resistance of filament/woven-reinforced fabric composites. (NH: non-thermally treated, YH: thermally treated).	99
Figure 5.7 The strength-displacement curve of the static puncture resistance of filament/woven-reinforced fabric composites.	99
Figure 5.8. Dynamic puncture resistance of filament/woven-reinforced fabric composites. (NH: non-thermally treated, YH: thermally treated).	100
Figure 6.1 a) The composition of PET/TPU buffering sandwiches. b) and c) are the diagrams of a TPU honeycomb grid, and d) is the lateral view of the PET/TPU buffering sandwiches.	110
Figure 6.2 Images of the assembly of a drop-weight impact instrument.	112
Figure 6.3 The bursting strength of the PET/TPU buffering sandwiches as related to different basic weights.	113
Figure 6.4 The air permeability of with a basic weight of a) 150, b) 200, and c) 250 g/m ² as related to the number of lamination layers.	115
Figure 6.5 The air permeability of PET/TPU buffering sandwiches as related to the basic weight (150, 200, and 250 g/m ²) and the number of the nonwoven cover sheets (1- and 2-layered).	115
Figure 6.6 The resilience rate of PET nonwoven fabrics with a basic weight of a) 150, b) 200, and c) 250 g/m ² as related to the number of lamination layers (1-, 2-, 3-, 4-, and 5-layered).	117
Figure 6.7 The resilience rate of PET/TPU buffering sandwiches with a basic weight of a) 150, b) 200, and c) 250 g/m ² as related to the number of nonwoven cover sheets (1- 2-, 3-, 4-, and 5-layered).	118
Figure 6.8 The residual stress of PET nonwoven fabrics with a basic weight of a) 150, b) 200, and c) 250 g/m ² as related to the number of lamination layers (1-, 2-, 4-, and 6-layered).	120
Figure 6.9 The residual stress of PET/TPU buffering sandwiches with a basic weight of a) 150, b) 200, and c) 250 g/m ² as related to the number of nonwoven cover sheets on both upper and lower sides (1-, 2-, and 3-layered).	120

List of Tables

Table 2.1 Denotation of recycled fabric.....	35
Table 3.1 Physical and mechanical properties of aramid woven fabric.....	52
Table 3.2 Sample named and code of this study	54
Table 4.1 Physical properties of basalt, carbon fiber, and aramid plain woven fabrics..	73
Table 4.2 Denotation and composition of hybrid-fabric fibrous planks.	75
Table 4.3 Physical properties of high strength PET matrices	78
Table 5.1 Comparison of puncture resistances between N/L/W/F/L/N sample and other products.....	101

CHAPTER 1

Introduction

1.1 Current status of textile waste

In recent years, fibrous and textile products are applied to many other fields than garments and decorations. Due to the flexibility, lightweight, and easy process, they can easily combine with other materials. In addition to the intrinsic properties, they can also yield other required properties via the employment of different organizational structures and manufacturing processes. Fibrous and textile materials have a great diversity of applications, from domestic and industrial purposes to custom-made special functionality requests. Therefore, with the rapid development of the textile industry, and a large amount of textile waste has been produced. Textile waste includes waste from fiber processing, waste from spinning engineering, waste from textile processing, and discarded textiles in people's lives. The development of fast fashion clothing culture in recent years, its process of using cheap but not sustainable production has also promoted the production of a large amount of textile waste. Huge amounts of fiber, yarn and fabric waste are produced in the manufacture of textiles and garments, and a significant proportion of textile waste occurs at the end of the product life cycle. In addition, the manufacturers produce increasingly requirement protective textiles, consuming a large volume of protective fibers and fabrics. The amounts of selvages and textile wastes increase as a result of the considerable mass production of textiles inevitably, including those high prices, high strength, and high modulus fibrous materials. Due to previous various reasons, people produce a large amount of textile waste every year. How to deal with these textile wastes has been a problem faced by countries all over the world for a long time. In particular, the most urgent countries in the world are mainly textile exports, such as China, the European Union, India, the United States, Turkey, South Korea, and Taiwan (the export trade volume in 2017 is the seventh-largest in the world, as shown in Figure 1.1)[1].

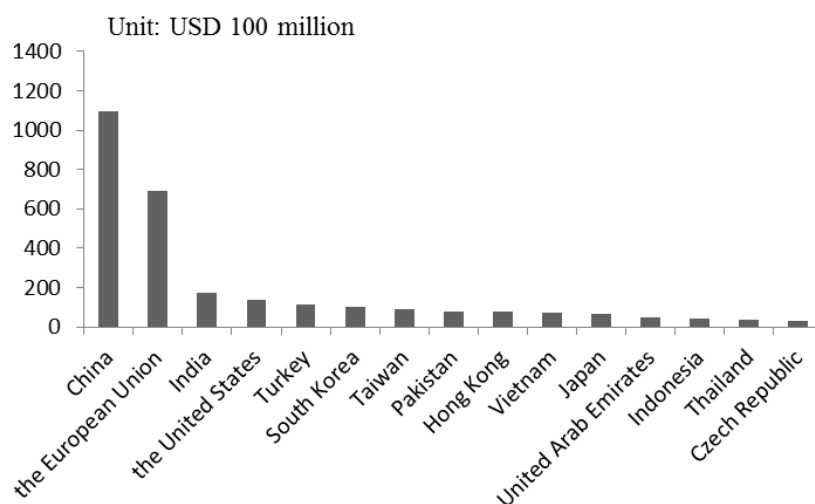


Figure 1.1 World's Major Textile Exporters in 2017[1]

Take Taiwan as an example. According to the statistics of the Taiwan Environmental Protection Administration [2], the fiber content of waste in the period from 2008 to 2014 averaged about 78,000 metric tons per year, while the fiber cloth content from 2015 to 2017 was about 134,000 metric tons per year. It accounts for about 4.63% of total waste in Taiwan (in 2017). On the other hand, according to the 2016 statistics of the Waste & Resources Action Programme (WRAP) in the UK [3], 1,130,000 tons of clothing was purchased in the UK, and 800,000 tons of process waste from the UK clothing requirement. The US Environmental Protection Association (EPA) estimates that approximately 16.89 million tons of textile waste were generated in 2017 [4], of which only 15.2% was recycled, 18.8% was combustion with Energy Recovery, and 66.0% was landfilled.

It is well known that the earth's resources may face a crisis of depletion. As the population grows, the requirement for food continues to increase, while the area of arable land for food and textile crops is shrinking. It is necessary to find a better way to utilize and conserve existing resources. Recycle of wastes can save resources and energy. Hence, highly efficient recycling and reclaiming design can process the materials to have new additive values. Various technologies have been developed so

far, mainly focused on reinforcing fibers and have not yet been commercialized. The main recycling methods can be divided into mechanical recycling, heat recovery and chemical recycling [5-6]. To discard the high-performance textile waste by means of direct disposal, burning, or the use as fillers seems rather a pity [7-8]. Improperly discarded waste increases the possibility of emitting carbon dioxide or toxic gas which is a burden to the environment [9-11]. In response, people increasingly pay more attention to recycle and reclamation techniques and related studies. For example, high strength uni-directional fabrics or woven fabrics are trimmed or scattered and then produced into a new reinforcing materials.

1.1.1 High performance textile waste

Fibers generally refer to materials consisting of continuous or discontinuous filaments, objects that are slender and soft in shape and longer in length than the width, and are the basis for all textile-related products. According to the source of raw materials, it can be mainly divided into natural fibers and artificial or chemical fibers. Fibers that can be obtained from animals, plants, and minerals are called natural fibers such as wool, silk, cotton, hemp and asbestos. The fibers processed by artificial methods are called artificial or chemical fibers, such as polyester fibers, glass fibers, metal fibers, and polyparaphenylene benzobisoxazole fibers (PBO) fibers. Puncture-proof materials need to be lightweight and safe to use, so the fibers used should have high strength, high modulus, shear resistance, and impact resistance. Commonly used are ultra-high molecular weight polyethylene fiber (UHMWPE), high strength Nylon fiber (Nylon), para-aramid fiber (PPTA), polyparaphenylene benzobisoxazole fiber (PBO).

Aramid fiber is mainly used as a protective material, it is widely used in various fields. The most famous aramids are Kevlar®, Twaron®, Nomex®, Newstar® and

Chapter 1

Teijinconex®. Because the aramid fiber usually has a significant performance degradation under UV light. Therefore, the outer layer is usually covered with a protective material during use. These protective products will be discarded after the end of their useful life. However, the high modulus fibers used in these protective products may only be slightly damaged.

In addition, as mentioned earlier, a large amount of textile waste is also produced during the production of high-performance textiles. These textile wastes include irregular pieces, sheets, filaments, staple fibers, and selvages (as shown in Figure 1.2). Therefore, we believe that an efficient recycling process and design can re-add new value to the material. This study focuses on the recycling technique of Aramid fabrics with the premise of minimizing the damage to the fibers. The main purpose of this study was to recover the selvage of high modulus woven fabrics in a one-step method using a non-woven process. The long strip of the waste selvage is broken into short fibers and directly formed into a non-woven fabric (as shown in Figure 1.3). The main difficulty is to achieve a highly efficient recycling process. The waste Aramid fibers are reclaimed to make high-performance fibers with a relatively much lower cost, thereby replacing the demands of using expensive resources of raw materials. Moreover, recycling textile waste is environmentally protective in terms of the reduction of wastewater, waste heat, and exhaust gas, making the development of protective materials more feasible and with more advantages in the industrial and livelihood protection fields. Therefore, the purpose of this thesis is to propose a new method for recycling waste textile materials. The main recycling object is high-performance woven fabric edges, and the recovered waste textile materials are used to make woven fabrics and explore the performance and feasibility.

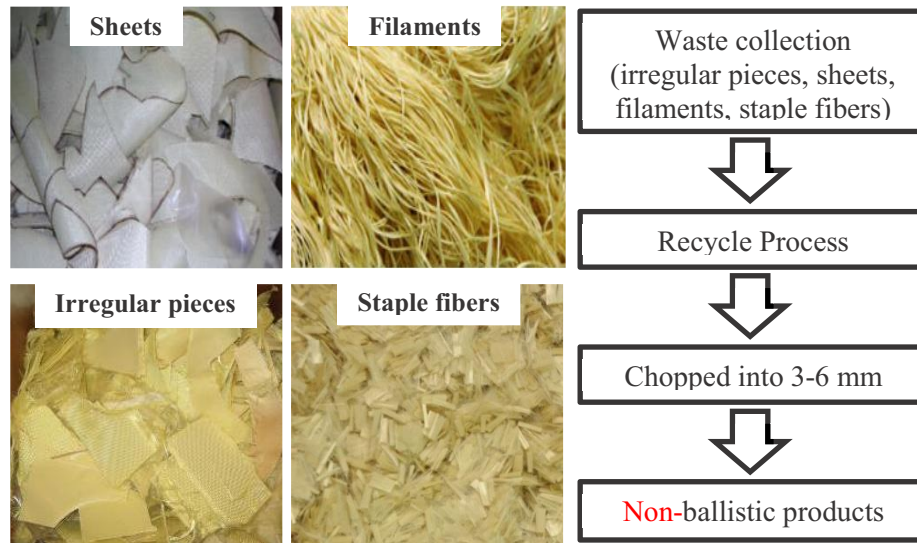


Figure 1.2 high-performance textile wastes and reuse/recycle process [12]

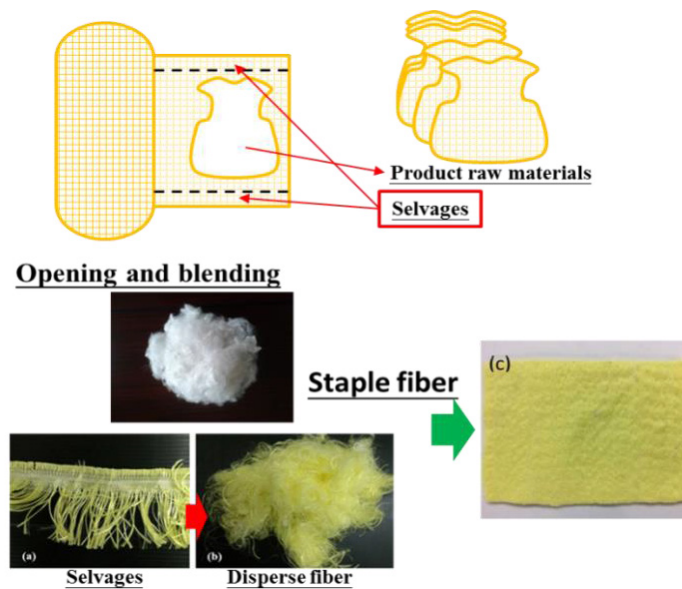


Figure 1.3 Recycle of the waste Kevlar® (ρ -aramid) woven selvages

1.1.2 The selvage of high modulus woven fabrics

With the wide application of Kevlar® (ρ -aramid), the recycling of Kevlar® products has also become an important issue in recent years. The selvage of the high modulus Kevlar® woven fabric was used in this study. High-modulus Kevlar® woven fabrics currently on the market are generally woven by using a rapier looms. Figure 1.4 shows the production process of high modulus Kevlar® woven fabrics.

Chapter 1

High-modulus Kevlar® filaments are woven through a rapier looms machine to form a Kevlar® woven fabric. For quality requirements, the width of the woven fabric must usually be slightly larger than the actual width required. When during the production process, the producer cuts the excess width, so that the produced woven fabric has neat edges to improve the quality and looks good of the product. The woven fabric is then packaged and sent to a processing plant for further processing into a wide variety of products. On the other hand, the cut edges will be scattered directly on the ground. After collection, they can only be handed over to the waste disposal recycling company for landfill or incineration treatment. However, the use of landfills or incineration to dispose of waste selvages, especially Kevlar® selvages, is not a good idea.

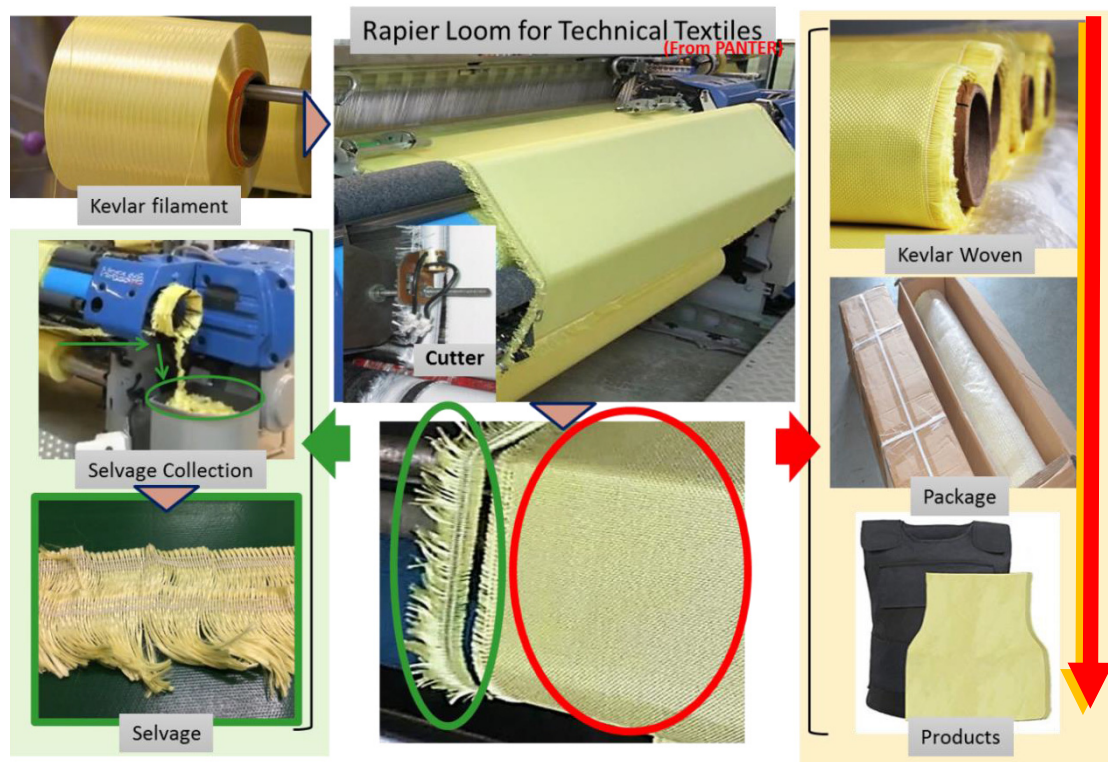


Figure 1.4 High-modulus Kevlar® woven fabrics (photo of the rapier loom is from PANTER, Italy)

Kevlar® fibers have high fiber physical strength, mainly due to the benzene

Chapter 1

rings, hydrogen bonds (as shown in Figure 1.5), and ordered molecular arrangements and crystals in their molecular structure [13-16]. So if it is buried in a landfill, it will not decompose even for a long time. In addition, according to 1982 United States Environmental Protection Agency literature, the combustion products of Kevlar® fibers which have been identified as presenting some potential for health-related hazards[17]. Therefore, if it is incinerated, toxic exhaust gas may be generated, and the waste liquid will impact the environment and endanger human health.

Figure 1.6 shows the structure of Kevlar® selvage which used in this study. As shown in the figure, the Kevlar® selvage can be divided into two parts, warp side selvage and weft side selvages. Weft selvage fibers are cut from long Kevlar® filament bundles with a fiber length of about 40-80 mm. The Weft selvage fibers generally use cheaper yarn materials, such as polyester yarn or cotton yarn, which is used to fix the edge of the woven fabric. The main purpose of warp selvage fibers is to make the fabric structure neat at the edges of the woven fabric, so the tight weave structure can be clearly seen from Figure 1.6. In addition, these waste selvages are usually continuous strips, and 1/3 of them with weave structure may cause reusing or recycling difficulties. Due to the weave structure in the waste selvage is tight and difficult to remove. In the past, when this type of waste selvage was recycled, the waste selvage was usually directly twisted to form thick ropes. However, the uneven weave structure may produce more hairiness and is rather wasteful for high-performance Kevlar® fibers. As a result, with the widespread use of Kevlar®, a large number of Kevlar® selvages are produced and waiting to be processed. At present, in order to effectively recycle these wastes Kevlar®, usually Kevlar® textile waste or waste fiberboard is directly broken into small fragments, staple fibers or pulp through physical and mechanical methods. It can be re-spun into new yarns, and can also be used for filling or pulp.

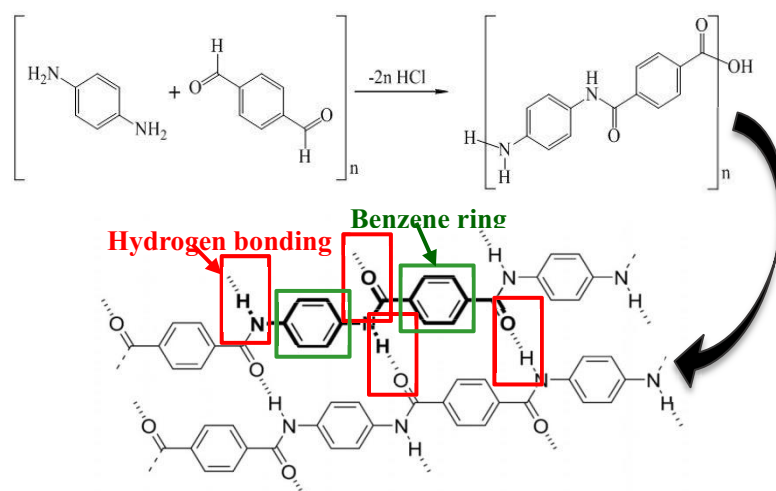


Figure 1.5 Synthetic molecular reaction formula of Kevlar®, benzene ring and the hydrogen bonding [16]

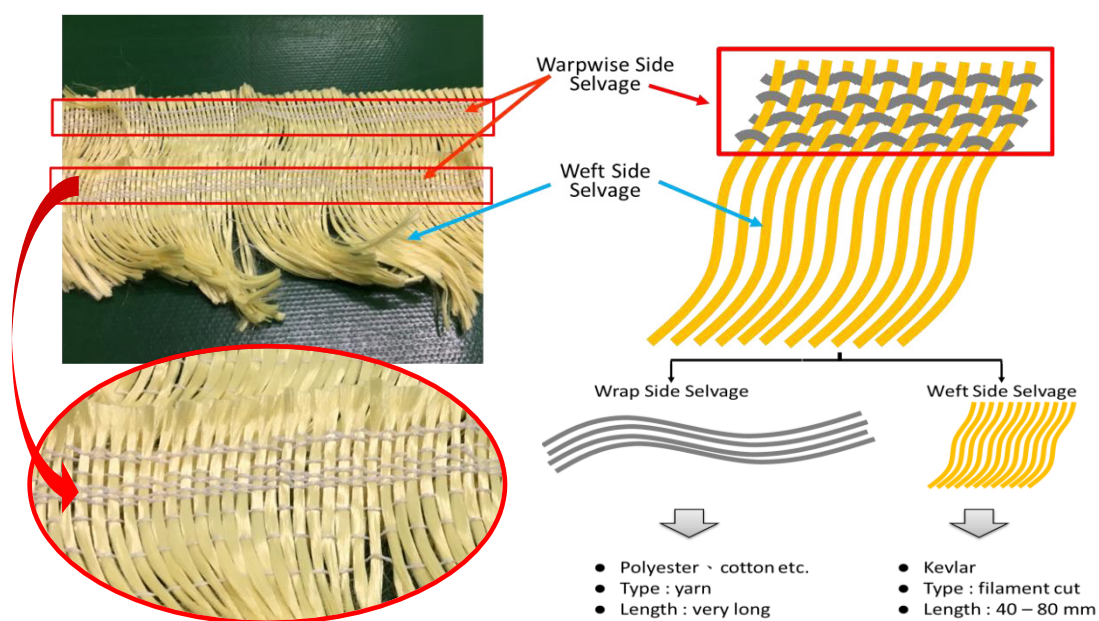


Figure 1.6 Structure of Kevlar® selvage

1.2 Reusing methods and current status of other high modulus fibrous materials

The manufacturers produce increasingly demanded protective textiles, consuming a large volume of protective fibers and fabrics. The amounts of selvages and textile wastes increase as a result of the considerable mass production of textiles

inevitably, including some high price, high strength, and high modulus fibrous materials. In addition to the Kevlar® fiber introduced in the previous section, the recycling of other commonly used high-performance fibers has also received increasing attention, such as carbon fiber, glass fiber, and so on.

Various technologies have been developed so far, mainly focused on reinforcing fiber composite materials and have not yet been widely commercialized. In addition, environmental regulations have become more stringent due to population growth and land area restrictions. Previously, the direct landfilling of these waste materials was convenient, but the time required for the decomposition of these wastes was too long and could have many adverse effects on the environment. Therefore, there is an urgent need to find more industrial-scale solutions to recover composite materials. Currently, the main recycling methods can be divided into heat recovery, chemical recycling and mechanical recycling [5-6].

1.2.1 Heat recovery and chemical recycling

Fibers recovered from thermal cracking and solvolysis generally cause a significant reduction in mechanical properties. The glass fiber recovered by fluidized bed pyrolysis at 450 °C showed a 50% reduction in tensile strength, while at 550 °C, the tensile strength decreased by 80% [18]. Other, for example, recycled carbon fibers which are subjected to thermal cracking (ELGCF process [19], FBP [20] and MIT-LLC process [21]) and solvolysis (ATI process [19]) are added to the thermoplastic resin. Materials containing ELGCF rCF exhibit properties that are very similar to those of materials with vCF. However, the stiffness and strength properties of the ATI rCF material are reduced by an average of about 36%; one of the reasons for the significant decrease in mechanical properties is also due to the residual resin on the fibers, which prevents good adhesion to the new matrix. At the same time, the

Chapter 1

recycled fabric retains its rigidity, making it impossible for the new resin to effectively penetrate into the fabric. Secondly, the adhesion between the fiber and the substrate is weak. According to the results of Meredith J et al., the crimped long PP fibers were mixed with ELGCF pyrolyzed rCF, and then the layers were compressed and consolidated using hot press forming [22]. SEM analysis of the fracture surface of the sample showed that the failure mainly occurred in the fiber pull-out, indicating that the adhesion between the fiber and the PP matrix was weak. The smooth surface of the fiber may be detrimental to mechanical bonding to the PP matrix. Greco et al. studied the effects of different post-treatments of heat and chemistry on fibers [23]. The results of the thermal post-treatment showed more fiber damage, but the fiber/matrix interfacial shear strength (IFSS) increased by 40%. On the other hand, chemical treatment in nitric acid results in less fiber damage and improved surface chemistry (IFSS improved by about 70%). However, both heat treatment and chemical treatment can cause fiber damage. Thermal cracking and solvolysis are widely proposed for the recovery of high modulus fibers. However, due to the efficiency of recovery, the handling of solvents and by-products, it is limited in application.

1.2.2 Mechanical recycling

At present, the research on the recovery of fiber reinforced composite materials is mainly based on the research of carbon fiber, followed by glass fiber and Kevlar® fiber. In most studies, the recovered carbon fibers are cut, ground and sieved to form granules, small fragments or very short fibers. Then, a new fiber-reinforced composite material is prepared by impregnating a resin (for example, an epoxy resin, a polyurethane foam or a thermoplastic resin, etc.) at different recycled fiber content ratios. Kouparitsas et al. studied recycled carbon fiber, glass fiber and aramid fiber,

and the recycled fiber was ground and incorporated into a polypropylene resin [24]. The results show that the tensile strength of the ground glass fiber and the aramid fiber reinforced polypropylene resin can be compared with the same resin reinforced with virgin fiber. Takahashi et al. studied crushing thermosetting CFRP into square sheets of about 1 cm. It is then incorporated into a thermoplastic resin to make a carbon fiber reinforced composite [25]. When the fiber content is 30vol%, it has better mechanical properties than the unreinforced resin. Palmer et al. studied the reincorporation of ground thermosetting CFRP into new sheet molding compound (SMC) [26]. This study used a thermoset CFRP fiber bundle that was ground to 5-10 mm. This fiber length is similar to the glass fiber bundle typically used in automotive SMC. The results show that approximately 20wt% of the virgin glass fibers can be effectively replaced by these carbon fiber recyclates.

However, it is currently proposed that mechanical methods mostly cut or grind recycled fibers into granules, small pieces or very short fibers which are compounded in the resin. The length of the recycled fiber limits its mechanical properties and the application of the recycling process. When the length is too long, it is difficult to uniformly mix due to the viscosity of the resin. In addition, the recycled fibers are usually scattered and cannot be maintained in a single direction. Therefore, these findings are more suitable for use in bulk or sheet molding compounds and cannot be recycled/reused in structural applications [5].

1.3 Non-woven technology and mechanism

Nonwoven fabric processing technology is an important way to utilize recycled fibers. The raw materials that can be used for processing nonwoven fabrics are wide, and the requirements for fiber length and performance are relatively wide. Therefore, it is an advantageous, low-cost and high-efficiency processing technology for

Chapter 1

recycled fiber materials with mixed specifications. In addition, the recycle of high modulus fibers in product applications where lower strength requirements may be more interest than highly structured parts for people.

Non-woven is defined as a textile product that is made without spinning and weaving. A sheet of oriented or randomly arranged fibers (which may be long fibers or short fibers) formed by rubbing or bonding. Non-woven technology is a textile technology that has been developed for a long time in the textile industry and has been applied earlier. Compared with the traditional woven and knitted textiles, it belongs to the two-dimensional fabric, and the non-woven fabric has more Z-axis direction reinforcement belonging to the three-dimensional fabric. It is characterized by short process, high output, wide range of applicable raw materials, many types of products, wide range of functions, and easy secondary processing. Non-woven fabrics are widely used in clothing, filter materials, abrasive cloths, medical and sanitary materials, electronic, industrial or geotextiles - agriculture, civil engineering, construction materials, or as composite materials. It can be seen that non-woven fabrics occupy an important position in the entire textile market.

Non-woven technology can be roughly divided into four parts [27]: 1. Pre-processing-Opening and cotton blending. The main purpose is to make the cotton bales originally compacted in the cotton bales open into fiber bundles through the process of mechanical impact and tear through card clothing. During the opening process, two or more different fibers can be opened at the same time. Perform a mixing effect. ; 2. Carding and stripping. The finer impurities contained in the fibers are separated and the fibers are further carded to form a fiber web with a certain directionality. ; 3. Fold the cotton net. After the scattered fiber bundles are combed, a single-layer fiber web is formed on the surface of the doffer. After the fiber web is stripped from the doffer, the fiber web is passed to the cotton laminator, and the

single-layer fiber web is overlapped back and forth to form a multi-layer uniform thick web. ; 4. Needle rolling reinforcement process (as shown in Figure 1.7).

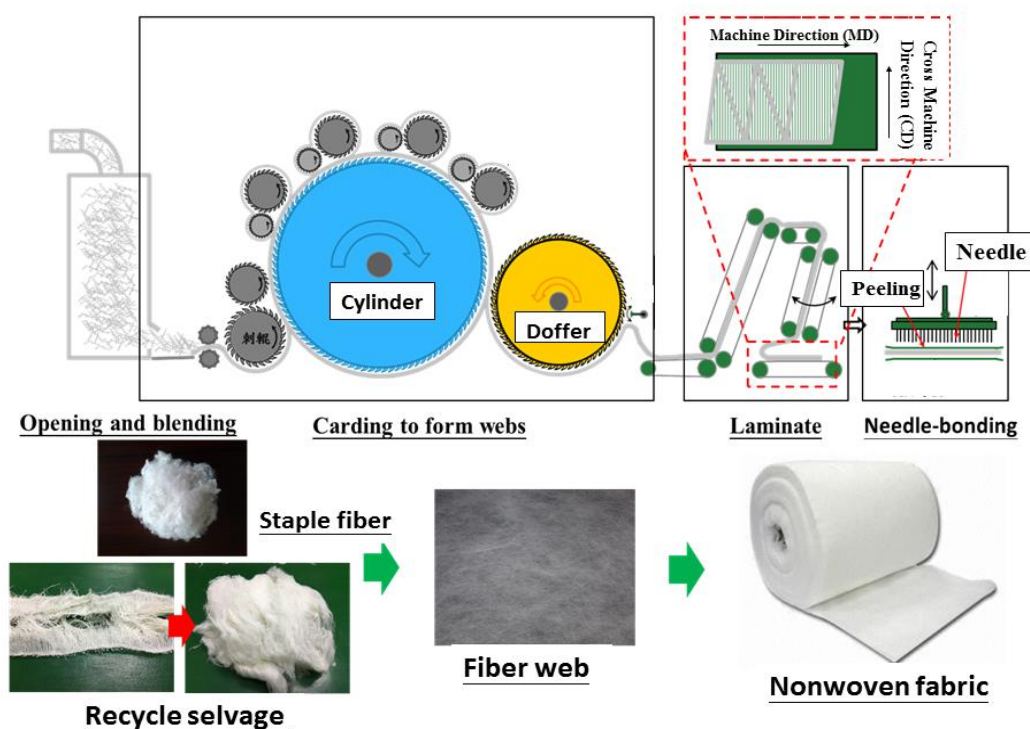


Figure 1.7 The process of recycled fabric.

During the needling process, the barbs on the needle can effectively hook the fibers in the fiber web, and the fibers are punctured from the surface through the fiber web to generate displacement (as shown in Figure 1.8), and the fiber web is compressed due to friction when the penetration of needles is deep. After that, the needle is lifted back, and at this time, the fiber is separated from the needle and left in the fiber web in an approximately vertical state due to the direction of the barbs. At the same time, the density of the non-woven fabric is greatly increased so that the uniformity is increased and the strength in each direction is increased. The main purpose of this study was to recover the Selvage of high modulus woven fabrics in a one-step method using a non-woven process. The principle and mechanism of nonwoven processing technology are used to destroy the structure of the waste

selvages and evenly comb and disperse these fibers. These dispersed short fibers are then made into a recycled nonwoven fabric through a complete nonwoven manufacturing process to facilitate subsequent processing and utilization (as shown in Figure 1.9 and 1.10).

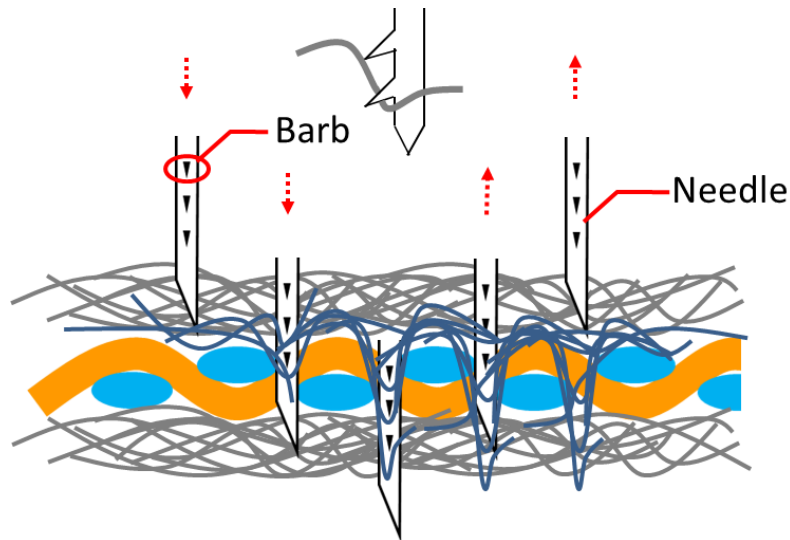


Figure 1.8 Needle-bonding process

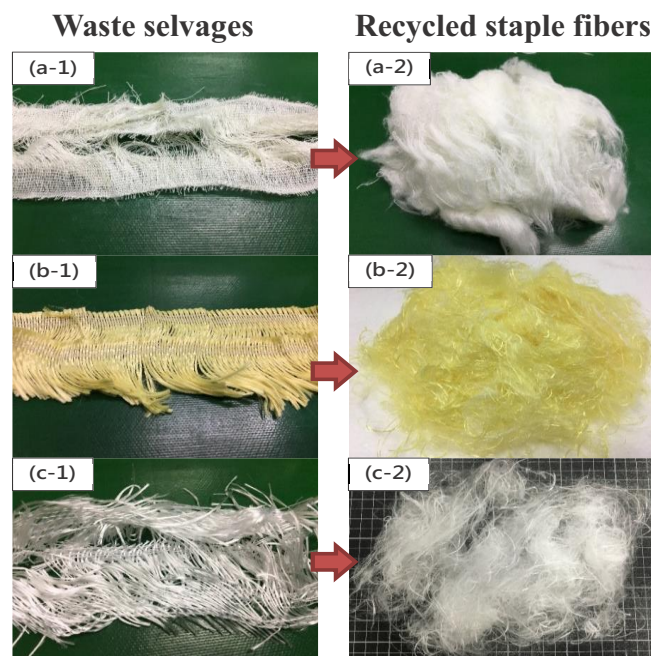


Figure 1.9 Recycled selvage and staple fibers. a-1) The left column shows the recycled Nomex®,(b-1) Kevlar®, and (c-1) polyester (PET) selvage. The right column shows the (a-2) Nomex®, (b-2) Kevlar®, and (c-2) PET staple fibers.

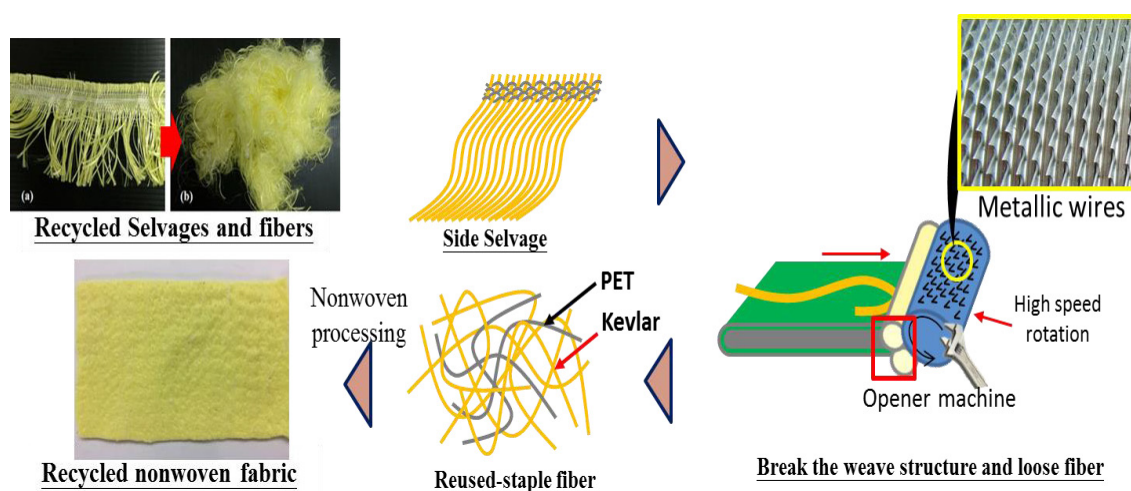


Figure 1.10 Schematic diagram of the waste selvage recycling process

1.4 Personal protective equipment (PPE)

Personal protective equipment (PPE) is defined as a device designed which is designed for personal wear or possession to protect people against one or more health and safety hazards or infection. Generally, the PPE devices include items such as protective clothing, helmets, goggles, or other garments or equipment depending on the area of the body protected you want and the types of hazards such as physical, electrical, thermal, chemical, biological hazards and airborne particulate matter [28-32]. Besides this, PPE usually can be divided by "Protective clothing" and "protective gear". "Protective clothing" is applied to traditional categories of clothing, and "protective gear" applies to items such as pads, guards, shields, or masks, and others. Therefore, PPE is needed to be required when there is a danger. And people wear protective equipment that may be worn for safety and health purposes as well as for sports and other activities.

Specifically, people are most concerned about safety protection at work and outdoors. Protective clothing is mainly used to protect the human body in professional fields and other harsh environments [33]. For example, firefighter protective clothing

Chapter 1

provides limited protection for firefighters in potentially hazardous environments. These hazards include heat (flame, radiation and convective heat), physical (impact, puncture and rough surfaces), biological (blood-borne pathogens), environment (extreme temperature and humidity) and chemistry (skin contact) [34]. Therefore, a variety of protective work clothes will become more and more important in the professional field as well as leisure and sports. Nowadays, in addition to the functionality, the comfort of protective clothing has gradually become one of the most important attributes required by modern consumers. Among them, when producing industrial work clothes, protective clothing, protective gloves, and engineering shoes, stab resistance and impact resistance are the most common and basic concerns in various fields [35-36].

1.4.1 Stab-resistance materials

With the continuous development of technology and the recognition of self-protection, protective materials have been continuously developed from bark, leather, metal to advanced composite materials. A variety of protective materials have been developed for the needs of industry and manufacturers [27-32]. The most common need in different fields is the stab-resistant material [35-36]. On the one hand, the incidence of knife stick injuries is more commonly used in fights and robberies due to gun control restrictions and easy access to knives [37]. According to Taiwan's occupational injury statistics, 15% of injuries are caused by stab wounds, cuts and abrasions. The main injuries are on the hands and feet. Although the limb amputation is not fatal, it still causes a lot of inconvenience to the injured person's life. Therefore, there have been many published studies on the stab resistance properties of industrial textiles [35-39]. Stab resistance is one of the important features of materials, especially in the case of fabrics for safety clothing and personal protective clothing.

Chapter 1

Protective gloves, law enforcement and safety personnel, body armor, firefighter protective clothing and inflatable structures are required to have stab resistance [7, 40].

Achieving good puncture resistance is mainly based on sufficient fiber density, high friction among fibers, a profound aggregation of fibers where the spike strikes, and firmly secured fibers. In this section, the displacement, friction, deformation and damage between the puncture needle and the puncture fabric during the puncture will be explained. In the first stage, the puncture process begins with the contact of the puncture needle with the puncture fabric. As the puncture needle moves, the structure of the puncture fabric begins to stretch and tighten, and the puncture load is slowly increased. In the second phase, the puncture load is increased until the tip of the puncture needle pierces the surface of the fabric, causing a sudden drop in load. In this process, the fibers or yarns, which are primarily puncture points, form yarn slippage and severing due to the tip pressure of the puncture needle. It was also the cause of the sharp drop in the puncture load, and no fiber breakage was observed at this time. Then, in the third stage, when the puncture needle is continuously moved, the diameter of the needle penetrating past becomes larger, and the friction between the yarn around the needle tip and the needle is rapidly increased, and the puncture load is also rapidly increased. During this process the yarn will produce significant slip and yarn breakage. In the fourth stage, the diameter of the conical portion that penetrates the past is maximized, and the area of fabric damage does not increase. The puncture load reaches a maximum and the post-stress decreases (penetration process is shown in Figure 1.11).

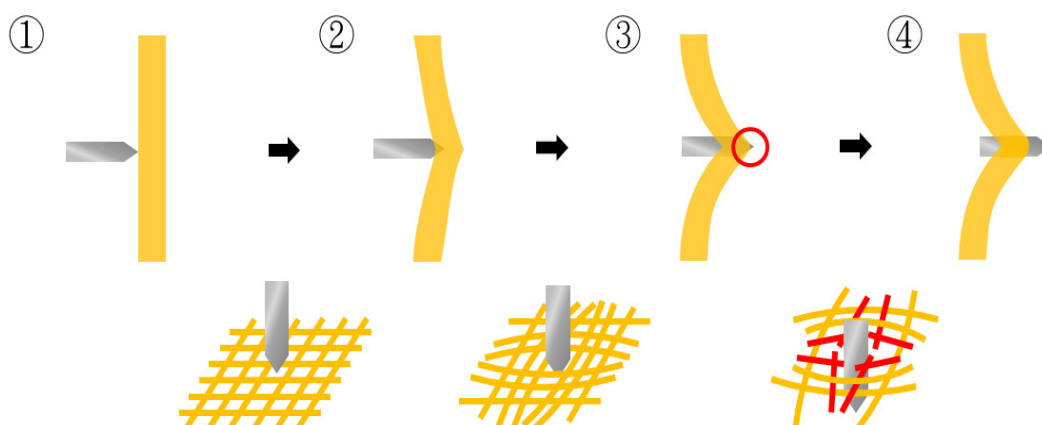


Figure 1.11. Schematic of puncture process

In addition, it has been found from many studies that the puncture force can be decomposed into different forces for analysis and discussion. As shown in Figure 1.12, the puncture target gradually deforms as the puncture blade penetrates the target during the puncture. The puncture load and the puncture displacement are gradually increased. According to the puncture load and the puncture displacement, the current puncture energy (J) (Equation 1) can be obtained by formula calculation. P is the penetration load and δ is the displacement of the penetrator. In addition, the puncture load can be further decomposed by magnifying the puncture tip. According to the resistance of the puncture tip during the puncture and the deformation and damage of the fabric, the puncture load can be decomposed into three types: (1) the friction force between the puncture target and the blade (2) the puncture target applies the press force on the blade (3) Stress concentration damage at the tip of the blade. In general, if it is possible to design and improve the effects of these forces, it will definitely improve the puncture resistance of the material.

$$\text{Penetration Energy (J)} = \frac{P\delta}{2} \quad (\text{Equation 1})$$

P (N) is the load during the penetrate process ; δ (mm) is the displacement of the penetrator.

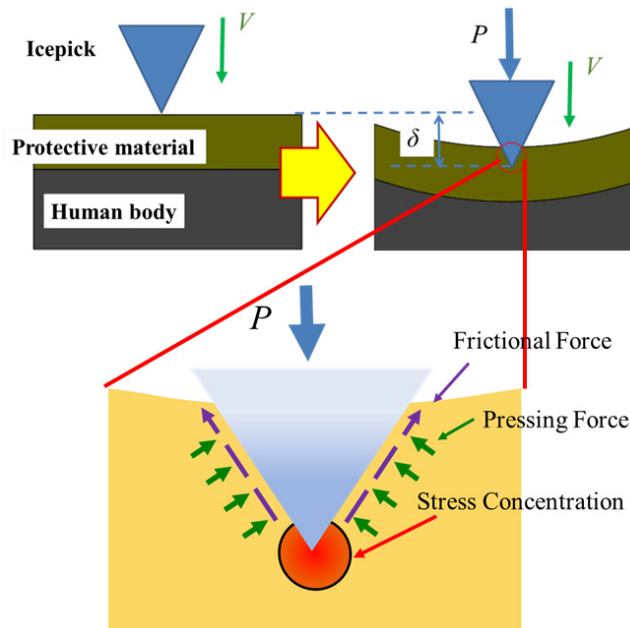


Figure 1.12 Penetrate model of the penetrate process

1.4.2 Buffer resistance materials

The main function of the cushioning material is to absorb energy effectively and reduce the damage to the object when it is impacted. The main function is to play the dual role of isolation and buffering. In recent years, many plastic materials have been used instead. Commonly used materials such as polyethylene, polypropylene, polyvinyl chloride, polystyrene, polyurethane and the like have been widely used in buffer protection devices and commercially available packaging materials [41-44]. The most important function of the buffer material is the absorption and consumption of impact energy. Especially when the object is subjected to vibration or impact, the cushioning material can avoid or mitigate the damage. The main mechanism of buffering can be divided into the following two points: 1. Disperse impact force: Distribute the external impact force on a large area by vibration and transmission, avoiding the impact energy concentrated on one point and causing stress concentration damage, thereby reducing or consuming impact energy. 2. Fixing and

reducing vibration: Fixing the protected body so that there is no pressure shock caused by additional vibration, collision or deformation caused by external force. The products include anti-collision mats, mattresses, floor mats and protective mats for sports, inner walls for construction, various protective gear, ridge materials for young children and the elderly, and cushioning for rehabilitation equipment. Further enhance the user's stability, comfort, and safety by increasing the cushioning protection of the product. From the above, it can be known that the development of the buffer composite structure is very important.

The main advantage of plastic materials as buffer materials are is that they can fulfill the space that is required by mass batches as their flexible form can be adjusted according to any irregularly shaped products. So that the contact area between buffer materials and products is increased, which efficiently distributes the damaging force occurring in shipping, securing the intact status of the products. In addition to their advantages of having a lightweight, ease of processing, good protection, broad adaptability, and a low production cost, but also has disadvantages of occupying a remarked volume and failing to be biodegraded, and it also releases toxic gas during incineration [45-48]. The bio-based foam and plastic are now available in the market; however, their strict treatment conditions and incomplete degradation restrict their applications [49-50].

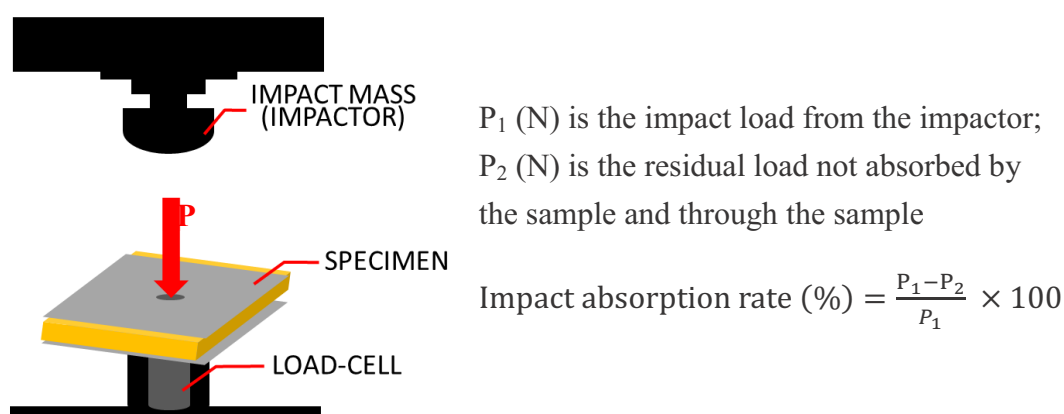


Figure 1.13 Drop-weight impact test arrangement

1.5 Constitution of this dissertation

In this thesis we investigate the recycled recycled fabrics in terms of characterizations and mechanical properties based on the constituent recycled staple fibers. The eco-friendly manufacturing design uses high performance of recycled m-aramid (Nomex®), p-aramid (Kevlar®), and polyester (PET) selvages. The recycled fibers take up 50, 70, and 90 wt% of the hybrid composites and corresponding low-melting polyester fibers (LMPET) account for 50, 30, and 10 wt%. In this study, the influence of a specified temperature of hot pressing of 130 °C on different properties is discussed. When base weight is excluded from consideration, K9 of the control groups has the optimal mechanical properties before hot-press treatment, and after hot-press treatment the P9 of the experimental groups has the optimal mechanical properties. The satisfactory test results are ascribed to the high performance of the recycled staple fibers and the reinforcement of LMPET fibers. In particular, the combination of recycled PET fibers and LMPET fibers has a synergistic effect in stabilized structure and mechanical improvement.

Secondly, in chapter three, I investigate the performance of hybrid-fiber-reinforced composite boards made of recycled Aramid composite matrices, LMPET matrices, and Aramid woven fabrics, which are laminated, needle punched and hot pressed. The test results show the tensile strength of hybrid-fiber-reinforced composite boards is 5 times greater than that of the control group, while its tearing strength is 8.5 times greater than that of the control group. The employment of hot pressing enhances the properties even more. And the composite boards with hot-pressed containing 90 % recycle Aramid fibers as the Aramid matrix has the optimal static puncture resistance, and the major factors are the compact plain woven structure and LMPET fibers. Hot pressing gives rise to the presence of thermal bonding points, which hampers the slipping of Aramid and

Chapter 1

LMPET fibers, secures the structure, and increases the friction of fibers against the powerful punch. As a result, the hybrid-fiber-reinforced composite boards containing 90 % of recycle Aramid fibers) have the optimal static puncture resistance.

In chapter four, I proposes flexible fabric-based protective planks, which are recycled high strength PET fibers by processed with minimum damage for secondary production, thereby obtaining recycled high-performance fibers with relatively lower production cost. In this study, the different reinforcing woven fabrics are combined with matrices to form hybrid-fabric fibrous planks. Despite multiple combining and carding processes, the recycled PET staple fibers are proven to provide the fibrous planks with high tensile and tear strengths. The test results indicate that recycled PET fibers remain high strength and can be made into protective products. The combination of nonwoven and woven fabrics provides the benefits of their different stab behaviors, strengthening the puncture resistance of the hybrid-fabric fibrous planks. Most of all, an efficient recycling process and using textile and fiber waste to make protective fibrous planks decreases the production cost considerably, which makes the industrial and livelihood protective products more advantageous and acceptable.

In chapter five, In order to improve the stab resistance from the fabric structure, I study to develop sandwich-structured puncture-resistant fabric composites, and the optimal N/L/W/F/L/N has good puncture resistance at level 3 (N: Nylon/aramid recycled nonwoven fabrics ; L: Low-melting PET fabrics ; W: reinforced woven fabric ; F: PET filament). The proposed fabric composites are characterized in terms of tearing strength, static puncture resistance, and dynamic puncture resistance. The test results indicate that thermally treated N/L/W/F/L/N has a 63.3 % greater tearing strength at CD orientation, 63.9 % greater static puncture resistance, and 32.5 % greater bursting strength than N/L/L/N. Compared to other studies, using the LMPET

Chapter 1

adhesive layer had a positive influence, preventing the slide of the filaments, but the poor interfacial combination only contributes limited reinforcement. Hence, improving the interfacial affinity between laminates is suggested to be conducted in future studies.

In chapter six, I study investigates the properties of the PET/TPU buffering sandwiches in terms of the different basic weights and the number of nonwoven cover sheets on both middles, upper and lower sides which made by the needle-punching method. The results are compared with the properties of the control group (i.e. pure PET nonwoven fabrics). Similarly, so far as the PET/TPU buffering sandwiches are concerned, the residual impact stress is decreased when the number of the nonwoven cover sheets increases, and then reaches 3248 N when the buffering sandwiches are composed of 3-layered nonwoven cover sheets on both upper and lower sides. Moreover, the optimal bursting strength of the experimental group is 1336 N. To sum up, compared to the control group, the experimental group has 23.2 % lower residual impact force and 5.2 times the bursting strength, but slightly lower LOI. The proposed buffering sandwiches are composed of environmentally friendly TPU honeycomb grids and traditional nonwoven fabrics and are proven to have excellent buffering and protective properties.

Reference

- [1] Overview of Taiwan's textile industry in 2018, Taiwan Textile Federation, 2019.
(In Chinese)
- [2] K.Y. Chiang, The Sampling and Analysis of Municipal Solid Waste Composition in Taiwan (2015-2017), Environmental Protection Administration of Taiwan, 2018.
- [3] The Waste & Resources Action Programme.
<https://www.wrap.org.uk/sustainable-textiles>.
- [4] Textiles: Material-Specific Data, Environmental Protection Association.
<https://www.epa.gov/facts-and-figures-about-materials-waste-and-recycling/textiles-material-specific-data>
- [5] G. Oliveux, L.O. Dandy, G.A. Leeke, Current status of recycling of fibre reinforced polymers: Review of technologies, recycle and resulting properties, *Progress in Materials Science* 2015, 72: 61–99.
- [6] Y.X. Yang, R. Boom, B. Irion, D.V. Heerden, P. Kuiper, H.D. Wit, Recycling of composite materials, *Chemical Engineering and Processing* 2012, 51:53-68.
- [7] J.B. Mayo, E.D. Wetzel, M.V. Hosur, S. Jeelani, Stab and puncture characterization of thermoplastic-impregnated aramid fabrics, *Int. J. Impact Eng.* 2009. 36 : 1095–1105.
- [8] S. Yasin, N. Behary, M. Curti, G. Rovero, Global consumption of flame retardants and related environmental concerns: A study on possible mechanical recycling of flame retardant textiles. *Fibers* 2016, 4:16–25.
- [9] S. Sidhu, B. Gullett, R. Striebich, J. Klosterman, J. Contrerasv, M. DeVito, Endocrine disrupting chemical emissions from combustion sources:diesel particulate emissions and domestic waste open burn emissions, *Atmos. Environ.* 2005, 39: 801–811.

Chapter 1

- [10] A. Kamal, U. Ali, M. I. Ramay, S. M. Z. Younis, S. Sumbal, R. N. Malik, A. Rashid, Principle component analysis of flue gas exhaust and health risk estimates for the population around a functional incinerator in the vicinity of Rawalpindi Pakistan, *Arab. J. Chem.* 2017, 10:2302-2306.
- [11] C. A. Pope III, D. W. Dockery, Health Effects of Fine Particulate Air Pollution: Lines that Connect, *J. Air Waste Manage. Assoc.* 2006, 56: 709-742.
- [12] Environmental Impact and Sustainability,
<https://kevlarweb.wordpress.com/environmental-impact-and-sustainability/>
- [13] Tiffany Vu. Kevlar, the “Not-so-Secretive” Bullet Proof Fiber
- [14] Michael C. Petty, *Molecular electronics: from principles to practice*, John Wiley & Sons, 2007, p. 310
- [15] J. Quintanilla, Microstructure and properties of random heterogeneous materials : a review of theoretical results. *Polymer Engineering and Science* 1990. 39 (3): 559–585. doi:10.1002/pen.11446
- [16] *Technical Guide for Kevlar® Aramid Fiber*, DuPont, 2017.
- [17] T. Lynch, L. Davies, J. Alchowiak, *Assessment of Future Environmental Trends and Problems of Increased Use, Recycling, and Combustion of Fiber-Reinforced, Plastic and Metal Composite Materials*. 1982
- [18] S.J. Pickering, R.M. Kelly, J.R. Kennerley, C.D. Rudd, N.J. Fenwick, A fluidised-bed process for the recovery of glass fibres from scrap thermoset composites. *Compos Sci Technol* 2000,60:509-523.
- [19] M.L. Connor, *Characterization of recycled carbon fibers and their formation of composites using injection molding*. Master thesis, North Caroline State University, Raleigh, NC, USA; 2008.
- [20] K.H. Wong, D.S. Mohammed, S.J. Pickering, R. Brooks, Effect of coupling agents on reinforcing potential of recycled carbon fibre for polypropylene

- composite. *Compos Sci Technol* 2012, 72:835-844.
- [21] K. Stoeffler, S. Andjelic, N. Legros, J. Roberge, S.B. Schougaard, Polyethylene sulphide (PPS) composites reinforced with recycled carbon fiber. *Compos Sci Technol* 2013, 84:65-71.
- [22] M.H. Akonda, C.A. Lawrence, B.M. Weager, Recycled carbon fibre-reinforced polypropylene thermoplastic composites. *Composites Part A* 2012, 43:79-86.
- [23] A. Greco, A. Maffezzoli, G. Buccoliero, F. Caretto, G. Cornacchia, Thermal and chemical treatments of recycled carbon fibres for improved adhesion to polymeric matrix. *J Compos Mater* 2013, 47:369-377.
- [24] C.E. Kouparitsas, C.N. Kartali, P.C. Varelidis, C.J. Tsenoglou, C.D. Papaspyrides, Recycling of the fibrous fraction of reinforced thermoset composites. *Polym Compos* 2002, 23:682-689.
- [25] J. Takahashi, N. Matsutsuka, T. Okazumi, K. Uzawa, I. Ohsawa, K. Yamaguchi, et al. Mechanical properties of recycled CFRP by injection molding method. In: *Proceedings of the 16th international conference on composite materials 8–13 July 2007, Kyoto, Japan.*
- [26] J. Palmer, L. Savage, O.R. Ghita, K.E. Evans, Sheet moulding compound (SMC) from carbon fibre recycle. *Composites Part A* 2010, 41:1232-1237.
- [27] A.F. Turbak, *Nonwovens: Theory, Process, Performance, and Testing*, TAPPI Press, 1989, 101-106.
- [28] J.H. Verbeek, S. Ijaz, C. Mischke, J.H. Ruotsalainen, E. Mäkelä, K. Neuvonen, M.B. Edmond, R. Sauni, F.S. Kilinc Balci, R.C. Mihalache, Personal protective equipment for preventing highly infectious diseases due to exposure to contaminated body fluids in healthcare staff, *Cochrane Database of Systematic Reviews* 2016. DOI: 10.1002/14651858.CD011621.pub2.
- [29] G. Bartkowiak, A. Dąbrowska, A. Marszałek, Assessment of an active liquid

Chapter 1

- cooling garment intended for use in a hot environment. *Appl. Ergon.* 2017. 58: 182-189.
- [30] E. Małek, D. Miedzińska, M. Stankiewicz, Heat resistance research and surface analysis of fireproof textiles with titanium silicide coating. *Procedia Struct. Integr.* 2017. 5: 508-515.
- [31] M.C. Silva-Santos, M.S. Oliveira, Giacomini, A.M.; Laktim, M.C.; Baruque-Ramos, J. Flammability on textile of business uniforms: Use of natural fibers. *Procedia Eng.* 2017. 200: 148-154.
- [32] Y. Xu, J. Sheng, X. Yin, J. Yu, B. Ding, Functional modification of breathable polyacrylonitrile/polyurethane/TiO₂ nanofibrous membranes with robust ultraviolet resistant and waterproof performance. *J. Colloid Interface Sci.* 2017. 508: 508-516.
- [33] J. Legerská, P. Lizák, Evaluation of the specific physiological properties for the selected assortment of work clothes, *Procedia Engineering* 2016. 136: 227-232.
- [34] A. Coca, W.J. Williams, R.J. Roberge, J.B. Powell, Effects of fire fighter protective ensembles on mobility and performance, *Applied Ergonomics* 2010. 41:636-641.
- [35] Y. Termonia, Puncture resistance of fibrous structures. *International Journal of Impact Engineering.* 2006. 32:1512-1520.
- [36] Q.S. Wang, R.J. Sun, X. Tian, M. Yao, Y. Feng, Quasi-static puncture resistance behaviors of high-strength polyester fabric for soft body armor. *Results in Physics.* 2016. 6:554-560.
- [37] H. Kim, I. Nam, Stab resisting behavior of polymeric resin reinforced p-aramid fabrics, *J. Appl. Polym. Sci.* 2012. 123: 2733-2742.
- [38] M.J. Decker, C.J. Halbach, C.H. Nam, N.J. Wagner, E.D. Wetzel, Stab resistance of shear thickening fluid [STF]-treated fabrics, *Compos. Sci. Technol.*

2007. 67: 565–578.

- [39] Z. Song, C. Zhang, M. Song, S. Wu, Advanced Stab Resistance fabrics utilizing shear thickening fluids, *Adv. Mater. Res.* 2011. 300:73–76.
- [40] E. Triki, P. Dolez, T. Vu-Khanh, Tear resistance of woven textiles – criterion and mechanisms, *Compos: Part B* 2011. 42: 1851–1859.
- [41] M. Hosur, M. Abdullah, S. Jeelani, Manufacturing and low-velocity impact characterization of foam filled 3-D integrated core sandwich composites with hybrid face sheets. *Compos. Struct.* 2005, 69: pp.167-181.
- [42] Rasoul N and Ali Reza S. Study of foam density variations in composite sandwich panels under high velocity impact. *Int. J. Impact Eng.* 2014, 63:129–139.
- [43] Z. Sun, X.Z. Hu, S.Y. Sun, H. Chen. Energy-absorption enhancement in carbon-fiber aluminum-foam sandwich structures from short aramid-fiber interfacial reinforcement. *Compos. Sci. Technol.* 2013, 77:14–21.
- [44] F. Xia, X.Q. Wu, Study on impact properties of through-thickness stitched foam sandwich composites. *Compos Struct* 2010, 92:412-421.
- [45] C. Yang L. Fischer, S. Maranda, J. Worlitschek, Rigid polyurethane foams incorporated with phase change materials: A state-of-the-art review and future research pathways. *Energ. Buildings* 2015, 87(1) : 25-36.
- [46] A. Tinti, A. Tarzia, A. Passaro, R. Angiuli, Thermographic analysis of polyurethane foams integrated with phase change materials designed for dynamic thermal insulation in refrigerated transport. *Appl. Therm. Eng.* 2014, 70(1):201-210.
- [47] N. Pargana, M.D. Pinheiro, J.D. Silvestre, J. Brito, Comparative environmental life cycle assessment of thermal insulation materials of buildings, *Energ. Buildings* 2014,82 : 466-481.

Chapter 1

- [48] H. Sasaki, K. Saito, K. Abe Development of an Air Cushioning Material Based on a Novel Idea. *Pack-aging Technology and Science* 1999, 12(3):143-150.
- [49] H. Kobayashi, M. Daimaruya, T. Kobayashi, Dynamic and static compression tests for paper honeycomb cores and absorbed energy. *JSME International Journal Series A* 1998; 41(3):338-344.
- [50] K. Chidambarampadmavathy, O.P. Karthikeyan, K. Heimann, Sustainable bio-plastic production through landfill methane recycling. *Renewable and Sustainable Energy Reviews* 2017, 71:555–562.

CHAPTER 2

Mechanical properties of recycled fabric made of waste Nomex[®], Kevlar[®], and polyester selvages

2.1 Introduction

There are always contradictions with advancement regardless of whether it is evolution, religion, or industrial progress. Weapons are one martial creation of the progressing technology, which is used in wars and also in crimes. Protective products, armors, and equipment are popular items on the market. The range of self-protection generally involves people's lives and property. People are concerned about the safety and have increasing demands on self-protection in terms of the working/living environment, accidents, and raising crime rates. Practically, the safety of the working environment is what people are deeply concerned about. The developments of body armor, safety shoes, and other protective products are necessary due to the possibly inflicted injuries, loss of lives and property. For industries, protective clothing, protective gloves, and safety shoes are commercially popular, and protective materials also require stab resistance [1-4]. The increasing demands of protective textiles cause the mass production of high-performance fabrics [5-6], leaving a considerable amount of high-performance selvages. As high-performance fabrics have a higher cost, it is a waste to leave the selvages as garbage to be outsourced to be abandoned, burnt, or used as fillers. In addition, improper disposal of textile waste may result in emissions of carbon dioxide and toxic gas, which causes damage to the environment and human health [7-9]. Thus, people pay more attention to recycling and reclamation technology, which has a positive influence on recycling textile waste [10-12]. Liu, Zhu, Xu, and Bao (2018) and Wan and Takahashi (2016) studied investigating the benefits of recycling and reclaiming high-performance fibers and fabrics [13-14]. For example, high-performance unit-directional fabrics and woven fabrics are recycled and severed in order to be made into reinforcing materials which are tested whether they are effective to make composite mechanically strong. Therefore, this study proposes using recycled high-performance selvages (e.g. Nomex®, Kevlar®, and

Chapter 2

high-performance Polyester woven) and the selvage fibers we used in this study are collected from the edges of the waste woven fabrics for recycle. The woven fabric is woven into a fabric by the textile yarns and it is usually a ‘continuous filament’. Therefore, the waste fibers obtained by recycling the waste woven fabric selvage are ‘smooth short fibers’ which has a length of 40–80mm and making the recycled fabric. And then processed with the least damage, producing high value-added protective materials. Using a great amount of recycled fibers can reduce the presence of wastewater, heat, and gas caused by improper disposal, and is considered eco-friendly and economical. As a result, the proposed protective materials have feasibility for the use in the industrial and livelihood fields and will be preferred by the manufacturers and users.

2.2 Experimental

2.2.1 Materials

Recycled Nomex® staple fibers are obtained from Nomex® selvages. The recycled Nomex® selvages are produced by DuPont (USA) and imported by Formosa Taffeta, Taiwan. Nomex® is a kind of flame-resistant meta-aramid material, and it is high-temperature resistant fiber that does not melt and does not support combustion in the air. Recycled Kevlar® staple fibers are obtained from Kevlar® woven selvages (K129 and K29, DuPont, Wilmington, DE, USA). The recycled Kevlar® selvages are produced by DuPont and imported by Formosa Taffeta, Taiwan. It is lightweight, high performance and high toughness, mainly used in bulletproof products, ropes and protective clothing (such as cut resistant gloves). Recycled polyester (PET) staple fibers are obtained from high performance PET woven selvages that are purchased from Chien Chen Textile, Taiwan. Low-melting-point polyester (LMPET) fibers (Far Eastern New Century, Taiwan)

have a fineness of 4D and a length of 51 mm. LMPET fibers are composed of a PET skin of a melting point of 110 °C and a regular PET core of a melting point of 265°C . It has good wrinkle resistance and shape retention, and has high strength and elastic recovery.



Figure 2.1 Recycled selvage and staple fibers. a-1) The left column shows the recycled Nomex®,(b-1) Kevlar®, and (c-1) PET selvage. The right column shows the (a-2) Nomex®, (b-2) Kevlar®, and (c-2) PET staple fibers.

2.2.2 Preparation of recycled staple fibers

These selvage fibers we used in this study were obtained by recycling the waste woven fabric selvage, and these recycled fibers are smooth staple fibers which has a length of 40 to 80 mm. These waste woven fabric selvages are still neat and keep a portion of the weave structure (as shown in Figure 1.6). Therefore, the first step was made these Recycled Nomex®, Kevlar®, and PET selvages are processed into staple

fibers using an opening machine, as seen in Figure 1 (b-2、c-2 and d-2). Then the recycled staple fibers were ready for making the recycled fabric.

2.2.3 Preparation of recycled fabric

The Nomex®, Kevlar®, and PET staple fibers are separately combined with LMPET fibers at ratios of 9:1, 7:3, and 5:5 to form nine types of recycled fabric by a needle punching machine (needle punching machine, SNP120SH6, Shoou Shyng Machinery Co., Ltd., New Taipei City, Taiwan) with a needle-punched speed of 200 needles/min and a line speed of 2.3 m/min. Then hot pressing treated at 130 °C at a speed of 0.2 m/min and hot pressure with 10 MPa (two-wheel hot press machine, CW-NEB, Chiefwell Engineering Co., Ltd., New Taipei City, Taiwan).

Samples are denoted as N9, N7, N5, K9, K7, K5, P9, P7, and P5 based on the proportion of recycled staple fibers. For example, N9 means Nomex®/LMPET ratio of 9:1; K5 means the Kevlar®/LMPET ratio is 5:5; and P7 means the PET/LMPET ratio is 7:3. The recycled fabric are thermally compressed at 130 °C and then evaluated for air permeability, tensile strength, tearing strength, and bursting strength.

Table 2.1 Denotation of recycled fabric.

Sample	Recycled staple fibers content (wt%)	LMPET Content (wt%)
P9	90	10
P7	70	30
P5	50	50
K9	70	10
K7	50	30
K5	50	50
N9	90	10
N7	70	30
N5	50	50

2.2.4 Test methods and standards

2.2.4.1 Air permeability

The air permeability of recycled fabric is measured using an air permeability tester (TEXTTEST FX3300) as specified in ASTM D737 (standard test method for air permeability of textile fabrics). Sample size is 25 cm × 25 cm. Ten samples for each specification are used for the measurement in order to have the mean.

2.2.4.2 Scanning electron microscopy (SEM) characterization

Recycled fabrics undergo trimming, vacuum drying, and metallizing, after which they are photographed and observed using an SEM (S-3000N, HITACHI, Japan).

2.2.4.3 Tensile strength test

As specified in ASTM D5035 (standard test method for breaking force and elongation of textile fabrics), the tensile strength of recycled fabrics is measured at a cross head tensile speed of 300 mm/min using an Instron 5566 (Instron, US). The distance between a pair of pneumatic clamps is 75 mm. Ten samples for each specification along the cross-machine direction (CD) and machine direction (MD) are used. Samples have a size of 25.4 mm x 180 mm.

2.2.4.4 Tearing test

The tearing strength of recycled fabrics is measured as specified in ASTM D5587 (standard test method for tearing strength of fabrics by trapezoid procedure). Samples are prepared according to the trapezoid method and have two equal altitudes and two parallel bases of 75 mm and 150 mm. The short base has a perpendicular cut with a length of 15 mm in the center. The distance between two clamps is 25 mm and the test rate is 300 mm/min. Ten samples for each specification along the CD and MD are used in order to have the mean.

2.2.4.5 Bursting strength test

As specified in ASTM D3787 (standard test method for bursting strength of

textiles—constant-rate-of-traverse (CRT) ball burst test), a universal tester (Instron 5566, Instron, US) that is equipped with a 25.4-mm-diameter hemispherical probe is used to measure the bursting strength of recycled fabrics at a rate speed of 100 mm/min. Ten samples (150 mm x 150 mm) for each specification are used and the maximum bursting strength is recorded.

2.3 Results and discussion

2.3.1 Areal density and air permeability

Figures 2.2 and 2.3 show the areal density and air permeability of recycled fabrics of N9, N7, N5, K9, K7, K5, P9, P7, and P5. Before the hot pressing process, P9 and P7 have an areal density of 180 g/m² and the other samples have an area density of 100±15 g/m². The distinctive differences in areal density between samples could be attributed to two factors. One is the fibers are all obtained from scattering the recycled selvages. The length and fineness of the fibers are changed due to the nonwoven process, and there are no specific and corroborated values of the processed fibers. Therefore, when composed of the same type of recycled fibers, the recycled fabrics have different base weights. The other is due to the addition of a lower melting point of polyester fiber in recycled fabric, which causes shrinkage during hot pressing. The shrinkage will result in different shrinkage based on the major fiber properties of recycled fabric. And according to the different intrinsic properties of Nomex®, Kevlar®, and PET fibers, including the smoothness, moisture content, and softness. The nonwoven process that involves opening and carding causes differences in the basis weight of webs.

Figure 2.3 shows the air permeability of the recycled fabrics. Comparing to the area density, the air permeability is inversely proportional to the area density. Theoretically, a high areal density implies a greater number of fibers, which decreases

the voids between fibers. Needle punching repeatedly entangles fibers that create friction among them, and provides the webs with a highly compact structure that prevents ventilation of air flows under the same gas flow pressure, resulting in low air permeability. In particular, when the hybrid composites are hot pressed, they exhibit thermal contraction. Hot pressing has a remarkable influence on the areal density and air permeability.

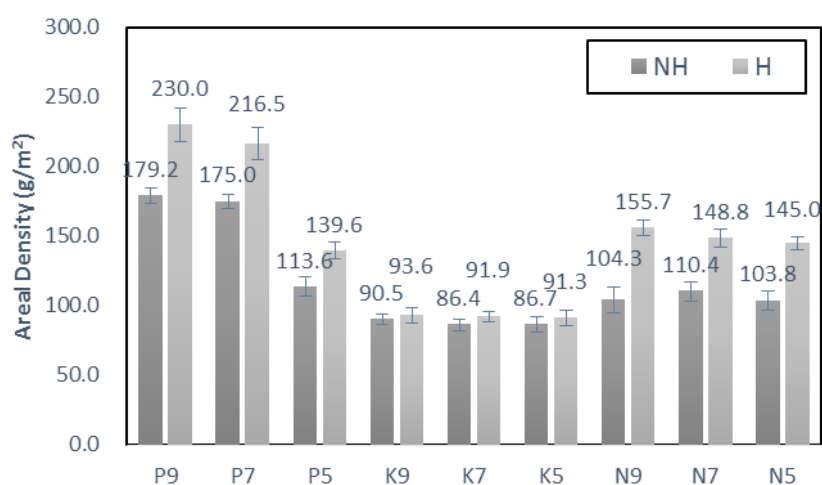


Figure 2.2 Areal density of recycled fabrics. “NH” means no heat treatment (i.e. the control group) and “H” means hot-pressed samples (i.e. the experimental group.)

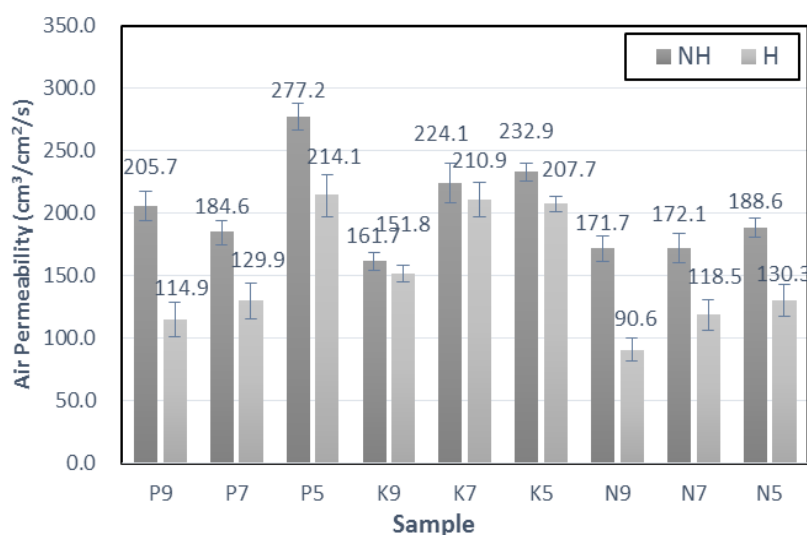


Figure 2.3 Air permeability of recycled fabrics. “NH” means no heat treatment (i.e. the control group) and “H” means hot pressed samples (i.e. the experimental group.)

2.3.2 Tensile strength

Figure 2.4 shows the tensile strength of recycled fabrics of N9, N7, N5, K9, K7, K5, P9, P7, and P5. The hot pressed samples have greater tensile strength, especially those composed of recycled PET staple fibers. As hybrid composites have Nomex®, Kevlar®, or PET recycled fibers as the prime composition, they have different base weights. The data collected from the tensile strength test are divided with their base weight as seen in Figure 2.5. The tensile strength of hybrid composites ranked from highest to lowest based on corresponding recycled fibers as Kevlar®, PET, and then Nomex®.

On the other hand, the tensile strength along the cross-machine direction (CD) is significantly higher than that along the machine direction (MD). The majority of fibers in the nonwoven fabrics are aligned along the CD, and the high orientation of fibers can efficiently disperse the force onto each fiber. In addition, needle punching enhances the friction among fibers, increasing the tensile strength of hybrid composites. In addition, the employment of hot pressing renders the hybrid composites with considerable melting points where the fibers cross or contact (as shown in Figure 2.6), thereby increasing the displacement of fibers (as shown in Figure 2.7) and increasing the friction among the fibers in the fabric. This distinctively improves the tensile strength along the CD and MD of the hybrid composites.

As far as the amounts of recycled Nomex®, Kevlar®, PET staple fibers are concerned, the tensile strength of hybrid composites show different trend base on the amount of LMPET fibers. For recycled Nomex® and Kevlar® staple fibers, when either of them is combined with more LMPET fibers, the hybrid composites have greater tensile strength. In contrast, for the recycled PET staple fibers, the hybrid composites have a lower tensile strength when they are composed of more LMPET

fibers. The recycled PET fibers are obtained from high-strength PET selvage, and thus have higher strength than LMPET fibers. Therefore, the combination of more LMPET fibers and less PET staple fibers leads to a decrease in the tensile strength of PET/LMPET hybrid composites. Conversely, recycled Kevlar® and Nomex® staple fibers have comparable strength to that of LMPET fibers, which facilitates the hybrid composites to disperse a force over fibers. As a result, the Kevlar®/LMPET and Nomex®/LMPET hybrid composites have greater tensile strength when they are composed of more LMPET fibers.

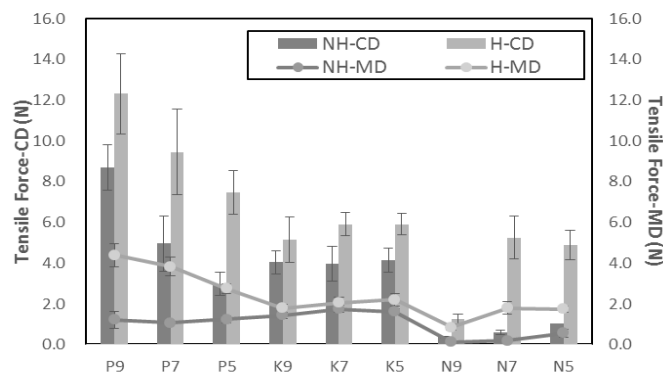


Figure 2.4 Tensile force along the CD and MD of recycled fabric. “NH-” means no heat treatment (i.e. the control group) and “H-” means hot pressed samples (i.e. the experimental group.) “CD” is the cross machine direction and “MD” is machine direction.

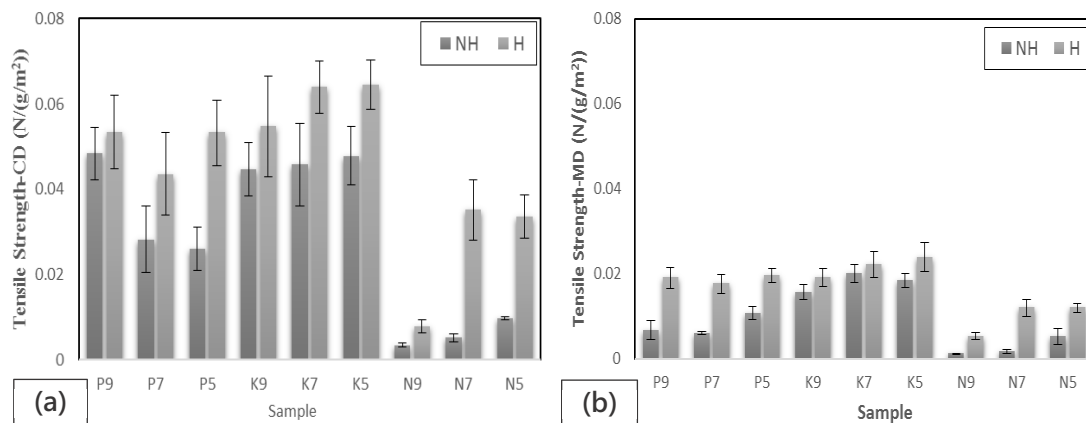


Figure 2.5 The tensile strength of recycled fabric along the (a) CD and (b) MD

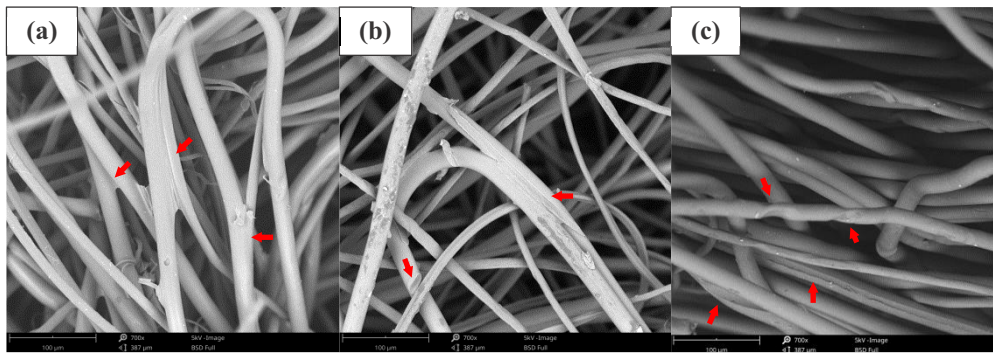


Figure 2.6 SEM images of thermal-bonding points in the recycled fabric of (a) K5 (b) N5 and (c) P5.

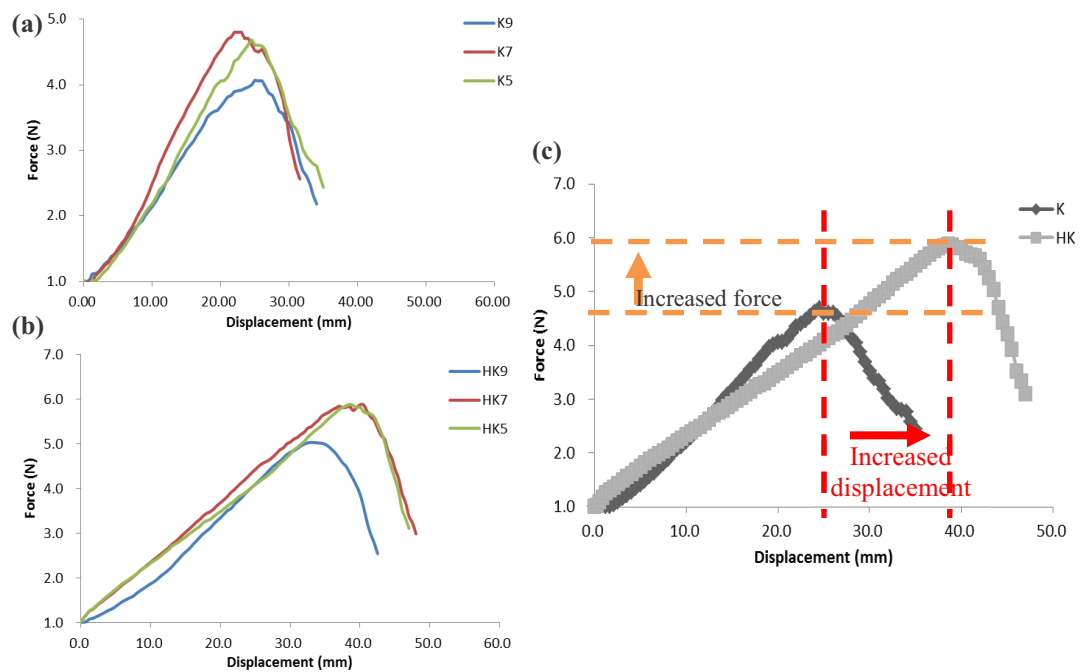


Figure 2.7 Force-displacement curve of recycled Kevlar[®] fabric-CD (a) without heat treatment (b) with heat treatment (c) data comparison of K9

2.3.3 Tearing test

The experimental groups are recycled fabrics that are processed with hot pressing, and the control groups are recycled fabrics that are not processed with hot pressing. Figure 2.8 shows the tearing strength of the experimental groups. When base weight is excluded from consideration, the hybrid composites made of recycled PET

staple fibers have the optimal tearing strength, especially P9, as seen in Figure 8 (b). For the control group, K9 has the optimal tearing strength.

During a tearing strength test, the notched cut of the samples is perpendicular to the CD, the direction that the majority fibers are aligned. Namely, the notched cut is parallel to the MD. The tearing force exerted by the tester needs to overcome the shear friction caused by the entangled fiber along the axis. The control groups that are composed of recycled Kevlar® staple fibers have the highest shear friction resistance. The experimental groups that are hot pressed have thermal bonding points caused by LMPET fibers, and the structure is stabilized without fiber displacement. Therefore, the experimental groups that are composed of recycled PET fibers are significantly reinforced, and have the highest tearing strength. However, the recycled Nomex® fibers have the lowest fiber strength, and regardless of whether it is the control group or experimental group, the hybrid composites made of recycled Nomex® fibers have the lowest tearing strength.

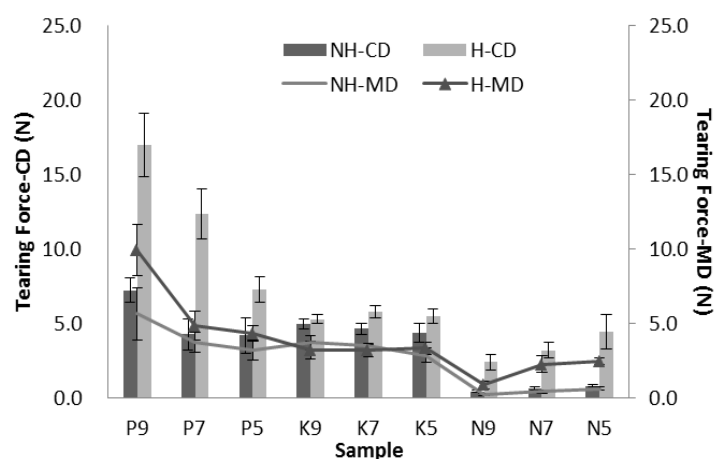


Figure 2.8 The tearing force of along the CD and MD of the recycled fabrics as related to the employment of hot pressing. “NH” means no heat treatment (i.e. the control group) and “H” means hot pressed samples (i.e. the experimental group.)

2.3.4 Bursting strength test

Figures 2.9 and 2.10 show the bursting strength performance of recycled fabrics. When base weight is excluded from consideration, for the experimental control groups, hybrid composites made of recycled PET fibers have better bursting strength (Figure 2.10), especially P9 (Figure 2.9). Among the control group, K9 has the maximum bursting resistance. A cylindrical burst punch head is used to punch the samples, the damage area of which starts to show remarkable deformation. The structure of hybrid composite falls apart following the presence of fiber displacement, deformation, the loss of fiber intertwined stress and friction, as well as the breakage of fiber, after which the punch head penetrates the sample eventually.

Kevlar® fibers have the feature of a high abrasion resistance. Thus, among the control groups, the hybrid composites composed of Kevlar® fibers have the highest bursting strength than those composed of recycled PET or Nomex® fibers. Noticeably, hot pressing does not improve the bursting strength of Kevlar®/LMPET hybrid composites, and the control and experimental groups of Kevlar®/LMPET hybrid composites have comparable bursting strength. Among the experimental and control group, the hot pressed PET/LMPET (9:1) hybrid composites (i.e. P9) have the highest bursting strength. The prime cause is the addition of LMPET fibers. LMPET fibers are melted and form the thermal bonding points, thereby reinforcing and stabilizing the structure of hybrid composites. In addition, according to the results of Figure 2.10, PET / LMPET has the best reinforcement after the same recycling and production process. The biggest difference in the hot pressing process is the thermal melting point formed by the high temperature and pressure in the composites fabric. It is formed by the melting of a lower melting point of polyester fibers and is attached between the fibers or between the intersections of the fibers. Therefore, the interface bonding force between the hot bonding point and the fiber will affect the mechanical

properties of the sample. The low melting point PET fiber and the recycled PET fiber are also one type of polyethylene terephthalate. Therefore, it is possible to have a better interface function to effectively transfer stress and achieve better mechanical property reinforcing the effect.

As a result, the recycled PET fibers thus can fully contribute high fiber strength and P9 outperforms the others in bursting resistance.

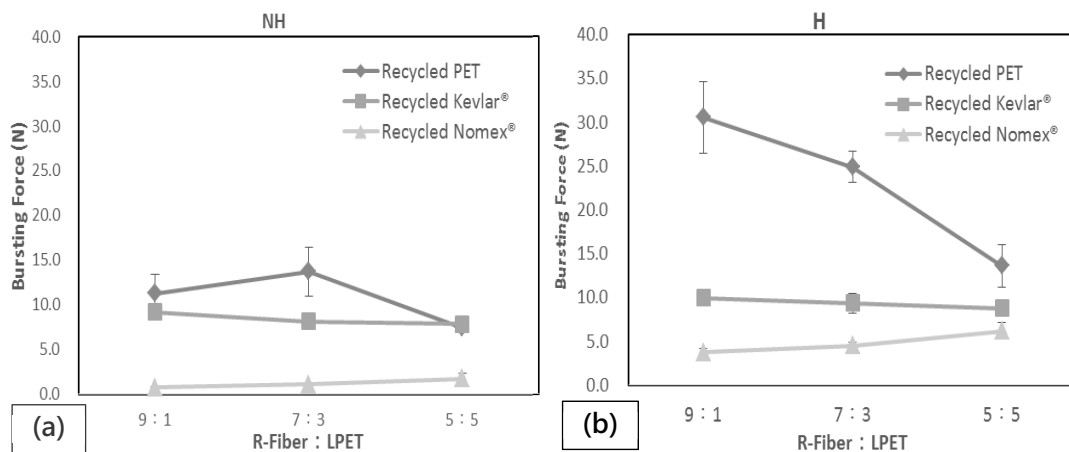


Figure 2.9 Bursting force of recycled fabrics that are processed (a) with or (b) without the heat treatment. “R- “stands for “recycled.” “NH” means no heat treatment (i.e. the control group) and “H” means hot pressed samples (i.e. the experimental group.)

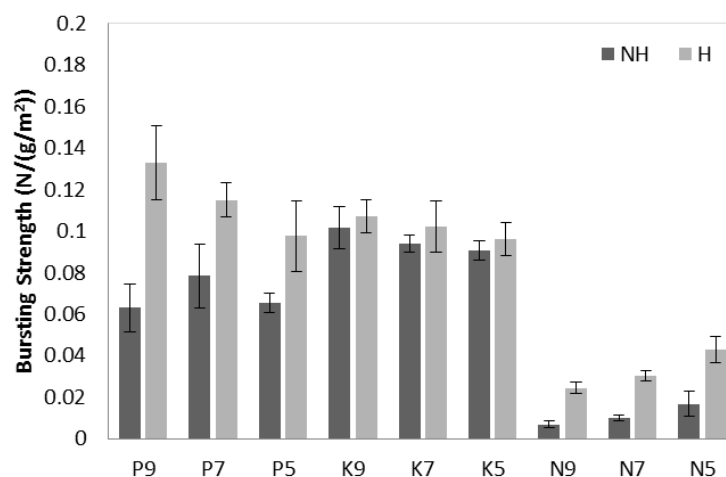


Figure 2.10 Bursting strength of recycled fabrics. “NH” means no heat treatment (i.e. the control group) and “H” means hot pressed samples (i.e. the experimental group.)

2.4 Conclusions

This study investigates the high-performance hybrid composites in terms of characterizations and mechanical properties based on the constituent recycled staple fibers. The eco-friendly manufacturing design uses high performance of recycled Nomex®, Kevlar®, and PET selvages. The recycled fibers take up 50, 70, and 90 wt% of the hybrid composites, and corresponding LMPET fibers account for 50, 30, and 10 wt%. When base weight is excluded from consideration, K9 of the control groups has the optimal mechanical properties before hot-press treatment, and after hot-press treatment the P9 of the experimental groups has the optimal mechanical properties. The satisfactory test results are ascribed to the high performance of the recycled staple fibers and the reinforcement of LMPET fibers. In particular, the combination of recycled PET fibers and LMPET fibers has a synergistic effect in stabilized structure and mechanical improvement. In this study, the influence of a specified temperature of hot pressing of 130 °C on different properties is discussed. On the other hand, the influences of hot pressing in terms of temperature and pressures of hot pressing are not discussed in this study, and thus provide opportunities for the future studies to carry on the further investigation examining whether these parameters are related to the reinforcement of high performance hybrid composites.

References

- [1] Bleetman A, Watson CH, Horsfall I, Champion SM, Wounding patterns and human performance in knife attacks: optimising the protection provided by knife-resistant body armour. *Journal of Clinical Forensic Medicine*, 2003, 10(4):243-248.
- [2] Decker MJ, Halbach CJ, Nam CH, Wagner NJ, Wetzzel ED, Stab resistance of

Chapter 2

- shear thickening fluid (STF)-treated fabrics, *Composites Science and Technology*, 2007, 65(3-4):565-578.
- [3] Jessie BMJ, Eric DW, Mahesh VH, Shaik J, Stab and puncture characterization of thermoplastic-impregnated aramid fabrics [J]. *International Journal of Impact Engineering*, 2009, 36(9): 1095-1105.
- [4] Termonia Y, Puncture resistance of fibrous structures, *International Journal of Impact Engineering*, 2006, 32(9):1512-1520.
- [5] Batista APMC, Tinô SRL, Fontes RS, Nóbrega SHS, Aquino EMF. Anisotropy and holes in epoxy composite reinforced by carbon/glass and carbon/aramid hybrid fabrics: Experimental and analytical results. *Composites Part B: Engineering*, 2017, 125:9-18.
- [6] Na W, Ahn H, Han S, Harrison P, Park JK, Jeong E, Yu WR, Shear behavior of a shear thickening fluid-impregnated aramid fabrics at high shear rate. *Composites Part B: Engineering*, 2016, 97:162-175.
- [7] Atif K, Usman A, Muhammad IR, Syed MZY, Syeda S, Riffat NM, Audil R. Principle component analysis of flue gas exhaust and health risk estimates for the population around a functional incinerator in the vicinity of Rawalpindi Pakistan. *Arabian Journal of Chemistry*. 10(2): s2302-2306, 2017.
- [8] Pope CA 3rd, Dockery DW. Health effects of fine particulate air pollution: lines that connect. *Journal of the Air & Waste Management Association*. 56(6):709-742, 2006.
- [9] Sukh S, Brian G, Richard S, Joy K, Jesse C, Michael D. Endocrine disrupting chemical emissions from combustion sources: diesel particulate emissions and domestic waste open burn emissions. *Atmospheric Environment*, 39(5):801-811, 2005.
- [10] Hadded A, Benltoufa S, Fayala F, Jemni A. Thermo physical characterisation of

Chapter 2

- recycled textile materials used for building insulating. *Journal of Building Engineering*, 5:34-40, 2016.
- [11] Hu YZ, Du CY, Leu SY, Jing HD, Li XT, Lin CSK. Valorisation of textile waste by fungal solid state fermentation: An example of circular waste-based biorefinery. *Resources, Conservation and Recycling*. 129:27-35, 2018.
- [12] Nunes LJR, Godina R, Matias JCO, Catalão JPS. Economic and environmental benefits of using textile waste for the production of thermal energy. *Journal of Cleaner Production*, 171(10):1353-1360, 2018.
- [13] Liu B, Zhu P, Xu AC, Bao L. Investigation of the recycling of continuous fiber-reinforced thermoplastics. *Journal of Thermoplastic Composite Materials*, doi.org/10.1177/0892705718759388, 2018.
- [14] Wan Y, Takahashi J. Tensile and compressive properties of chopped carbon fiber tapes reinforced thermoplastics with different fiber lengths and molding pressures. *Composites: Part A*, 87:271–281, 2016.

CHAPTER 3

Hybrid-fiber-reinforced composite boards made of recycled aramid fibers: preparation and puncture properties

3.1 Introduction

Primitives used barks and hides to make their garments, which were shabby but considered the early known protective cloth in that regard. Protective cloth is composed of a diversity of materials, from barks, hides, leather, metal, to composite materials. The advancing technical development also expedites different demands of industrial fields for innovative materials of protective clothing. Protective materials or armors are made by different requests, as in warm wear, thermally insulating suit, fire resistant suit, UV-cut suit, and water-proof suit [1-5]. Specifically, people are most concerned about the safety protection at work and outdoors. The stab resistance is the superior concern when producing industrial protective materials, packaging materials or wearing textile used in protective clothing, protective gloves, and engineering shoes [6,7]. At first, people used rigid materials such as metal plates or ceramic plates to resist puncture attacks, but they were bulky and heavy [7,8]. The impact resistance and flexible geometry of flexible textile composite materials have made them favorable materials for both military and civil protective applications. The design of this study belongs to the flexible composite materials. It is formed by the lamination of multiple layers of fabric. The strength of the flexible textile composite materials is weaker than that of the general fiber reinforcement composite. However, due to its softness, it is easy to process into various products or as a reinforcing material for secondary recombination. And due to its flexible, it is easy to process into various products or as a reinforcing material for secondary recombination [7-9]. For example, shear thickening fluid (STF) has been one of the most popular flexible stab resistant material. It was long developed by the U.S. army research laboratory in order to protect and provide the soldiers with a liquid bulletproof material [10-12]. But there are some studies proved that it was the particles of the STF that increased the friction between the yarns of fabrics, thereby improving the stab resistance [13]. Regardless of

Chapter 3

the types of stab resistant materials, the generated friction is the major factor for the stab resistance.

The manufacturers produce increasingly demanded protective textiles, consuming a large volume of protective fibers and fabrics. Subsequently, there is considerable waste of high strength fabrics. To discard the high performance textile waste by means of direct disposal, burning, or the use as fillers seems rather a pity. Recycling can save resources and energy. Various technologies have been developed so far, mainly focused on reinforcing fibers and have not yet been commercialized. The main recycling methods can be divided into mechanical recycling, heat recovery and chemical recycling [14,15]. Improperly discarded waste increases the possibility of emitting carbon dioxide or toxic gas which is a burden to the environment [16-18]. In response, people increasingly pay more attention to the recycle and reclamation techniques and related studies [19-21]. For example, high strength uni-directional fabrics or woven fabrics are trimmed or scattered and then produced into reinforcing materials [22]. Or re-using the para-aramid fiber as a mechanical reinforcement in the polyamide 6.6 (PA66) matrix [8].

Aramid fiber is mainly used as a protective material, it is widely used in various fields. Because the aramid fiber usually has a significant performance degradation under UV light. Therefore, the outer layer is usually covered with a protective material during use. These protective products will be phased out after the end of their useful life. However, the high modulus fibers used in these protective products may only be slightly damaged. Therefore, we believe that an efficient recycling process and design can re-add new value to the material. Therefore, this study focuses on the recycling technique of aramid fabrics with a premise of minimizing the damage to the fibers. The main purpose of this study was to recover the Selvage of high modulus woven fabrics in a one-step method using a non-woven process. The long strip of

waste selvage is broken into short fibers and directly formed into a non-woven fabric. The main difficulty is to achieve a highly efficient recycling process. The waste aramid fibers are reclaimed to make high-performance fibers with a relatively much lower cost, thereby replacing the demands of using expensive resources of raw materials. Moreover, recycling the textile waste is environmentally protective in terms of the reduction of waste water, waste heat, and exhaust gas, making the development of protective materials more feasible and with more advantages in the industrial and livelihood protection fields.

3.2 Experimental

3.2.1 Materials

Recycled aramid staple fibers (Kevlar®-K129, Kevlar®-K29, DuPont, USA) have a length of 40-65 mm and fineness of 2820 D and 1000 D, and are obtained from the recycled aramid selvages (recycled Kevlar® woven selvage) that are purchased from Formosa Taffeta, Taiwan). And the woven fabric sealed edge was weaving with a general cotton yarn. In the recycling process of waste woven selvage, the cotton sealed edge will be broken directly by the force of mechanical striking to achieve better recovery efficiency. Low-melting-point PET (LMPET) staple fibers (Far Eastern New Century, Taiwan) have a fineness of 4 D and a length of 51 mm, and are composed of a skin-core structure. The melting points of the skin and core are 110 °C and 265 °C. Aramid woven fabrics are purchased from Jinsor-Tech Industrial Co., Taiwan. Figure 3.1 shows the images of the materials whose mechanical properties are shown in Table 3.1.

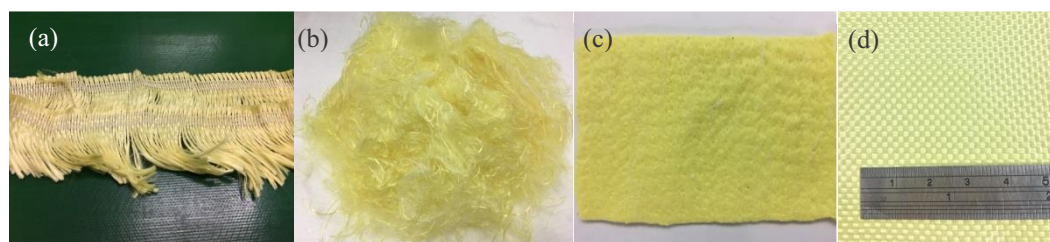


Figure 3.1 Images of the a) aramid selvage, b) aramid staple fibers, c) aramid composite matrix and d) aramid woven fabrics.

Table 3.1 Physical and mechanical properties of aramid woven fabric

Fabrics	Fineness (D)	Basis Weight (g/m ²)	Thickness (mm)	Density (/inch)	Modulus (GPa)
Aramid woven fabric	1000	180	0.31	28 × 28	4.76
Recycled Aramid matrix	2~3	120	2	-	-
LMPET matrix	4	150	2	-	-

3.2.2 Preparation of aramid composite matrices

Because the recycled aramid fiber used in this study is the waste selvage of the woven fabric. It is different from the fiber type of short fibers generally used for non-woven fabrics. In general, short fibers for non-woven fabrics are wavy or crimp in order to increase the friction. However, the woven fabric is woven using long yarns and has no wavy or crimp fiber form. In addition, the surface of the recycled aramid fiber is very smooth, thus causing uneven distribution of fibers in the nonwoven fabric. In the study, after considering the subsequent process design, some low-melting PET fibers were selected for the process. Increase the friction between the recovered aramid fiber and the machine, and distribute the low-melting PET fiber in the recycled aramid fiber for heat treatment in subsequent research.

Recycled aramid staple fibers (recycled Kevlar® woven selvage) and LMPET fibers at ratios of 9:1, 7:3 and 5:5 are made into recycled aramid matrices, which are denoted as K9, K7, and K5. And, The LMPET matrix is made by using pure LMPET

fibers. The basic weight of LMPET matrix is approximately 150 g/m^2 . Because the melting point of the LMPET fiber is lower than that of the aramid fiber, it is compounded as an adhesive layer between the recycled aramid matrices and the aramid woven fabric. Two aramid matrices are used as the top and bottom layers and two LMPET matrices are used as the interlayer of a sandwich. The combinations are needle punched to form aramid composite matrices, and serve as the control group (hereafter referred as “C”). Then, one batch of the aramid composite matrices is hot pressed (hereafter referred as “HC”). Figure 3.2 shows the manufacturing process.

3.2.3 Preparation of hybrid-fiber-reinforced composite boards

The composite boards are made of five layers, including an aramid matrix, an LMPET matrix, and an aramid woven fabric, an LMPET matrix, and an aramid matrix. Namely, the composite boards are actually aramid composite matrices with an additional aramid woven fabric as the interlayer. The five layers are needle punched to form hybrid-fiber-reinforced composite boards (hereafter referred as “B”). Then, one batch of the composite boards is hot pressed (hereafter referred as “HB”).

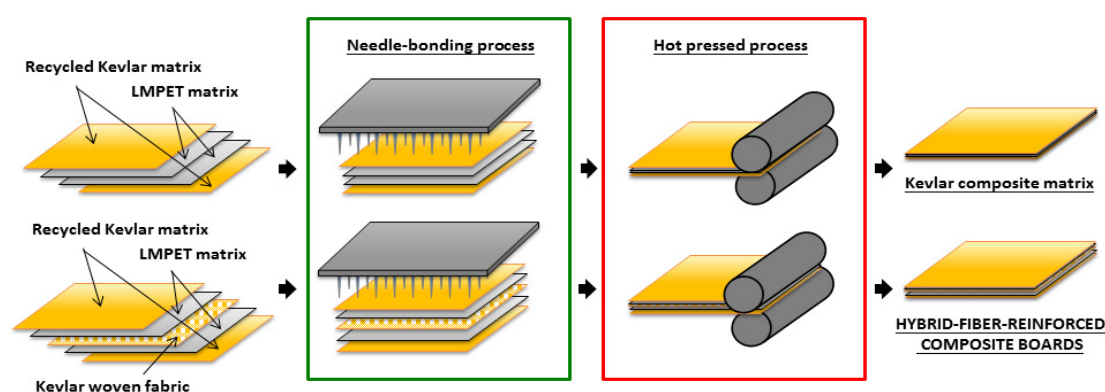


Figure 3.2 Schematic diagrams of aramid composite matrix and hybrid-fiber-reinforced

Table 3.2 Sample named and code of this study

Named	R-aramid content (wt%)	LMPET content (wt%)	Code	Hot pressed	Reinforcing layer
K9	90	10	C	No	No
K7	70	30	HC	Yes	No
K5	50	50	B	No	Yes
			HB	Yes	Yes

3.2.4 Test methods and standards

3.2.4.1 Scanning electron microscopy (SEM) characterization

High-performance aramid composites matrices undergo trimming, vacuum drying, and metallizing, after which they are photographed and observed using an SEM (S-3000N, HITACHI, Japan).

3.2.4.2 Tensile strength

As specified in ASTM D5035, the tensile strength of aramid composite matrices is measured at a cross head tensile speed of 300 mm/min using an Instron 5566 (Instron, US). The distance between a pair of pneumatic clamps is 75 mm. Samples for each specification along the cross-machine direction (CD) and machine direction (MD) are used. Samples have a size of 25.4 mm x 180 mm.

3.2.4.3 Tearing strength

The tearing strength of high-performance hybrid-fiber-reinforced composite boards is measured as specified in ASTM D5587. According to the trapezoid method, samples have two equal altitudes and two parallel bases of 75 mm and 150 mm. The short base has a perpendicular cut with a length of 15 mm in the center. The distance between two clamps is 25 mm and the test rate is 300 mm. Samples for each specification are taken along the CD and MD in order to have the mean.

Chapter 3

3.2.4.4 Air permeability

The air permeability of high-performance hybrid-fiber-reinforced composite boards is measured using an air permeability tester (TEXTTEST FX3300) as specified in ASTM D737 (Standard Test Method for Air Permeability of Textile Fabrics). Sample size is 25 cm × 25 cm. Samples for each specification are used for the measurement in order to have the mean.

3.2.4.5 Bursting strength

As specified in ASTM D3787, a universal tester (Instron 5566, Instron, US) that is equipped with a 25.4-mm-diameter hemispherical probe is used to measure the bursting strength of high-performance hybrid-fiber-reinforced composite boards at a rate speed of 100 mm/min. Samples (150 mm x 150 mm) for each specification are used and the maximum bursting strength is recorded.

3.2.4.6 Static puncture resistance

An Instron 5566 (Instron, US) is used to measure the static puncture resistance of the samples as specified in ASTM F1342 (standard test method for protective clothing material resistance to puncture). The acicular punch damages the samples with a constant speed of 508 mm/min, and the maximum applied force is recorded. Ten samples for each specification are taken and samples have a size of 100 mm × 100 mm.

3.3 Results and discussion

3.3.1 Effect of hot pressing on tensile strength of aramid composite matrices

Employing hot pressing improves the tensile strength of the aramid composite matrices to different extents (Figure 3.3). The difference in the tensile strength is due to LMPET fibers, the skin of which melts to form thermal bonding points that bond the fibers in vicinity as shown in the SEM image (Figure 3.4). The

thermal bonding points prevent the fibers from slipping and increase the friction between fibers. As a result, the presence of thermal bonding points increases the tensile strength regardless of the directions. Moreover, the tensile strength along the cross-machine direction (CD) is higher than that along the machine direction (MD). CD has a greater fiber orientation (the direction that the majority of fibers are arranged along), allowing the tensile force to be efficiently dispersed. In the meantime, the recycled aramid fibers aligned along the MD are also rearranged to be perpendicular to the fibers along the CD, which causes the fibers to slip and the aramid composite matrix to deform. Therefore, the aramid composite matrices have greater tensile strength along the CD. The test results show that for the hot-compressed aramid composite matrices, the greater the content of LMPET fibers, the higher the tensile strength.

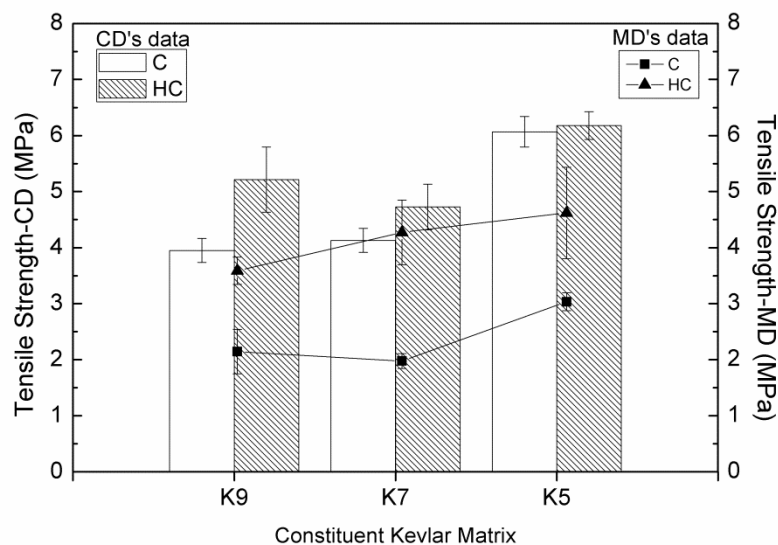


Figure 3.3 Tensile strength of recycled aramid composite matrices as related to the employment of hot pressing.

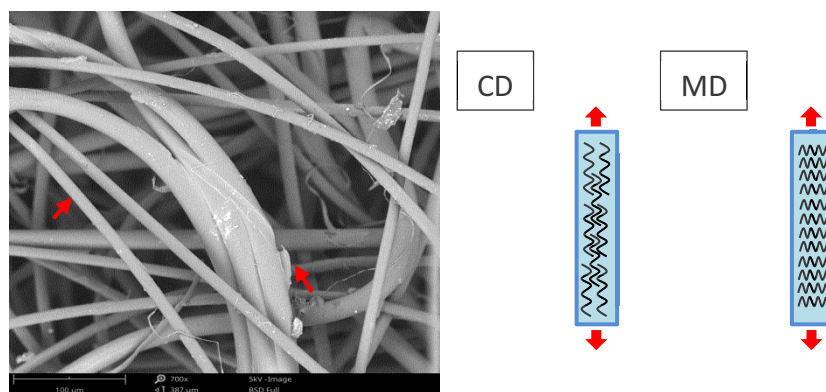


Figure 3.4 SEM images and schematic diagrams of the drawing mechanism of tensile strength.

3.3.2 Effect of hot pressing on tearing strength of aramid composite matrices

Figure 3.5 shows the tearing strength of the hot pressed aramid composite matrices, which displays the same trend as their tensile strength. Aramid composite matrix containing K5 has the maximum tearing strength as it contains the most of LMPET fibers. Like tensile strength, the tearing strength along the CD is also higher than that along the MD. The reason is the same as that mentioned previously in the section of tensile strength. Namely, the major factor for this result is also the high fiber orientation. Unlike the control group (C), the hot-pressed aramid composite matrices (HC) have tearing strength that shows a declining trend. Samples are cut with an opening beforehand. The tester needs to overcome the shear friction created by the axial fiber entanglement. Hot pressing provides the aramid composite matrices with thermal bonding points, though highly reinforcing the structure but limiting the elastic deformation of fibers. Despite having a lower strength than aramid fibers, LMPET fibers make good compensation for both the tensile strength and tearing strength. As a result, HC has the optimal tearing strength when being composed of the greatest amount of LMPET fibers.

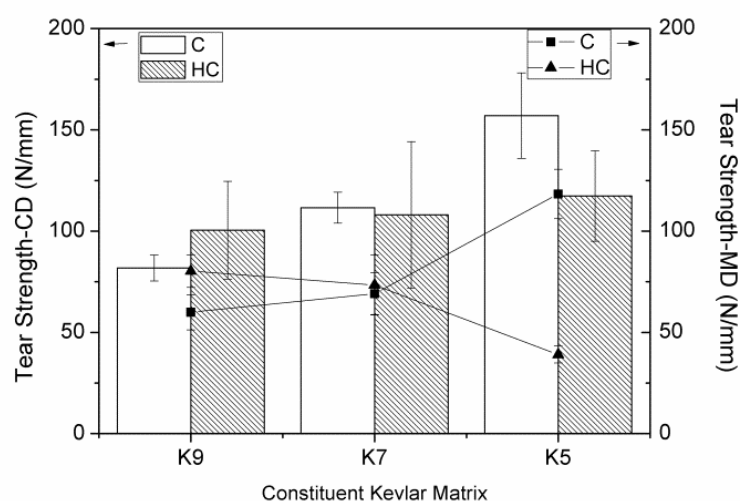


Figure 3.5 Tearing strength along the CD and MD of aramid composite matrices as related to the employment of hot pressing.

3.3.3 Tensile and tearing strengths of hybrid-fiber-reinforced composite boards

Figures 3.6 (a and b) show the tensile strength result and force-displacement curve tearing strength of C, HC, B, and HB. Figures 3.7 show the tearing strength result of C, HC, B, and HB. With containing an aramid woven fabric as the interlayer, B has distinctively improved tensile strength and tearing strength. The tensile strength of B is 5 times greater than that of C, while its tearing strength is 8.5 times greater than that of C. The employment of hot pressing enhances the properties even more. Comparing to HC, HB has 7 times greater tensile strength and 12 times greater tearing strength. B and HB consist of an aramid woven fabric that is made of filaments. Woven fabrics have higher intrinsic strength than nonwoven fabrics made of staple fibers. Hence, aramid woven fabric plays an important role in reinforcement. Likewise, the LMPET matrix further increases the tensile and tearing strength with the help of hot pressing. The skin of LMPET fibers melts into polymer solution that solidifies and becomes thermal bonding points between the filaments of woven fabrics and the staple fibers of nonwoven fabrics, firmly securing the structure of the

Chapter 3

composite boards.

In addition, usually samples with higher LMPET fiber content should have better mechanical strength after hot pressing. Because some of the fibers are fixed by the molten fibers after the hot pressing treatment. This can reduce fiber slip and thus increase fabric strength. However, the strength of the bond point is lower than that of the recovered Kevlar® fiber and the relative recovered Kevlar® fiber content is reduced as the LMPET fiber content is higher. The strength of the composite board with the increased bond point is less than the strength lost due to the reduced content of the recovered aramid fiber. Therefore, the tensile strength and tear strength of the sample B (K5) were higher than the tensile strength and tear strength of the sample HB (K5).

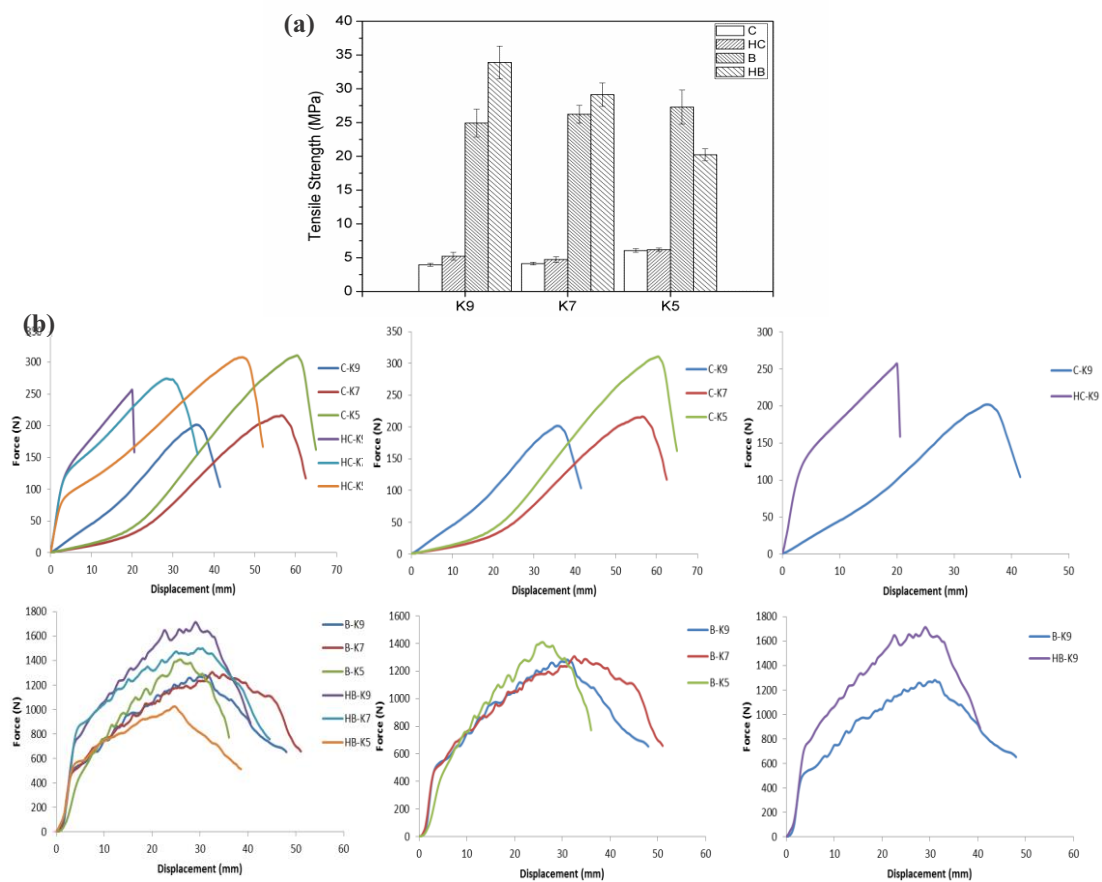


Figure 3.6 (a) tensile strength and (b) force-displacement curve of hybrid-fiber-reinforced composite boards.

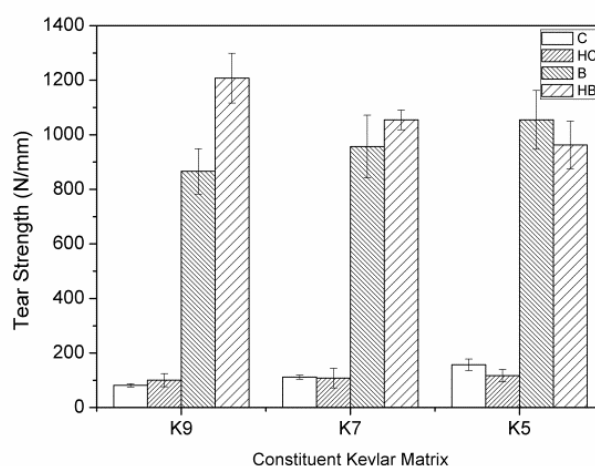


Figure 3.7 Tearing strength of hybrid-fiber-reinforced composite boards.

3.3.4 Air permeability of aramid composite matrices and hybrid-fiber-reinforced composite boards

Figure 3.8 shows the air permeability of the aramid composite matrices (C, HC) and the composite boards (B, HB) as related to the employment of hot pressing. The composite board has higher air permeability when its constituent aramid matrix contains a greater amount of LMPET fibers. This result is ascribed to the difference in the fineness and friction coefficient between LMPET and aramid fibers, which impacts the evenness of the two fibers during the carding process. LMPET fibers have a greater fineness, and are thicker than aramid fibers. When the unit mass is identical, there are a less number of LMPET fibers than there are aramid fibers. A greater number of fibers relatively render the composite boards with a complex structure and a smaller size of pores. Namely, the LMPET fibers form a relatively larger pore size, which in turn provides B with higher air permeability.

Moreover, the air permeability of the composite boards decreases as a result of employing hot pressing. Because the prior needle punching process entangles a greater amount of fibers, and the friction between fibers is strengthened, creating a

compact web structure. Afterwards, hot pressing melts the skin of LMPET fibers and thermally bonds the fibers where they cross, during which the thermal bonding points may form flakes involving more jointed fibers. Subsequently, HB is featured with pores overcoming a high blocking possibility, which adversely impact the air permeability.

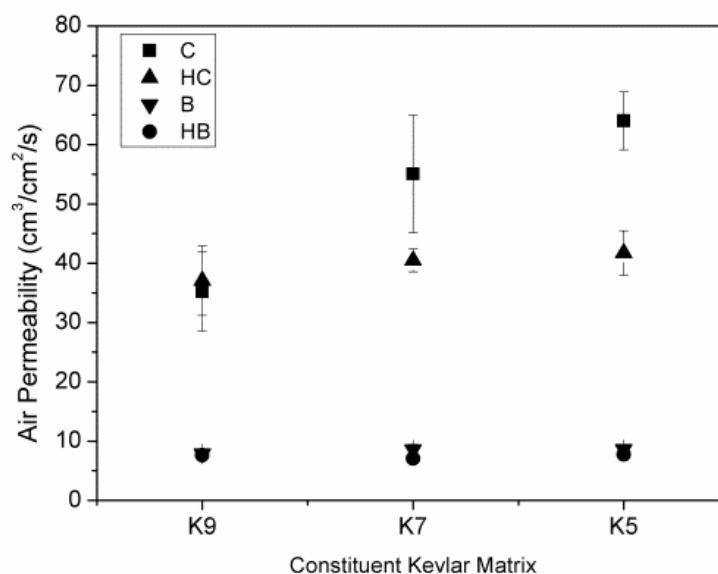


Figure 3.8 Air permeability of aramid composite matrices and hybrid-fiber-reinforced composite boards.

3.3.5 Bursting strength of aramid composite matrices and hybrid-fiber-reinforced composite boards

Figure 3.9 shows the bursting strength of the aramid composite matrices (C, HC) and composite boards (B, HB) as related to the employment of hot pressing. There is a distinctive raise in bursting strength of the composite boards (B)—the bursting strength of B is 2 to 3 times that of C. For the bursting strength test, a cylindrical burst punch head is used to damage the samples. Instead of expelling the fibers, the punch head distorts and deforms the sample conspicuously, debilitating the friction against the entangled fibers and exerting displacement and deformation on the samples until

the fibers fracture and the punch head penetrates the samples. In particular, B that is composed of K7 as the aramid matrix has the maximum bursting strength.

HB has thermal bonding points as a result of hot pressing, after which fibers are highly inhibited from slipping. In this case, the composite boards are strengthened. In the bursting strength test, B has higher bursting strength than HB. The bursting force can be dissipated by means of deformation of composite boards and the slipping of fibers, which are two efficient ways to release the stress energy. The punch head has a bigger diameter, and the deformation of composite boards thus have greater influence than the slipping of fibers. By contrast, HB is hot pressed composite boards whose thermal bonding points hinder the deformation. As a result, B has a higher bursting strength than HB. Specifically, B that containing K7 as the aramid matrix has the greatest bursting strength.

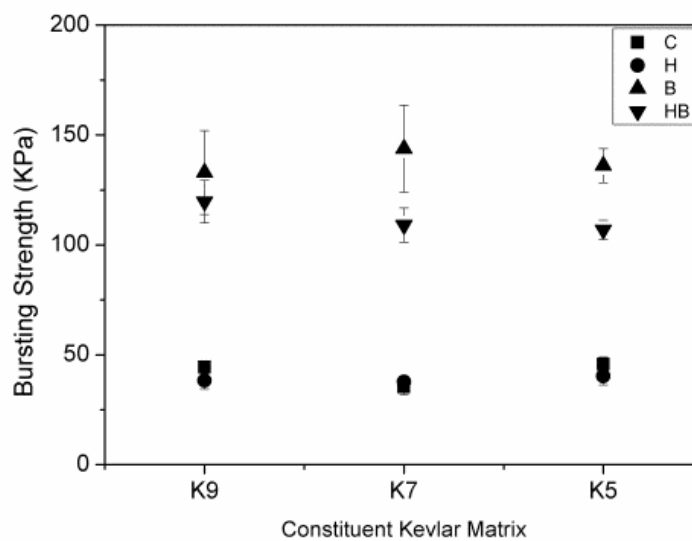


Figure 3.9 Bursting strength of aramid composite matrices and hybrid-fiber-reinforced composite boards.

3.3.6 Static puncture resistance of aramid composite matrices and hybrid-fiber-reinforced composite boards

Figure 3.10 shows the static puncture resistance of the aramid matrices (C, HC) and composite boards (B, HB) as related to the employment of hot pressing. The static puncture resistance-displacement (SD) curves of aramid composite matrices are displayed in Figure 3.11. Moreover, Figure 3.12 shows the SD curves of C, HC, B, and HB that have K9 as the specified constituent aramid matrix.

The composite boards have a compact plain structure and thermal bonding points which are a result of the hot pressing. The two features can effectively decrease the slipping of fibers and increase the friction of fibers against the penetration of the pointed punch (Figures 3.10 and 3.11). During the constant rate puncture test, when the puncture head starts to contact the sample, the puncture resistance value is slowly increased. As the penetration depth increases, the sample is gradually tightened and the puncture resistance value is rapidly increased. At the same time, the puncture opening on the sample gradually increases with the puncture depth and the tip end of the puncture needle. When the tip size of the puncture needle reaches the limit, the puncture resistance value reaches the highest and then decreases rapidly. At this time, only the frictional resistance of the sample and the surface of the puncture needle remain. In addition, Figure 3.12 shows that HC and HB both have a lower deformation than C and B, indicating that the compact plain structure and the melted LMPET fibers prohibit the slipping of fibers. By contrast, an excessive amount of LMPET fibers mean that there is relatively less aramid fibers in the matrices, which adversely influence the puncture and shear resistances exemplified by B and HB. Specifically, HB that contains K9 as the aramid matrix has the maximum static puncture resistance.

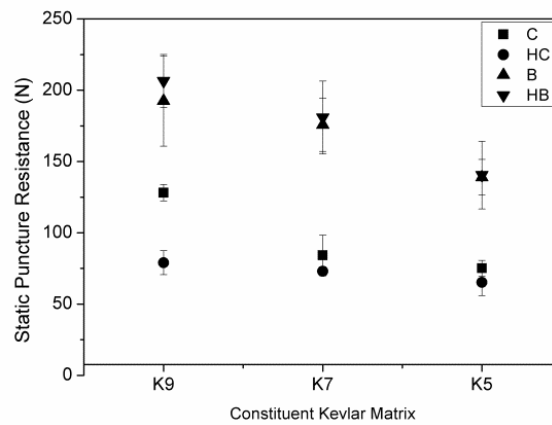


Figure 3.10 Static puncture resistance of aramid composite matrices and hybrid-fiber-reinforced composite boards.

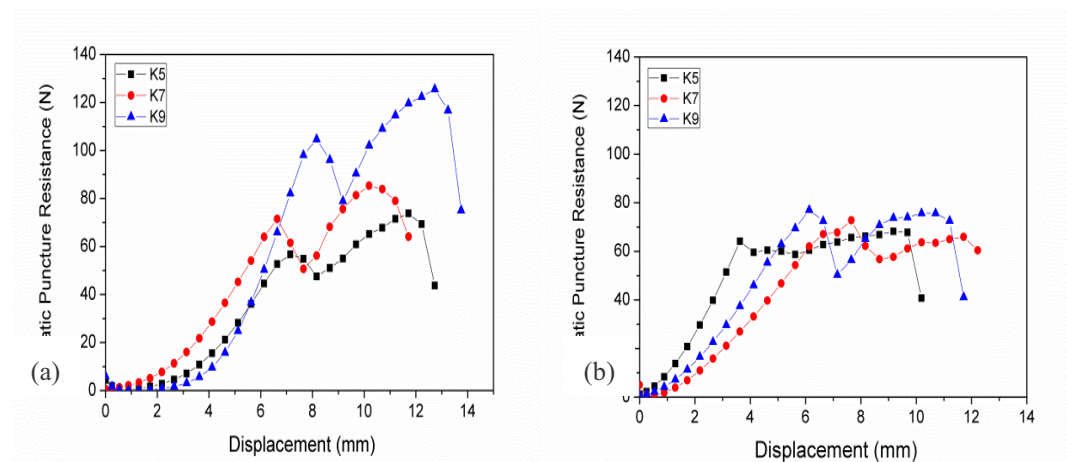


Figure 3.11 Static puncture resistance-displacement curves of a) non hot-pressed and b) hot-pressed aramid composite matrices.

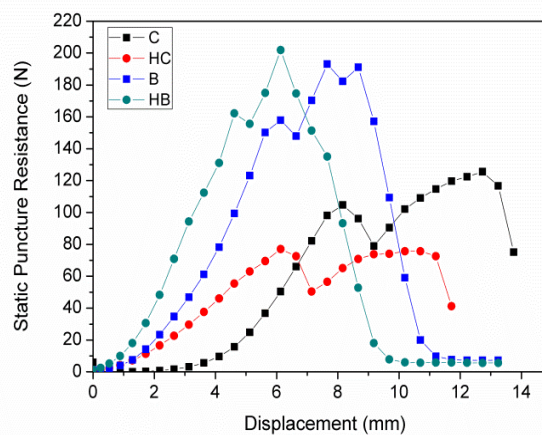


Figure 3.12 Static puncture resistance-displacement curves of aramid composite matrices and hybrid-fiber-reinforced composite boards as related to the employment

of hot pressing. C, HC, B, and HB are made of a specified aramid matrix of K9.

3.4 Conclusions

This study investigates the performance of hybrid-fiber-reinforced composite boards made of recycled aramid composite matrices, LMPET matrices, and aramid woven fabrics, which are laminated, needle punched and hot pressed. The test results show the tensile strength of B is 5 times greater than that of C, while its tearing strength is 8.5 times greater than that of C. The employment of hot pressing enhances the properties even more. Comparing to HC, HB has 7 times greater tensile strength and 12 times greater tearing strength. And the HB containing K9 as the aramid matrix have the optimal static puncture resistance, and the major factors are the compact plain woven structure and LMPET fibers. Hot pressing gives rise to the presence of thermal bonding points, which hampers the slipping of aramid and LMPET fibers, secures the structure, and increases the friction of fibers against the powerful punch. As a result, the hybrid-fiber-reinforced composite boards with K9 (an aramid matrix containing 90 % of aramid fibers) have the optimal static puncture resistance.

References

- [1] Francesco F. Water vapor transport in carbon nanotube membranes and application in breathable and protective fabrics. *Current Opinion in Chemical Engineering*. 2017; 16:1-8.
- [2] Bartkowiak G, Dabrowska A, Marszalek A. Assessment of an active liquid cooling garment intended for use in a hot environment. *Applied Ergonomics*. 2017; 58 : 182-189.
- [3] Małek E, Miedzińska D, Stankiewicz M. Heat resistance research and surface analysis of fireproof textile with titanium silicide coating. *Procedia Structural*

- Integrity. 2017; 5:508-515.
- [4] M.C. Silva-Santos, M.S. Oliveira, Giacomini, A.M.; Laktim, M.C.; Baruque-Ramos, J. Flammability on textile of business uniforms: Use of natural fibers. *Procedia Eng.* 2017. 200: 148-154.
- [5] Y. Xu, J. Sheng, X. Yin, J. Yu, B. Ding, Functional modification of breathable polyacrylonitrile/polyurethane/TiO₂ nanofibrous membranes with robust ultraviolet resistant and waterproof performance. *J. Colloid Interface Sci.* 2017. 508: 508-516.
- [6] Y. Termonia, Puncture resistance of fibrous structures. *International Journal of Impact Engineering.* 2006. 32:1512-1520.
- [7] Q.S. Wang, R.J. Sun, X. Tian, M. Yao, Y. Feng, Quasi-static puncture resistance behaviors of high-strength polyester fabric for soft body armor. *Results in Physics.* 2016. 6:554-560.
- [8] L. Loureiro, V. H. Carvalho, S. H. P. Bettini, Recycle of p-aramid from industrial waste as reinforcement fiber in, polyamide 6.6 *Polym. Test.* 2016, 56: 124-130.
- [9] C.C. Yang, T. Ngo, P. Tran, Influences of weaving architectures on the impact resistance of multi-layer fabrics, *Mater. Design* 2015, 85: 282–295.
- [10] Barnes HA. Shear-Thickening ("Dilatancy") in Suspensions of Nonaggregating Solid Particles Dispersed in Newtonian Liquids. *J. Rheol.* 1989; 33 (2):329.
- [11] Egres Jr. RG, Halbach CJ, Decker MJ, Wetzel ED, Wagner NJ. Stab performance of shear thickening fluid (STF)–fabric composites for body armor applications. *SAMPE 2005: New Horizons for Materials and Processing Technologies.* 2005.
- [12] Decker MJ, Halbach CJ, Nam CH, Wagner NJ, Wetzel ED, Stab resistance of shear thickening fluid (STF)-treated fabrics. *Composites Science and*

Chapter 3

- Technology. 2007; 67:565-578.
- [13] Bao LM, Sato S, Wang YL, Wakatsuki K, Morikawa H. Development of Flexible Stab-proof Textiles Impregnated with Microscopic Particles, *Journal of Textile Engineering*. 2017; 63(2):43-48.
- [14] Géraldine Oliveux, Luke O. Dandy, Gary A. Leeke, Current status of recycling of fibre reinforced polymers: Review of technologies, reuse and resulting properties, *Progress in Materials Science* 2015, 72: 61–99.
- [15] Y.X. Yang, R. Boom, B. Irion, D.V. Heerden, P. Kuiper, H.D. Wit, Recycling of composite materials, *Chemical Engineering and Processing* 2012, 51:53– 68.
- [16] Sidhu S, Gullett B, Striebich R, Klosterman J, Contreras J, DeVito M. Endocrine disrupting chemical emissions from combustion sources: diesel particulate emissions and domestic waste open burn emissions. *Atmospheric Environment*. 2005; 39(5):801-811.
- [17] Kamal A, Ali U, Ramay MI, Younis SMZ, Sumbal S, Malik RN, Rashid A. Principle component analysis of flue gas exhaust and health risk estimates for the population around a functional incinerator in the vicinity of Rawalpindi Pakistan. *Arabian Journal of Chemistry*. 2017; 10(2): s2302-2306.
- [18] C. A. Pope III, D. W. Dockery, Health effects of fine particulate air pollution: lines that connect, *J. Air Waste Manage. Assoc.*, 56(6), 709 (2006).
- [19] Y. Z. Hu, C. Y. Du, S. Y. Leu, H. D. Jing, X. T. Li, C. S. K. Lin, Valorisation of textile waste by fungal solid state fermentation: An example of circular waste-based biorefinery. *Resources. Resour. Conserv. Recycl.*, 129, 27 (2018).
- [20] A. Hadded, S. Benltoufa, F. Fayala, A. Jemni, Thermo physical characterisation of recycled textile materials used for building insulating. *Journal of Building Engineering*, 5, 34 (2016).
- [21] Nunes LJR, Godina R, Matias JCO, Catalão JPS. Economic and environmental

Chapter 3

benefits of using textile waste for the production of thermal energy. *Journal of Cleaner Production*, 171(10):1353-1360, 2018.

- [22] B. Liu, P. Zhu, A. Xu, L. Bao, Investigation of the recycling of continuous fiber-reinforced thermoplastics, *J. Thermoplast. Compos. Mater.* 2019, 32(3): 342-356.

CHAPTER 4

Mechanical and static stab resistant properties of hybrid-fabric fibrous planks: manufacturing process of nonwoven fabrics made of recycled fibers

4.1 Introduction

In recent years, fibrous and textile products are applied to many other fields than garments and decoration. Due to the flexibility, light weight, and easy process, they can be easily combined with other materials. In addition to the intrinsic properties, they can also yield other required properties via the employment of different organizational structures and manufacturing processes. Hence, fibrous and textile materials have a great diversity of applications, from domestic and industrial purposes to custom-made special functionality requests. The amounts of selvages and textile wastes increase as a result of the manufacturers producing increasingly demanded protective textiles, including some high price, high strength, and high modulus fibrous materials. In the production of weaving fabrics, due to the limitations of the machine and the quality of the product, the width of the fabric usually produced must be slightly larger than the actual required width. Therefore, almost all fabrics need to be cut and then sold. A large amount of discarded cloth selvages are produced in the process. On the other hand, these protective products will be phased out after the end of their useful life. However, the high modulus fibers used in these protective products may only be slightly damaged. It will be a pity to just discard or burn these materials or use them as fillers [1], especially the materials that are left after the production of protective products [2, 3]. Moreover, protective products with expired service life may be discarded when the constituent high modulus fibers are slightly damaged. Hence, a highly efficient recycling and reclaiming design can process the materials to have new additive values.

Recycling helps to reduce the demands for source and energy [1, 4-5]. It also involves many developed techniques, the majority of which is about fibers and not commercialized yet. The major recycling methods for functional fibers or composites are mechanical recycling, heat recovery, and chemical recovery [4, 5]. Heat recovery

Chapter 4

employs combustion which is able to separate resin and fibers, both of which have greatly different pyrolysis temperature. However, due to possible damage to fiber, heat recovery also requires the facility to generate and store the waste gas and liquid. When wrongly operated, heat recovery may cause considerable carbon dioxide and toxic substance that increases environmental burden [6-8]. By contrast, chemical recovery easily damages fibers and generates complex byproducts, which adds difficulty to the recycling. Additionally, machine crushing is suitable for recycling fibers with different lengths. It is easily operated and thus the most commonly used. In brief, recycling and reclaiming techniques and related studies engage increasingly more attention [9-11].

Therefore, this study aims to recycle and reclaim high strength PET waste fibers with minimum possible damage in order to regain comparatively cheaper high-performance fibers. Instead of using newly produced fibers, a great number of recycled fibers are made into nonwoven fabrics, which are then combined with different reinforcing woven fabrics, thereby producing stab resistant hybrid-fabric fibrous planks. However, we believe that an efficient recycling process and design can re-add new value to the material. There are many studies indicating that the stab resistance of protective items is created by the friction force between fabrics and yarns [12-15]. For example, fabrics that are immersed in a shear thickening fluid (STF) exhibit better stab resistance because the presence of STF particles strengthens the friction force between the fabrics and yarns [16-18]. Similarly, friction force between the fabrics and yarns can also be obtained when the fabrics are made with a higher fabric density, immersed in resin, or stabilized with rubber threads [2, 19]. Regardless of the stab resistant materials, the stab resistance performance is primarily dependent on the friction of the materials against the impact objects. This study aims to propose an efficient method to recycle the waste woven selvages and recycle these fibers to

develop a flexible stab resistance hybrid fabric composites that may be used in the protective clothing field and geotextiles field. Rather than the traditional rigid protective materials, this study designs flexible protective materials with a multi-layered fabric structure. The combination of nonwoven and woven fabrics provides hybrid planks with highly improved stab resistance. The resulted flexible hybrid-fabric fibrous planks do not render as much burden to the human body as the traditional stiff composite protective items [20, 21], and can be easily made into diverse products or serve as a reinforcing item in any required secondary process. In addition, we used a nonwoven process in this study. The process technology has the advantages of fast, low cost and high output, and can fully mix two or more kinds of fiber materials and composite multi-layer fabrics to make a flexible stab-resistant hybrid fabric composite material designed by us.

4.2 Materials and methods

4.2.1 Materials

Recycled high strength polyester (PET) selvages (Chien Chen Textile, Taiwan) have a fiber fineness of 1000D/192f, fiber length of 40-65 mm, and single fiber strength of 8g/d (Figure 4.1). Both carbon and aramid plain woven fabrics are purchased from Jinsor-Tech Industrial Co., Taiwan and the physical properties are listed in Table 1. Basalt woven fabrics (Yurak International, Taichung City, Taiwan) are composed of basalt fiber bundles at both warp and weft directions with a fineness of 2970 D and an areal density of 328 g/m² (as shown in Table 4.1 and Figure 4.2). Low-melting-point PET (LMPET) staple fibers (Far Eastern New Century, Taiwan) have a fineness of 4 D and a length of 51 mm, and are composed of a skin-core structure. The melting points of the skin and core are 110 °C and 265 °C.



Figure 4.1 Images of recycled high strength PET selvages.

Table 4.1 Physical properties of basalt, carbon fiber, and aramid plain woven fabrics.

Reinforced Woven Fabric	Fineness	Base Weigh (g/m ²)	Thickness (mm)	Tensile Load (N)
Basalt	2970 D	328	0.31	118.45
Carbon	12 K	390	0.60	164.63
Kevlar®	1000 D	180	0.31	512.23

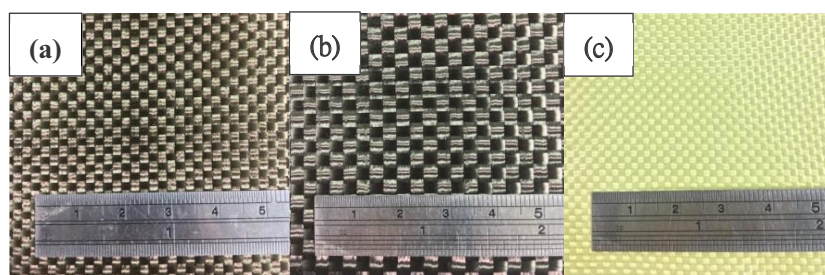


Figure 4.2 Images of (a) basalt, (b) carbon-fiber, and (c) aramid plain woven fabrics.

4.2.2 Method

The principal material in this study is recycled high strength PET selvages. In general, the staple fibers which used in non-woven fabrics are wavy or crimp in order to increase the friction. However, the waste selvages of woven fabric are usually cut from the edge of woven fabric made by the filament or continue yarn and still with woven fabric structure. So we have to break, dispersion, recycled and then reused these fibers. Therefore, the high strength PET waste selvages which are processed with the opening into recycled PET staple fibers. The PET staple fibers are mixed with low-melting point polyester (LMPET) fibers at ratios of 9:1, 7:3, and 5:5 to form high strength PET matrices by a needle punching machine (needle punching machine,

SNP120SH6, Shoou Shyng Machinery Co., Ltd., New Taipei City, Taiwan) with a needle-punched speed of 200 needles/min and a line speed of 2.3 m/min. And during the needle-punching process, the needles are pressed in from the direction of the vertical fabric surface to laminate and bonded the multilayer web or multilayer fabric together. Next, pure LMPET fibers are also made into LMPET layer by the nonwoven process, which serves as the adhesive layer between the PET matrix and reinforcing the woven fabric. Different reinforcing woven fabrics are used, including basalt, carbon-fiber, and aramid plain woven fabrics. The sandwich-structured laminates are hot pressed into the hybrid-fabric fibrous planks which treated at 130 °C at a speed of 0.2 m/min and hot pressure with 10 MPa (two-wheel hot press machine, CW-NEB, Chiefwell Engineering Co., Ltd., New Taipei City, Taiwan). The manufacturing process are denoted as Figure 4.3 and Table 4.2. Finally, the air permeability, tensile strength, and tearing strength, bursting strength, and static stab resistance of hybrid-fabric fibrous planks are tested to examine the influence of content of recycled high strength PET fibers and the employment of hot pressing.

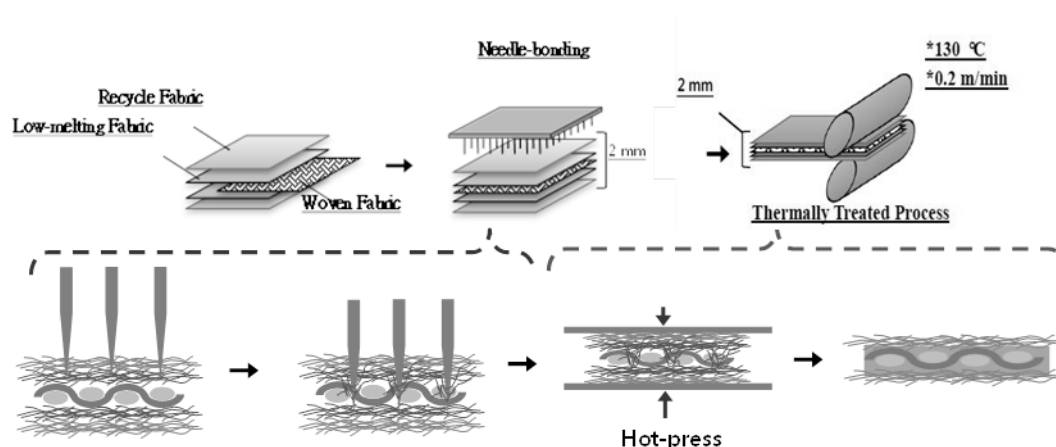


Figure 4.3 Manufacturing process of hybrid-fabric fibrous planks.

Table 4.2 Denotation and composition of hybrid-fabric fibrous planks.

Sample	Recycled PET fiber Content (wt%)	LMPET Content (wt%)	Reinforcing Layer	Employment of Hot Press
P9	90	10	-	N
P7	70	30	-	N
P5	50	50	-	N
HP9	90	10	-	Y
HP7	70	30	-	Y
HP5	50	50	-	Y
HP9C	90	10	Carbon	Y
HP7C	70	30	Carbon	Y
HP5C	50	50	Carbon	Y
HP9B	90	10	Basalt	Y
HP7B	70	30	Basalt	Y
HP5B	50	50	Basalt	Y
HP9K	90	10	Kevlar®	Y
HP7K	70	30	Kevlar®	Y
HP5K	50	50	Kevlar®	Y
LMPET Bonding Layer	-	100	-	-

4.2.3 Test methods and standards

4.2.3.1 Air permeability

The air permeability of hybrid-fabric fibrous planks is measured using an air permeability tester (TEXTTEST FX3300) as specified in ASTM D737 (Standard Test Method for Air Permeability of Textile Fabrics). Sample size is 25 cm × 25 cm. Ten samples for each specification are used in order to have the mean.

4.2.3.2 Tensile strength

As specified in ASTM D5035, the tensile strength of hybrid-fabric fibrous planks is measured at a cross head tensile speed of 300 mm/min using an Instron 5566 (Instron, US). The distance between a pair of pneumatic clamps is 75 mm. Six samples for each specification along the cross machine direction (CD) and machine direction (MD) are used. Samples have a size of 25.4 mm x 180 mm.

Chapter 4

4.2.3.3 Tearing strength

The tearing strength of hybrid-fabric fibrous planks is measured as specified in ASTM D5587. Samples are prepared according to the trapezoid method and have two equal altitudes and two parallel bases of 75 mm and 150 mm. The short base has a perpendicular cut with a length of 15 mm in the center. The distance between two clamps is 25 mm and the test rate is 300 mm. Six samples for each specification along the CD and MD are taken in order to have the mean.

4.2.3.4 Bursting strength

As specified in ASTM D3787, a universal tester (Instron 5566, Instron, US) that is equipped with a 25.4-mm-diameter hemispherical probe is used to measure the bursting strength of hybrid-fabric fibrous planks at a rate of 100 mm/min. Six samples (150 mm x 150 mm) for each specification are used and the maximum bursting strength is recorded.

4.2.3.5 Static-stab resistance test

The static puncture resistance of samples is measured at a puncture rate of 508 mm/min using a universal strength testing machine (Instron5566, US) as specified in ASTM F1342. Samples have a size of 100 mm × 100 mm. The diameter of the puncture probe is 4.5 mm. Six samples for each specification are used for the test in order to have the average static puncture resistance, standard deviation, and coefficient of variation (as shown in Figure 4.4).

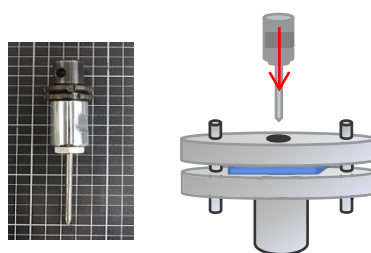


Figure 4.4 The equipment and puncture needle of static puncture resistance test.

4.3 Results

4.3.1 Mechanical property of recycle high strength pet matrices

Table 4.3 shows the mechanical property of recycled high strength PET matrices, including tensile strength, tearing strength, and air permeability. The mechanical properties are discussed based on the employment of hot pressing, the content of recycled PET fibers, and fiber orientation (i.e., the direction that the majority of fibers are aligned). Except for the tensile load, the employment of hot pressing significantly influences the elongation, tearing strength, tearing elongation, and air permeability. The LMPET fibers are melted to form thermal bonding points in the high strength PET matrices as a result of hot pressing. The thermal bonding points primarily stabilize the fabric structure and restrain the slip of fibers, which is proven by the results of tensile elongation of the matrices [22, 23]. However, the thermal bonding points have a lower strength than single fiber strength of high strength PET fibers, and employment of hot pressing can hardly affect the tensile strength of the matrices.

As for the tearing strength test, the matrices have a large area, which enable thermal bonding points to resist the tearing force as well as restrain the slip of fibers. Therefore, hot pressing has a positive influence on the tearing strength and elongation of the matrices. In particular, when composed of more recycled high strength PET fibers, the matrices exhibit greater tensile and tearing strengths. Because PET fibers are gathered from PET woven selvages, they are less crimped. Subsequently, the nonwoven fabrics (i.e., PET matrices) have a low porosity and compact structure, which is proven by the low air permeability. The employment of hot pressing creates a great amount of thermal bonding points and decreases the thickness of the matrices. Hence, the matrices have low air permeability due to the high fabric density and low porosity. Moreover, when composed of 50 wt% or 70 wt% of recycled high strength PET fibers, the matrices exhibit similar tensile and tearing performances. The results

are ascribed to the fact that PET fibers undermine the synergistic effect with highly crimped LMPET fibers. Comparatively, hot pressed PET matrices exhibit greater mechanical properties, and are thus used for following discussions.

Table 4.3 Physical properties of high strength PET matrices

	Recycled PET content (wt%)	Tensile Strength, (MPa)	CV (%)	Elongation, (%)	Tearing Strength, (N/mm)	CV (%)	Elongation, (%)	Air Permeability, (cm ³ /cm ² /s)
Without Hot-press	50 (P5)	13.3±1.29	9.72	40.38±1.36	267.9±32.96	12.30	66.1±7.13	49.3±4.63
	70 (P7)	16.7±1.92	11.48	33.17±2.22	258.2±27.63	10.70	68.7±8.70	45.1±3.75
	90 (P9)	16.0±1.32	8.26	33.85±2.40	354.4±47.32	13.35	65.9±9.42	40.1±2.71
Hot-press	50 (P5)	13.8±0.67	4.3	15.02±1.04	376.7±34.75	9.22	51.9±7.09	28.4±2.98
	70 (P7)	15.6±0.80	5.79	16.82±2.03	375.1±14.68	3.91	59.0±5.84	20.5±3.53
	90 (P9)	17.0±1.03	6.04	17.61±1.79	422.0±60.44	14.32	65.1±2.58	15.8±1.39

4.3.2 Tensile strength of hybrid-fabric fibrous planks

Figure 4.5 shows the tensile strength properties of high strength PET matrices as related to the fiber blending ratios. When the content of LMPET fibers is lower than 50 wt%, the resulted PET matrices exhibit greater tensile strength. Furthermore, three plain woven fabrics are separately combined with the PET matrices for reinforcement. The hybrid-fabric fibrous planks containing basalt woven fabrics and carbon-fiber woven fabrics have comparable mechanical properties. Basalt fibers and carbon fibers have similar properties, and both fibers are fragile and cannot be bent (Figure 4.5). According to the curve in Fig. Figure 4.5(c), it can be proved that the fiber properties affect the tensile properties of the sample. From the picture, it can be found that the curves of HP7B and HP7C decrease instantaneously after reaching the maximum force. This is also the moment when the fibers of the reinforcing fabric break. However, because of the high toughness of the Kevlar fiber, the slope of the curve rising at the beginning of the test is smaller. And after reaching the maximum, the

Chapter 4

curve appears wavy, which represents the process of slipping and pulling out the reinforcing yarn. Hence, when using a basalt or carbon-fiber plain woven fabric as the reinforcement, the fibrous planks exhibit similar trends in tensile strength tests.

The maximum tensile strength occurs when the fibrous planks are composed of 70 wt% of PET fibers. Specifically, the planks composed of aramid woven fabrics outperform planks composed of basalt or carbon-fiber woven fabrics in terms of tensile strength. Figure 4.6 shows the fractured images of different woven fabrics. Furthermore, Figure 4.7 indicates that the fibrous planks composed of aramid woven fabrics exhibit the highest tensile elongation due to the greater elongation rate of aramid fibers. As a result, the fibrous planks composed of aramid woven fabrics do not have a sudden decrease in the tensile strength when the aramid woven fabric is damaged. However, the high modulus fibers are commonly coated with oiling agent during the spinning and weaving process, which hampers the melted LMPET fibers to adhere. Therefore, the thermal bonding effect of LMPET fibers is insignificant, and aramid fibers slip to a greater extent. The test results show that HP9K that is composed of a lower content of LMPET fibers has the maximum tensile strength.

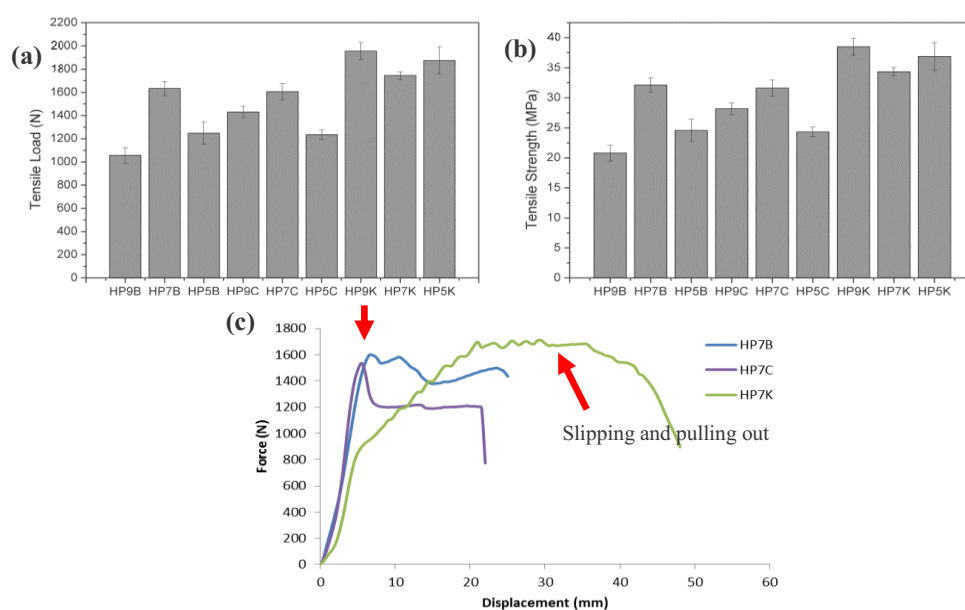


Figure 4.5 a) Tensile load, b) tensile strength of hybrid-fabric fibrous planks as related

to fiber blending ratios and c) force-displacement curve.

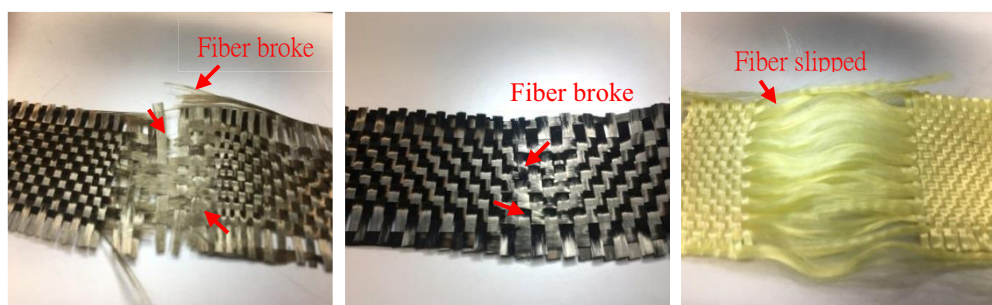


Figure 4.6 Damage level of (a) basalt, (b) carbon-fiber, and (c) aramid woven fabrics after tensile tests.

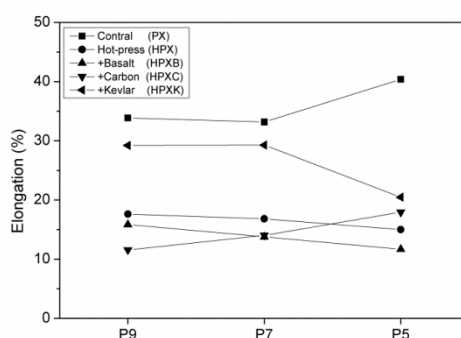


Figure 4.7 Elongation of hybrid-fabric fibrous planks as related to fiber blending ratios.

4.3.3 Tearing strength of hybrid-fabric fibrous planks

Figure 4.8 shows the tearing strength and elongation of hybrid-fabric fibrous planks as related to fiber blending ratios. Samples are prepared with a perpendicular cut in the center beforehand. The test results show that hybrid-fabric fibrous planks consisting of aramid woven fabrics have the maximum tearing strength. Figure 4.9 shows that fibrous planks that are composed of greater LMPET and not hot pressed exhibit low tearing elongation, which suggests that the employment of hot press creates thermal bonding points, preventing the slip of fibers and stabilizing the structure. By contrast, both basalt and carbon-fiber woven fabrics have fragile fibers.

The breakage of basalt or carbon-fiber woven fabrics causes a sudden decrease in the tearing properties, which in turn stops the test immediately. In particular, consisting of 10 wt% of LMPET fibers and 90 wt% of recycled high strength PET fibers, HP9K exhibits the highest tearing strength. The high strength PET fibers are repeatedly processed with combing and scattering to form staple fibers, and then made into nonwoven fabrics. Based on the test results, the tensile and tearing strength of the PET fibers are comparable to those of the embossing fibers, which indicates that the recycling has effective value [25-27].

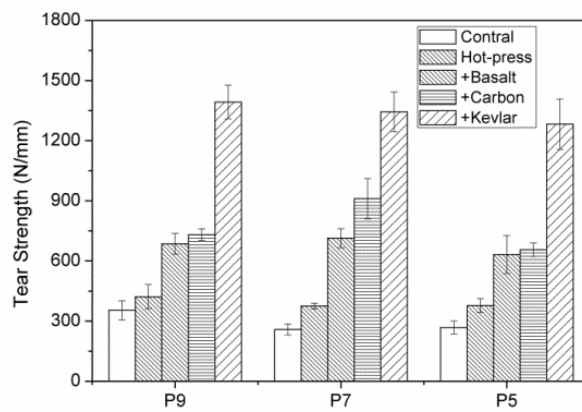


Figure 4.8 Tear strength of hybrid-fabric fibrous planks as related to fiber blending ratios.

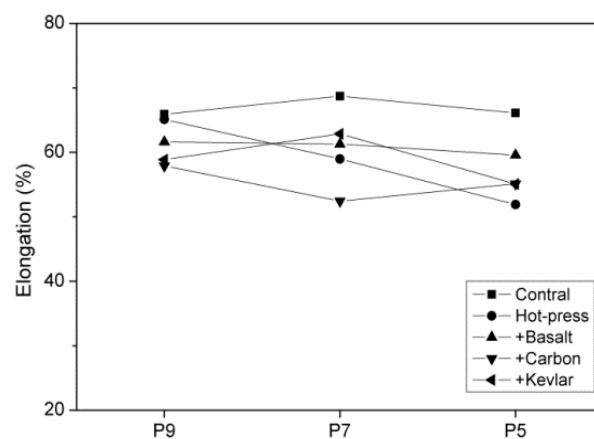


Figure 4.9 Elongation of hybrid-fabric fibrous planks as related to fiber blending ratios.

4.3.4 Bursting strength of hybrid-fabric fibrous planks

Figure 4.10 shows the bursting strength of hybrid-fabric fibrous planks as related to the fiber blending ratios. The fibrous planks that consist of a higher content of recycled PET fibers have higher bursting strength. The recycled PET fibers undergo the combing and carding processes repeatedly to form the staple fibers for nonwoven fabrics. Unlike the commonly used staple fibers in nonwoven fabrics, the recycled PET fibers are not crimped or embossing. Usually, crimped or embossing fibers contribute relatively higher friction and a uniform distribution to the nonwoven fabrics. In addition, the recycled PET fibers are chopped from complete bundles, which may possibly leave more filling and oiling agent that restrain the subsequent combing and opening processes. Based on the bursting strength, all hybrid-fabric fibrous planks have comparable bursting strength and coefficient of variation. Only when containing uneven fiber distribution or obvious fiber packing do the planks exhibit uneven and diversity in the bursting strength. Moreover, the fibrous planks consisting of a greater amount of recycled PET fibers demonstrate higher bursting strength, which suggests that the fibers are evenly distributed and the recycling PET fibers for the production of nonwoven fabrics is proven effective. The test results show that HP9K that is composed of a lower content of LMPET fibers has the maximum bursting strength about 146.8 % better than the sample of HP9.

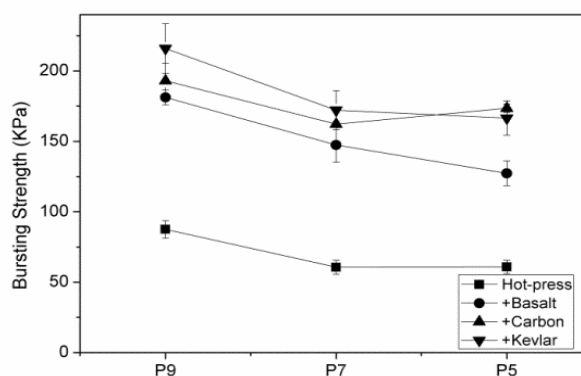


Figure 4.10 Bursting strength of hybrid-fabric fibrous planks as related to fiber

blending ratios.

4.3.5 Static stab-resistance of hybrid-fabric fibrous planks

Figure 4.11 shows the static stab resistance of hybrid-fabric fibrous planks as related to the fiber blending ratios. Consisting of 90 wt% of recycled PET fibers in the PET matrix and Kevlar® woven fabric as reinforcement, P9K demonstrates the maximum static stab resistance. This test uses a pointed probe with a diameter of 4.5 mm, and the stab resistance mechanism of fibrous planks is via the resistance against the tip of the probe as well as the frictional resistance of fibers against the pointed probe. The displacement of the fibrous planks is relatively smaller in Figure 4.12 The hybrid-fabric fibrous planks to resist the pointed probe via the compact plain structure of woven fabric as well as the melting status and adhesion effects caused by a great amount of LMPET fibers. The specified design of the fibrous planks is to stop the slip of fibers and increase the friction between fibers and the probe effectively. However, the recycled high modulus PET fibers are coated with oiling agent, which prevents LMPET fibers to form an adhesive layer during the hot pressing, and thus the interface bonding strength is low. Furthermore, the fibrous planks exhibit highest static stab resistance when consisting of the greatest amount of recycled PET fibers and the smallest amount of LMPET fibers about 212.6 N. Based on the test results, the static stab-resistance of the hybrid-fabric fibrous planks are comparable to those of the embossing fibers, which indicates that the recycling has effective value [25, 28]. The future studies need to remove the filling and oiling agent before conducting the test for further discussion.

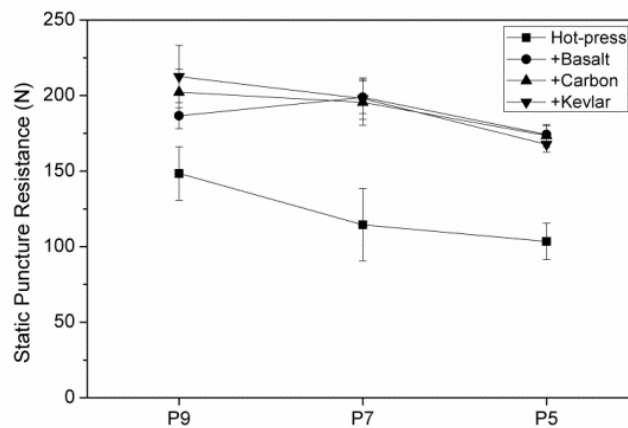


Figure 4.11 Static puncture resistance of hybrid-fabric fibrous planks as related to fiber blending ratios.

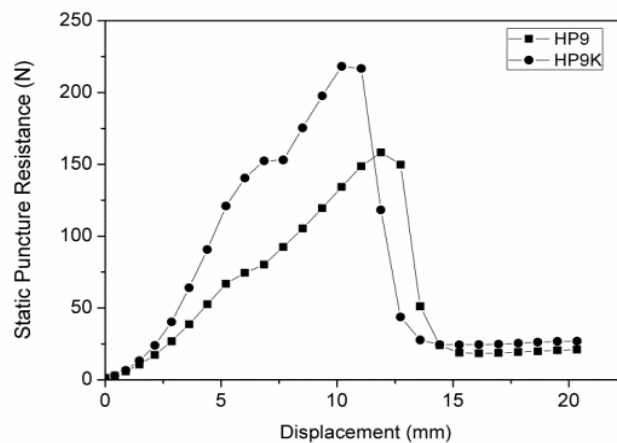


Figure 4.12 Static puncture resistance-displacement curve of hybrid-fabric fibrous planks of HP9 and HP9K.

4.4 Conclusions

This study proposes flexible fabric-based protective planks, which are recycled high strength PET fibers by processed with minimum damage for secondary production, thereby obtaining recycled high performance fibers with relatively lower production cost. In this study, the different reinforcing woven fabrics are combined with matrices to form hybrid-fabric fibrous planks. Despite multiple combining and

Chapter 4

carding processes, the recycled PET staple fibers are proven to provide the fibrous planks with high tensile and tearing strengths. The test results indicate that recycled PET fibers remains the high strength and can be made into protective products.

The test results indicate that recycled PET fibers remains high strength and can be made into protective products. The sample consisting of 10 wt% of LMPET fibers and 90 wt% of recycled high strength PET fibers, HP9K exhibits the optimal mechanical properties those we tested in this study with 38.5 Mpa of tensile strength, 1392.8 N/mm of tearing strength, 215.9 KPa of bursting strength and 212.6 N of static stab resistance force. The combination of nonwoven and woven fabrics provides the benefits of their different stab behaviors, strengthening the puncture resistance of the hybrid-fabric fibrous planks. Most of all, an efficient recycling process and using textile and fiber waste to make protective fibrous planks decreases the production cost considerably, which makes the industrial and livelihood protective products more advantageous and acceptable.

In addition, due to the recycled high modulus PET fibers are generally coated with oiling agent when it produced, which prevents LMPET fibers to form an adhesive layer during the hot pressing, and thus the interface bonding strength is low. The future studies need to remove the filling and oiling agent before conducting the test for further discussion.

References

- [1] Yasin, S.; Behary, N.; Curti, M.; Rovero, G. Global Consumption of Flame Retardants and Related Environmental Concerns: A Study on Possible Mechanical Recycling of Flame Retardant Textiles. *Fibers* 2016, 4, 16-25.
- [2] Mayo, J.B., Jr.; Wetzel, E.D.; Hosur, M.V.; Jeelani, S. Stab and puncture characterization of thermoplastic-impregnated aramid fabrics. *Int. J. Impact Eng.*

- 2009, 36, 1095-1105.
- [3] Hejazi, S.M.; Kadivar, N.; Sajjadi, A. Analytical assessment of woven fabrics under vertical stabbing-The role of protective clothing. *Forensic Science International* 2016, 259, 24-233.
- [4] Oliveux, G.; Dandy, L.O.; Leeke, G.A. Current status of recycling of fibre reinforced polymers: Review of technologies, reuse and resulting properties, *Prog. Mater. Sci.* 2015, 72, 61-99.
- [5] Yang, Y.X.; Boom, R.; Irion, B.; Heerden, D. V.; Kuiper, P.; Wit, H.D. Recycling of composite materials, *Chem. Eng. Process.* 2012, 51, 53- 68.
- [6] Sidhu, S.; Gullett, B.; Striebich, R.; Klosterman, J.; Contreras, J.; DeVito, M. Endocrine disrupting chemical emissions from combustion sources: diesel particulate emissions and domestic waste open burn emissions. *Atmos. Environ.* 2005, 39(5),801-811.
- [7] Kamal, A.; Ali, U.; Ramay, M.I.; Younis, S.M.Z.; Sumbal, S.; Malik, R.N.; Rashid, A. Principle component analysis of flue gas exhaust and health risk estimates for the population around a functional incinerator in the vicinity of Rawalpindi Pakistan. *Arab. J. Chem.* 2017, 10(2), s2302-2306.
- [8] Pope C.A. III; Dockery D.W. Health effects of fine particulate air pollution: lines that connect. *J. Air Waste Manage. Assoc.* 2006, 56(6), 709-742.
- [9] Hu, Y.; Du, C.; Leu, S.Y.; Jing, H.; Li, X.; Lin, C.S.K. Valorisation of textile waste by fungal solid state fermentation: An example of circular waste-based biorefinery. *Resour. Conserv. Recycl.* 2018, 129, 27-35.
- [10] Nunes, L.J.R.; Godina, R.; Matias, J.C.O.; Catalão, J.P.S. Economic and environmental benefits of using textile waste for the production of thermal energy. *J. Clean Prod.* 2018, 171(10), 1353-1360.
- [11] Hadded, A.; Benltoufa, S.; Fayala, F., Jemni, A. Thermo physical

Chapter 4

- characterisation of recycled textile materials used for building insulating. *Journal of Building Engineering* 2016, 5, 34-40.
- [12] Termonia, Y. Puncture resistance of fibrous structures. *Int. J. Impact Eng.* 2006, 32,1512-1520.
- [13] Wang, Q.S.; Sun, R.J.; Tian, X.; Yao, M.; Feng, Y. Quasi-static puncture resistance behaviors of high-strength polyester fabric for soft body armor, *Results Phys.* 2016, 6, 554-560.
- [14] Bao L.; Sato, S.; Morikawa, H. Improving Stab-resistant Textile Materials with a Non-woven Fabric Structure. *Journal of Textile Engineering* 2016, 62(3), 37 – 42.
- [15] Bao L.; Wang, Y.L.; Baba, T.; Fukuda, Y.; Wakatsuki, K.; MORIKAWA, H. Development of a high-density nonwoven structure to improve the stab resistance of protective clothing material. *Ind. Health* 2017, 55, 1-8
- [16] Barnes, H.A.; Shear-Thickening ("Dilatancy") in Suspensions of Nonaggregating Solid Particles Dispersed in Newtonian Liquids, *J. Rheol.* 1989, 33 (2), 329.
- [17] Egres Jr., R.G.; Halbach, C.J.; Decker, M.J.; Wetzel, E.D.; Wagner, N.J. Stab performance of shear thickening fluid (STF)–fabric composites for body armor applications, *SAMPE 2005: New Horizons for Materials and Processing Technologies* 2005, Long Beach.
- [18] Decker, M.J.; Halbach, C.J.; Nam, C.H.; Wagner, N.J.; Wetzel, E.D. Stab resistance of shear thickening fluid (STF)-treated fabrics, *Compos. Sci. Technol.* 2007, 67, 565-578.
- [19] Mayo Jr, J.B., Wetzel, E.D., Hosur, M.V.; Jeelani S. Stab and puncture characterization of thermoplastic- impregnated aramid fabrics. *Int. J. Impact Eng.* 2009, 36(9), 1095-1105.

- [20] Bao L.; Sato, S.; Wang, Y.L.; Wakatsuki, K.; MORIKAWA, H. Development of Flexible Stab-proof Textiles Impregnated with Microscopic Particles. *Journal of Textile Engineering* 2017, 63(2), 43-48.
- [21] Park, H.; Branson, D.; Kim, S.; Warren, A.; Jacobson, B.; Petrova, A.; Peksoz, S.; Kamenidis, P. Effect of armor and carrying load on body balance and leg muscle function. *Gait Posture* 2014, 39, 430-435.
- [22] Dempsey, P.C.; Handcock, P.J.; Rehrer, N.J. Impact of police body armour and equipment on mobility. *Appl. Ergon.* 2013, 44, 957-961.
- [23] Yasin, S.; Sun, D.; Memon, H.; Zhu, F.; Jian, H.; Bin, Y.; Mingbo, M.; Hussain, M. Optimization of Mechanical and Thermal Properties of iPP and LMPP Blend Fibres by Surface Response Methodology. *Polymers* 2018, 10, 1135-1152.
- [24] Hussain, M.; Zhu, F.; Yu, B.; Han, J.; Memon, H.; Yasin, S. LMPP Effects on Morphology, Crystallization, Thermal and Mechanical Properties of iPP/LMPP Blend Fibres. *Fibres Text. East. Eur.* 2018; 26, 2(128), 26-31.
- [25] Correia, N.; Bueno, B. Effect of bituminous impregnation on nonwoven geotextiles tensile and permeability properties. *Geotext. Geomembr.* 2011, 29, 92-101.
- [26] Lin, M.C.; Lou, C.W.; Lin, J.Y.; Lin, T.A.; Lin, J.H. Mechanical property evaluations of flexible laminated composites reinforced by high-performance Kevlar® filaments: Tensile strength, peel load, and static puncture resistance. *Compos. Pt. B-Eng.* 2019, 166, 139-147.
- [27] Zakriya, G.; Ramakrishnan, G. Insulation and mechanical properties of jute and hollow conjugatedpolyester reinforced nonwoven composite. *Energy Build.* 2018, 158, 1544-1552.
- [28] Rawal, A.; Saraswat, H. Stabilisation of soil using hybrid needlepunched nonwoven geotextiles. *Geotext. Geomembr.* 2011, 29,197-200.

CHAPTER 5

Fabric composites reinforced with thermally bonded and irregularly aligned filaments: preparation and puncture resistant performance

5.1 Introduction

Owing to the increasing awareness of the importance of self-protection, protective materials are being efficiently developed, including barks, hides, leather, metal, and composites. The progressing technology gives rise to diverse industries and subsequently demands for the preparation of protective materials that require large amounts of advanced materials have risen [1-4], and stab resistant materials are the most pervasively used in different fields [5,6]. Statistically, stabs, cuts, and abrasions account for 15% of workplace injuries per year, which makes the development of puncture resistant products utterly essential. In addition to being used for personal protection, stab resistant products can also be used in clothing textiles, household textiles, and industrial textiles. However, the need for these products to have both low cost and high performance restricts the common application of puncture resistant products (e.g., geotextiles and other industrial protective materials).

In light of the material types and purposes, puncture resistant materials can be divided into flexible, semi-flexible, rigid, and liquid stab resistant materials. Ceramic and metal plates are commonly used rigid stab resistant materials. They have excellent stab resistance but are heavyweight, which restricts the mobility of users. By contrast, flexible or semi-flexible stab resistant materials, such as high-density polyethylene, aramid mixture fabric, and specially made composites [7], have good stab resistance, are lightweight and flexible, but require multi-layered lamination to attain a good stab resistance. Hence, many researchers still anticipate creating puncture resistant materials that can be lightweight and still attain good performance. Moreover, shear thickening fluid (STF) is one of the most popular materials with stab resistance [8-10]. As evidenced by previous studies, a combination of fabrics and STF can obtain highly strengthened stab-proof and bulletproof functions [11–14]. However, there are some studies that proved that it was the STF particles which increased the

friction force between fabrics and yarns, thereby improving the stab resistance of the STF-based fabrics [15-17].

To sum up, achieving good puncture resistance is mainly based on sufficient fiber density, high friction among fibers, a profound aggregation of fibers where the spike strikes, and firmly secured fibers. Hence, regardless of the type of stab resistant material, friction is one of the major factors influencing its stab resistance. This study aims to develop a flexible sandwich-structured puncture resistant fabric composites which can be used in the protective clothing field and geotextiles field. One of the materials we used in this study was the waste selvages of aramid plain woven fabrics (K129 and K29). Aramid fiber can usually be used in a wide variety of applications due to its light weight, high performance, and toughness. It is used in a variety of protective clothing and equipment to make it safer and more durable. Although aramid waste selvages can only be recycled into staple fibers, nonwoven fabrics can still take advantage of their original characteristics while reducing costs.

On the other hand, based on the fabric structure, knitted/woven fabrics have greater stab resistance against knives while nonwoven fabrics have puncture resistance against spikes [18-21]. Therefore, by combining the advantages of fibers and fabric structures, this study laminates filaments as a reinforcing interlayer to form the puncture resistant sandwich-structured fabric composites. A previous study shows that adding filament remarkably reinforces the puncture resistance of the composites, but the disadvantage is that the filaments slide severely. Hence, low-melting-point polyester (LMPET) layers are used in order to improve this drawback of filament reinforcement. The employment of thermal treatment then secures the reinforcing filaments and mitigates the slide of the filament, thereby achieving greater stab resistance. According to the test results and compared with other studies, using the LMPET adhesive layer has a positive influence, preventing the slide of filaments. At

the same time, the internal porosity of the fabric is reduced, the utilization ratio of the fiber to the puncture resistance is improved, and the stability of the stab resistance of the composite fabric is improved.

Besides this, we used the nonwoven fabric process in this whole study. This process technology has the advantages of being fast, low cost, and having a high output, and can fully mix two or more kinds of fiber materials and composite multi-layer fabrics to make the flexible sandwich-structured puncture resistant fabric composites we designed.

5.2 Materials and methods

5.2.1 Materials

Recycled aramid staple fibers (K129 and K29, provided by Jinsor-Tech Industrial Corporation, Taichung City, Taiwan) are obtained from aramid woven fabrics and have a fineness of 1.2 D and a length of 50–65 mm. High strength nylon 6 staple fibers (Formosa Chemicals & Fibre Corporation, Taipei City, Taiwan) have a fineness of 6.0 D, a length of 64 mm, single fiber strength of 10 g/d, and an elongation of 24.7%. Two-component low-melting-point polyester (LMPET) staple fibers (Far Eastern New Century Corporation, Taipei City, Taiwan) have a fineness of 4.0 D and a length of 51 mm. The melting temperatures of the sheath and the core are 110 °C and 265 °C, respectively. Basalt woven fabrics (Yurak International, Taichung City, Taiwan) are composed of basalt fiber bundles at both warp and weft directions with a fineness of 2970 D and an areal density of 328 g/m². PET continue filaments (Universal Textile, Taiwan) have a fineness of 500 D.

The commercially available geotextile is supplied by Hsinnjy Ltd. Co. (Taichung City, Taiwan), and the main material is PET fiber, which is a nonwoven fabric formed by multiple needle rolling and heat treatment. Its characteristics are based on the

relevant test standards of this study. The basis weight is 272.46 g/m²; the thickness is about 1 mm, the tearing strength force is 299.53 N at the cross machine direction (CD) and 291.75 N at the machine direction (MD), the static puncture strength is 55.90 N, and the dynamic puncture strength is 35.52 N.

5.2.2 Preparation of filament/woven-reinforced fabric composites

The symmetrically sandwich-structured composite fabrics are composed of double-layered surfaces and a reinforcing interlayer of a woven fabric and/or irregularly aligned filaments. As shown Figure 1, the surface layers are nylon/aramid recycled nonwoven fabrics (with an areal density of 200 g/m²) and pure LMPET fabrics (with an areal density of 200 g/m²). Waste aramid selvages are processed by opening (fiber opening machine, TYM-40, HongChio Machinery Co., Ltd., Taoyuan, Taiwan) to have staple fibers, after which they and nylon staple fibers are needle punched to form the nonwoven layers (needle punching machine, SNP120SH6, Shoou Shyng Machinery Co., Ltd., New Taipei City, Taiwan). Pure LMPET fabrics are composed of LMPET fibers, serving as the adhesion layer to stabilize the composite structure. All of the laminates are needle punched (needle punching machine, SNP120SH6, Shoou Shyng Machinery Co., Ltd., New Taipei City, Taiwan) and thermally treated at 130 °C at a speed of 0.2m/min (two-wheel hot press machine, CW-NEB, Chiefwell Engineering Co., Ltd., New Taipei City, Taiwan), forming the filamentor and woven-reinforced fabric composites. The first and second sub-figures in Figure 5.1 show the needle punching process and thermally treated process for forming the woven-reinforced fabric composites (N/L/W/L/N). The third sub-figure in Figure 5.1 shows the PET continuous filament lamination process which forms the filament-reinforced fabric composites (N/L/F/L/N). The total thickness of these sample are controlled at 2 mm. According to the materials we used in the

reinforcing interlayer, the experimental groups are denoted as N/L/W/L/N (the first sub-figure in Figure 1), N/L/F/L/N (the third sub-figure in Figure 5.1), and N/L/W/F/L/N where “N” stands for nonwoven layer, “L” stands for LMPET layer, “W” stands for woven interlayer, “F” stands for filament interlayer. The control group is thus denoted as N/L/L/N without reinforcing layers. The puncture resistance of the fabric composites is characterized in terms of their tear strength, static puncture resistance, and dynamic puncture resistance.

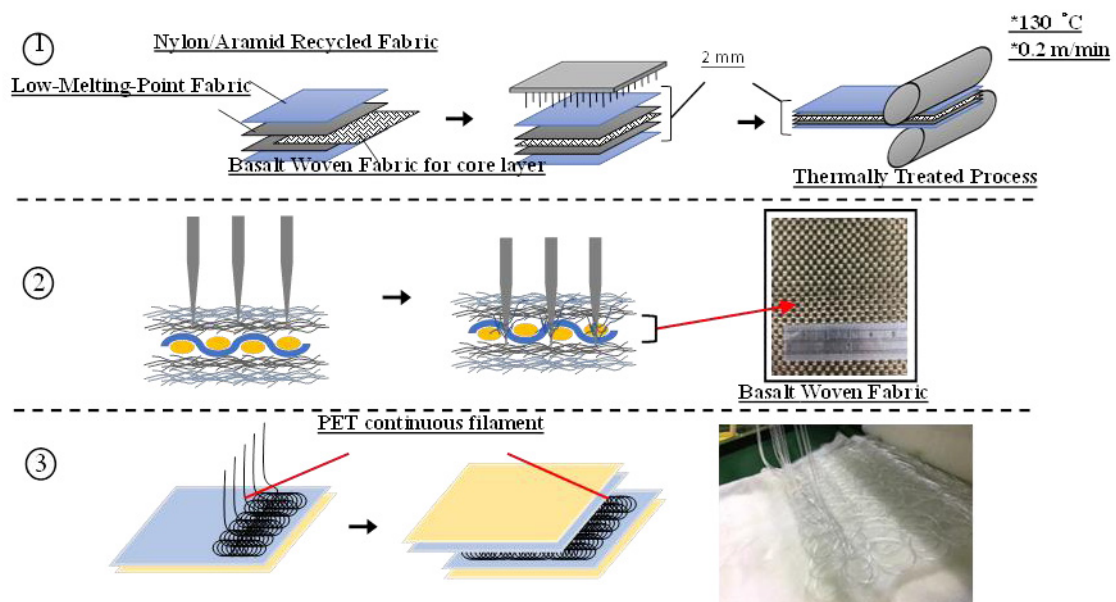


Figure 5.1 Schematic diagrams of the manufacture of fabric composites. (1) The laminates are needle punched and thermally treated to form the woven-reinforced fabric composites (N/L/W/L/N). (2) Sectional view during the needle punch process (N/L/W/L/N). (3) PET continuous filament lamination processing to form the N/L/F/L/N.

5.2.3 Test methods and standards

5.2.3.1 Tearing strength test

As specified in ASTM D5035-11 (2015) [22], fabric composites were tested for tearing strength using an Instron 5566 (Instron, Canton, Massachusetts, USA). As shown Figure 5.2, the test was conducted using a constant tearing rate of 300 ± 10 mm/min. The distance between the upper and lower fixtures was 25.4 mm. Samples had a size of 150 mm \times 75 mm and a 15 mm long notch. Ten samples for each specification were taken along the cross machine direction (CD) and machine direction (MD), respectively.

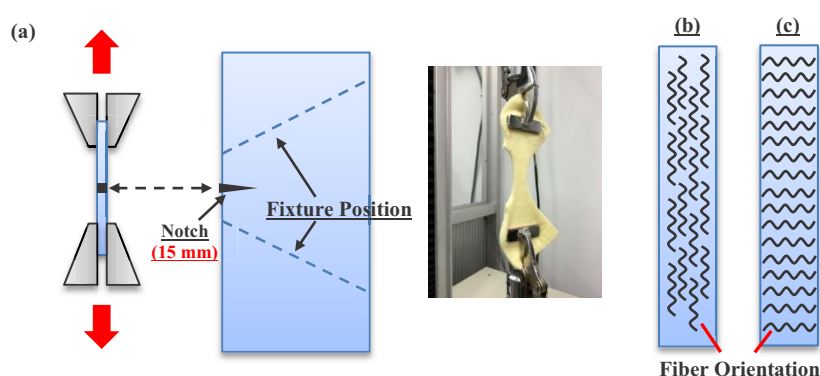


Figure 5.2 Schematic diagrams of the tearing test fabric composites. (a) Test schematic of the tearing strength test; (b) Cross Machine Direction (CD); (c) Machine Direction (MD).

5.2.3.2 Static puncture resistance test

The static puncture resistance of samples was measured at a puncture rate of 508 mm/min using a universal strength testing machine (Instron5566, Canton, Massachusetts, USA) as specified in ASTM F1342 [23]. Samples had a size of 100 mm \times 100 mm. The diameter of the puncture probe was 4.5 mm and was chosen to be similar to an ice pick. Six samples for each specification were used for the test in order to have the average static puncture resistance, standard deviation, and coefficient of variation.

5.2.3.3 Dynamic puncture resistance test

The dynamic puncture resistance of samples was measured by a drop-weight impact machine (Kuang Neng Factory, Taiwan) that was equipped with a data collector (PCD300A, San Lien Technology, Taipei City, Taiwan) according to the energy level of E1-1 (24 J) in the NIJ Standard-0115.00 (stab resistance of personal body armor)[24]. The puncture needle device contained a metal weight and a puncture probe, the total weight was 2.8 kg and the puncture probe was released from a height of 284 mm and fell freely (as shown in Figure 5.3). The maximum dynamic puncture resistance was obtained when the puncture probe penetrated the sample. Six samples for each specification were used for the test in order to have the average dynamic puncture resistance, standard deviation, and coefficient of variation.

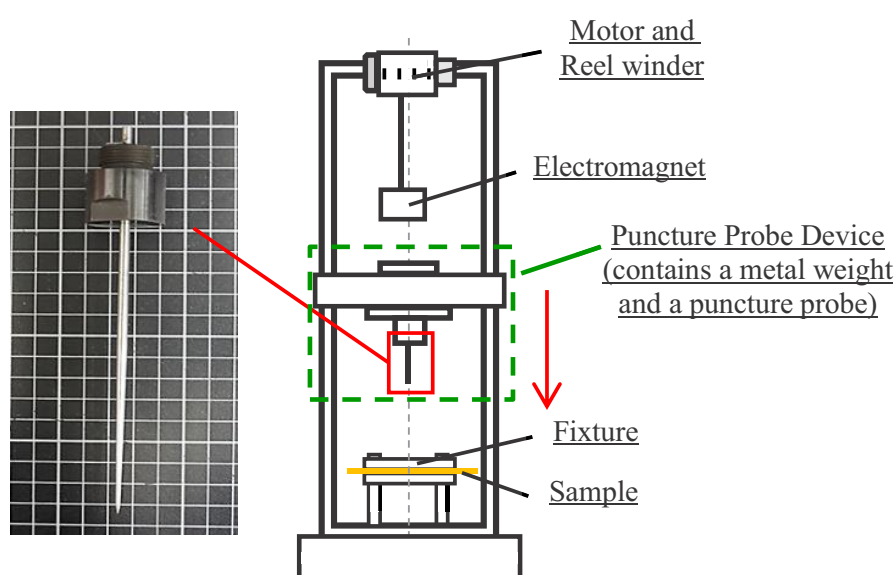


Figure 5.3 The equipment and puncture needle of dynamic puncture resistance test.

5.3 Results

5.3.1 Tearing strength

Figure 5.4 shows the tearing strength of the non-thermally treated filament/woven-reinforced fabric composites (denoted as NH) and Figure 5.5 shows

the tearing strength of thermally treated ones (denoted as YH). The tearing strength along the CD of N/L/W/F/L/N was higher than that of the other experimental groups (i.e., N/L/W/L/N, N/L/W/L/N) and the control group (i.e., N/L/L/N). Moreover, N/L/W/F/L/N had a greater tearing strength after it was thermally treated. N/L/W/L/N is woven-reinforced and plain woven fabric has a regular plain arrangement, whereas N/L/F/L/N is filament-reinforced and the filaments are irregularly aligned. Unlike woven fabrics that have high fiber-yarn and yarn-yarn friction, filaments tended to slide during the tearing test. Additionally, N/L/W/F/L/N had many thermal bonding points as a result of the heat treatment, which in turn effectively improved the phenomenon of filament slide and thus achieved a higher tearing strength of 1144.0 N (Figure 5.5).

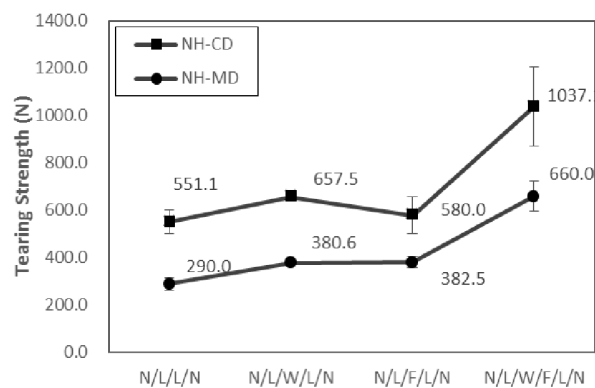


Figure 5.4 Tearing strength of filament/woven-reinforced fabric composites without heat treatment.

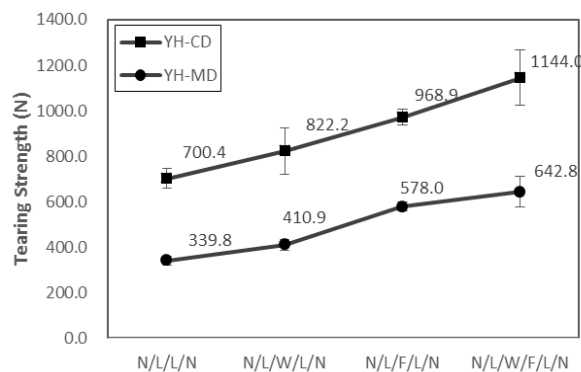


Figure 5.5 Tearing strength of filament/woven-reinforced composites fabrics that have

been thermally treated.

5.3.2 Static puncture strength

Figure 5.6 shows the static puncture resistance of filament/woven-reinforced fabric composites while Figure 5.7 shows their force-displacement curves. The non-thermally treated filament/woven-reinforced fabric composites are denoted as NH and the tearing strength of thermally treated ones is denoted as YH. Due to different features of the reinforcing woven- and filament-interlayers, N/L/W/F/L/N exhibited static puncture resistance in a combined manner. The shear force and friction between the probe and sample increased when the pointed probe further touched the sample (Figure 5.7). The resistance force against the probe sharply decreased (Figure 5.7a, 5.7b) right after the probe fully penetrated the sample (Figure 5.7c), leaving only the friction between the probe and the sample (Figure 5.7d). At the same time, the yarn-fabric structure of the samples underwent displacement, deformation, and final penetration damage, which makes the yarn-fiber friction and the slide of filament the two most important factors in this test. By comparison, the regularly formed plain-weave woven fabric provided greater puncture resistance than the irregularly aligned filaments for N/L/W/F/L/N. Furthermore, the thermal treatment generated thermal bonding points that can secure the whole structure of the fabric composites, preventing the slide of filaments. Unlike the woven fabrics with a fixed fabric pattern, filaments are freely aligned in loops as reinforcement and the slide of filaments adversely affects the static puncture resistance of thermally treated N/L/F/L/N. By contrast, N/L/W/F/L/N consists of both woven fabric and filaments as the reinforcing interlayers, both of which can be effectively combined. The irregularly arranged filaments can further improve the static puncture resistance at 0° and 90°. In particular, the thermally treated N/L/W/F/L/N had the maximum static puncture resistance of

243.2 N.

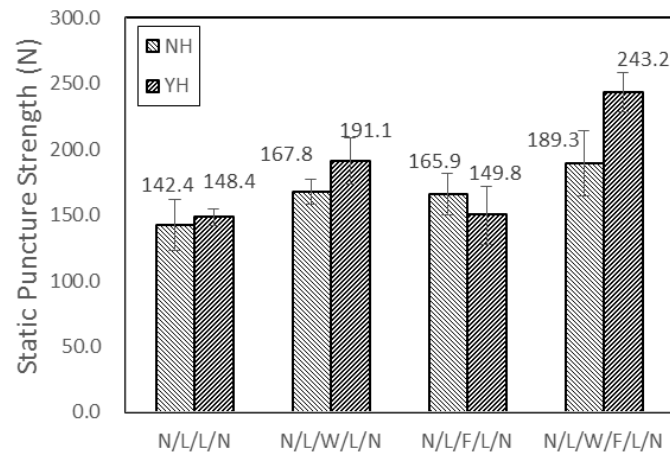


Figure 5.6 Static puncture resistance of filament/woven-reinforced fabric composites.

(NH: non-thermally treated, YH: thermally treated).

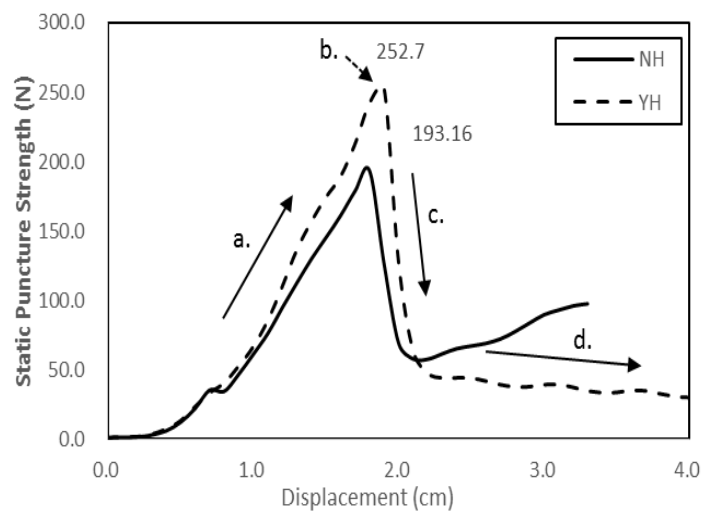


Figure 5.7 The strength-displacement curve of the static puncture resistance of filament/woven-reinforced fabric composites.

5.3.3 Dynamic puncture strength

Figure 5.8 shows the dynamic puncture resistance of N/L/W/F/L/N. Although both static and dynamic puncture strength tests used spike-shaped probes, the former used a constant rate of 508 mm/min, while the latter was added with an 8.5 kg weight

and released from a specified height to plummet. Hence, the dynamic puncture resistance was demonstrated in a different way. Without thermal treatment, all of the samples had comparable dynamic puncture resistance. Like its static puncture resistance, the thermally treated N/L/W/F/L/N also outperformed the other groups and had the optimal dynamic puncture resistance. The employment of thermal treatment made a remarkable contribution due to the presence of thermal bonding points that significantly secured the sandwich structure and prevented the slide of filaments, strengthening the compound laminates firmly. Specifically, the thermally treated N/L/W/F/L/N had the maximum dynamic puncture resistance of 104.7 N.

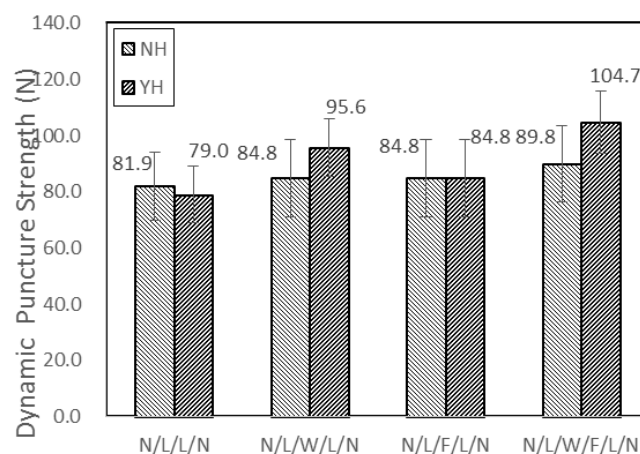


Figure 5.8. Dynamic puncture resistance of filament/woven-reinforced fabric composites. (NH: non-thermally treated, YH: thermally treated).

5.3.4 Summary of comparison

Table 5.1 shows the comparison of the proposed fabric composites, commercially available geotextiles, and the product of our previous studies [25]. Commercially available geotextiles have static and dynamic puncture resistances of 60 N and 37 N, indicating that the proposed N/L/W/F/L/N sample has greater puncture resistance. Similarly, the N/L/W/F/L/N sample also outperformed the

proposed products of our previous study in terms of static and dynamic puncture resistance. Conversely, pure filament-reinforced (N/L/F/L/N) did not exhibit significant puncture resistance as the filaments inevitably slide, indicating that a bonding layer of multi-layered composites can restrain the fibers from sliding. In addition, PET filaments provided a much lower reinforcement than that of nonwoven fabrics and thermal bonding points. Despite the presence of an LMPET adhesive layer, the combination of PET filaments and an LMPET layer only provided a limited reinforcing effect. Hence, the future study will focus on the interfacial bonding force between the adhesive layer and the reinforcing layer. In terms of the EN 388:2016 standard (protective gloves against mechanical risks), the puncture resistance of N/L/W/F/L/N reached level 3, which is between 100 N and 150 N and indicates good puncture resistance.

Table 5.1 Comparison of puncture resistances between N/L/W/F/L/N sample and other products.

	Static Puncture (N)		Dynamic Puncture (N)	
	Double-Layered Matrices	Matrix/F/Matrix	Double-Layered Matrices	Matrix/F/Matrix
Commercially Available Geotextiles	≈ 55.9		≈ 35.5	
Our Sample	148.4	149.4	79.0	84.8
EN 388:2016 Performance Levels	3 (100 < * < 150)	3 (100 < * < 150)	-	-

Note. "*" is the proposed the filament/woven-reinforced fabric composite.

5.4 Conclusions

This study aims to develop sandwich-structured puncture resistant fabric composites, and the optimal N/L/W/F/L/N has good puncture resistance at level 3. The proposed fabric composites are characterized in terms of tearing strength, static puncture resistance, and dynamic puncture resistance. The test results indicate that

thermally treated N/L/W/F/L/N has a 63.3% greater tearing strength at CD orientation, 63.9% greater static puncture resistance, and 32.5 % greater bursting strength than N/L/L/N.

Compared to other studies, using the LMPET adhesive layer had a positive influence, preventing the slide of the filaments, but the poor interfacial combination only contributes limited reinforcement. Hence, improving the interfacial affinity between laminates is suggested to be conducted in future studies.

References

- [1] Bartkowiak, G.; Dąbrowska, A.; Marszalek, A. Assessment of an active liquid cooling garment intended for use in a hot environment. *Appl. Ergon.* 2017, 58, 182–189.
- [2] Małek, E.; Miedzińska, D.; Stankiewicz, M. Heat resistance research and surface analysis of fireproof textiles with titanium silicide coating. *Procedia Struct. Integr.* 2017, 5, 508–515.
- [3] Silva-Santos, M.C.; Oliveira, M.S.; Giacomin, A.M.; Laktim, M.C.; Baruque-Ramos, J. Flammability on textile of business uniforms: Use of natural fibers. *Procedia Eng.* 2017, 200, 148–154.
- [4] Xu, Y.; Sheng, J.; Yin, X.; Yu, J.; Ding, B. Functional modification of breathable polyacrylonitrile/polyurethane/TiO₂ nanofibrous membranes with robust ultraviolet resistant and waterproof performance. *J. Colloid Interface Sci.* 2017, 508, 508–516.
- [5] Termonia, Y. Puncture resistance of fibrous structures. *Int. J. Impact Eng.* 2006, 32, 1512–1520.
- [6] Wang, Q.-S.; Sun, R.-J.; Tian, X.; Yao, M.; Feng, Y. Quasi-static puncture resistance behaviors of high-strength polyester fabric for soft body armor.

- Results Phys. 2016, 6, 554–560.
- [7] Gürgen, S.; Kuşhan, M.C. The ballistic performance of aramid based fabrics impregnated with multi-phase shear thickening fluids. *Polym. Test.* 2017, 64, 296–306.
- [8] Barnes, H.A. Shear-Thickening (“Dilatancy”) in Suspensions of Nonaggregating Solid Particles Dispersed in Newtonian Liquids. *J. Rheol.* 1989, 33, 329–366.
- [9] Hassan, T.A.; Rangari, V.K.; Jeelani, S. Synthesis, processing and characterization of shear thickening fluid (STF) impregnated fabric composites. *Mater. Sci. Eng. A* 2010, 527, 2892–2899.
- [10] Li, W.; Xiong, D.S.; Zhao, X.S.; Sun, L.L.; Liu, J. Dynamic stab resistance of ultra-high molecular weight polyethylene fabric impregnated with shear thickening fluid. *Mater. Des.* 2016, 102, 162–167.
- [11] Egres, R.G., Jr.; Halbach, C.J.; Decker, M.J.; Wetzel, E.D.; Wagner, N.J. Stab performance of shear thickening fluid (STF)–fabric composites for body armor applications. In *Proceedings of the Society for the Advancement of Material and Process Engineering (SAMPE 2005): New Horizons for Materials and Processing Technologies*, Long Beach, CA, USA, 1–5 May 2005.
- [12] Decker, M.J.; Halbach, C.J.; Nam, C.H.; Wagner, N.J.; Wetzel, E.D. Stab resistance of shear thickening fluid (STF)-treated fabrics. *Compos. Sci. Technol.* 2007, 67, 565–578.
- [13] Mayo, J.B., Jr.; Wetzel, E.D.; Hosur, M.V.; Jeelani, S. Stab and puncture characterization of thermoplastic-impregnated aramid fabrics. *Int. J. Impact Eng.* 2009, 36, 1095–1105.
- [14] Xu, Y.; Chen, X.G.; Wang, Y.L.; Yuan, Z.S. Stabbing resistance of body armour panels impregnated with shear thickening fluid. *Compos. Struct.* 2017, 163, 465–473.

- [15] Bao, L.M.; Sato, S.; Wang, Y.; Wakatsuki, K.; Morikawa, H. Development of Flexible Stab-proof Textiles Impregnated with Microscopic Particles. *J. Text. Eng.* 2017, 63, 43–48.
- [16] Baharvandi, H.R.; Alebooyeh, M.; Alizadeh, M.; Heydari, M.S.; Kordani, N.; Khaksari, P. The influences of particle–particle interaction and viscosity of carrier fluid on characteristics of silica and calcium carbonate suspensions-coated Twaron® composite. *J. Exper. Nanosci.* 2016, 11, 550–563.
- [17] Park, Y.; Kim, Y.H.; Baluch, A.H.; Kim, C.G. Numerical simulation and empirical comparison of the high velocity impact of STF impregnated aramid fabric using friction effects. *Compos. Struct.* 2015, 125, 520–529.
- [18] Rao, M.P.; Duan, Y.; Keefe, M.; Powers, B.M.; Bogetti, T.A. Modeling the effects of yarn material properties and friction on the ballistic impact of a plain-weave fabric. *Compos. Struct.* 2009, 89, 556–566.
- [19] Li, T.-T.; Wang, R.; Lou, C.W.; Lin, J.-Y.; Lin, J.-H. Static and dynamic puncture failure behaviors of 3D needle-punched compound fabric based on Weibull distribution. *Text. Res. J.* 2014, 84, 1903–1914.
- [20] Li, T.T.; Fang, J.; Huang, C.H.; Lou, C.W.; Lin, J.Y.; Lin, M.C.; Lin, J.H. Numerical simulation of dynamic puncture behaviors of woven fabrics based on the Finite Element Method. *Text. Res. J.* 2017, 87, 1308–1317.
- [21] Li, T.-T.; Wang, R.; Lou, C.-W.; Lin, J.-H. Acoustic absorption evaluation of high-modulus puncture resistance composites made by recycled selvages. *Text. Res. J.* 2012, 82, 1597–1611.
- [22] ASTM D5035-11(2015). Standard Test Method for Breaking Force and Elongation of Textile Fabrics; ASTM International: West Conshohocken, PA, USA, 2015.
- [23] ASTM F1342. Standard Test Method for Protective Clothing Material Resistance

Chapter 5

to Puncture; ASTM International: West Conshohocken, PA, USA, 2013.

[24] NIJ standard 0115.00. Stab Resistance of Personal Body Armor; Office of Law Enforcement Standards, National Institute of Standards and Technology: Gaithersburg, MD, USA, 2000.

[25] Li, J.H. Industrial-Grade High-Modulus Composite Geotextiles: Manufacturing Techniques and Property Evaluations. Ph.D. Thesis, Feng Chia University, Taichung City, Taiwan, 2016.

CHAPTER 6

Buffering sandwiches made of thermoplastic polyurethane (TPU) honeycomb grids: manufacturing technique and property evaluations

6.1 Introduction

The rapid industrial development improves the circulation of diverse commodities, which contributes to the rise of internationalization and modernization. Fierce competition makes the buffering packaging indispensable for commercial commodities as using buffering packaging markedly decreases the damage caused by transportation, especially for the products that have a high precision and fragility. Therefore, protective measures to the cargos are necessary in order to mitigate the negative influence of impacts caused by the bumping traffic and discharge [1-3], which makes the development of buffering packaging important. Buffering packaging is used to decrease the damage to the products during the transportation [4-5], preventing goods from any externally exerted forces while preserving their integrity and added value [6-7].

Buffering materials that are made of paper have been long used. However, paper-made buffering materials have a stiff surface which is not allowed to be in direct contact with the content. The voids formed by the content and the buffering material allow the content to move inside the packaging, and thus have damaged surface. Moreover, due to having the intrinsic disadvantages of low moisture resistance and low restorability, paper-made materials have a limited use as buffering materials [8]. Recently, Polyethylene, polypropylene, polyvinyl chloride, polystyrene, polyurethane, and plastic have been commonly used in commercially available buffering materials [9-12]. One great advantage of foam plastic is that they can fulfill the space that is required by mass batches as their flexible form can be adjusted according to any irregularly-shaped products. As a result, the contact area between foam plastic buffering materials and products is increased, which efficiently distribute the damage force occurring in shipping, securing the intact status of the products. In addition to their advantages of having a lightweight, ease of processing, good

Chapter 6

protection, broad adaptability, and a low production cost, foam plastic also has disadvantages of occupying a remarked volume and failing to be bio-degraded, and it also releases toxic gas during incineration [13-15]. The bio-based foam and plastic are now available in the market; however, their high price, strict treatment conditions, and incomplete degradation restrict their applications [16-20].

Among all buffering materials, the cardboard-type buffering materials can effectively provide a buffering efficacy, but it does not withstand the changes in weather [21]. Therefore, this study proposes an eco-friendly buffering materials using thermoplastic polyurethane (TPU) honeycomb grids and nonwoven fabrics that are composed of crimped PET fibers. The resulting buffering material has a light weight, high strengths, and a high impact resistance, and thus has broad applications. In addition, there are studies indicating that composite sandwiches have mechanical properties that are highly correlated with the constituent cover sheets and core layers. Although cover sheets that have high stiffness can bear the majority of an externally exerted force, which leaves the functions of the core layer less critical [22], the energy-absorbent capacity of the core layers still plays a significant role in improving the impact absorbent efficacy of the sandwiches in most cases [23-25]. As a result, the proposed TPU/PET buffering sandwiches are highly resistant against a compression pressure and an impact force. The buffering sandwiches can store a part of the energy from the dynamic stress and strain that are converted from an external force, while the remaining energy is transformed into heat that is then conducted and dissipated via the structure of the sandwiches [27-30]. As such, the TPU/PET sandwiches honey grids are featured by having compression resistance and viscoelastic recoverability and able to absorb the energy caused by a force of impacts or a shake during the delivery, keeping products in a good manner [31-32].

In this study, the TPU/PET buffering sandwiches are composed of a TPU

honeycomb grid (the core layer) and PET nonwoven fabrics (the cover sheets on both upper and lower sides) using the nonwoven manufacturing process. The PET fibers are crimped, three-dimensional, and flame retardant, and the PET nonwoven fabrics are designed to have differing basic weights. The TPU/PET buffering sandwiches consist of three parameters, including different layers and different basic weights of the cover sheets on both upper and lower sides, as well as the different thicknesses of the sandwiches. The bursting strength, air permeability, resilience rate, limited oxygen index (LOI), and drop-weight impact strength of the TPU/PET buffering sandwiches are finally evaluated in order to characterize the mechanical and impact properties.

6.2 Experimental

6.2.1 Materials

Crimped, three-dimensional polyester (PET) fibers (Far Eastern New Century Corporation, Taiwan) have a fineness of 7D, a length of 51 mm, a melting point of 265 °C, and the LOI is 37. Crimped, three-dimensional PET fibers are used to form fluffy nonwoven fabrics. Figure 6.1 (a) shows the structure of thermoplastic polyurethane (TPU) honeycomb grids (Art Giant Technology Corporation, Taiwan), which have a melting point of 120 °C, a thickness of 4 mm, and an eyelet of a diameter of 10 mm.

6.2.2 Preparation of PET/TPU buffering sandwiches

Crimped, three-dimensional, flame retardant PET fibers are made into PET nonwoven fabrics that have basic weights of 150, 200, and 250 g/m² using a nonwoven process. Based on a mechanism between nonwoven fabrics and TPU honeycomb grid, a needle punching machine is used to vertically punched the entangled fibers of nonwoven fabrics through the grids, thereby increasing the friction

between fibers, and frictions between fibers and grid walls. The resulting PET/TPU buffering sandwiches are thus highly mechanically strengthened when multiple layers of nonwoven fabrics are repeatedly laminated and continuously needle punched to firmly form the surface layers of the PET/TPU buffering sandwiches.

The control group is 1-, 2-, 3-, 4-, 5- and 6-layered pure PET nonwoven fabrics. The experimental group has 1-, 2-, and 3-layered PET nonwoven fabrics as the cover sheets on both upper and lower sides, and a TPU honeycomb grid as the core. The cover sheets and core are combined into PET/TPU buffering sandwiches as seen in Figure 6.1 (a) where the fibers of the upper and lower cover sheets can be intertwined through the TPU honeycomb grids, improving the strengths and buffering efficacy of the sandwiches. The buffering sandwiches are tested in terms of bursting strength, air permeability, resilience rate, limited oxygen index (LOI), and drop-weight impact strength, thereby examining the optimal parameters.

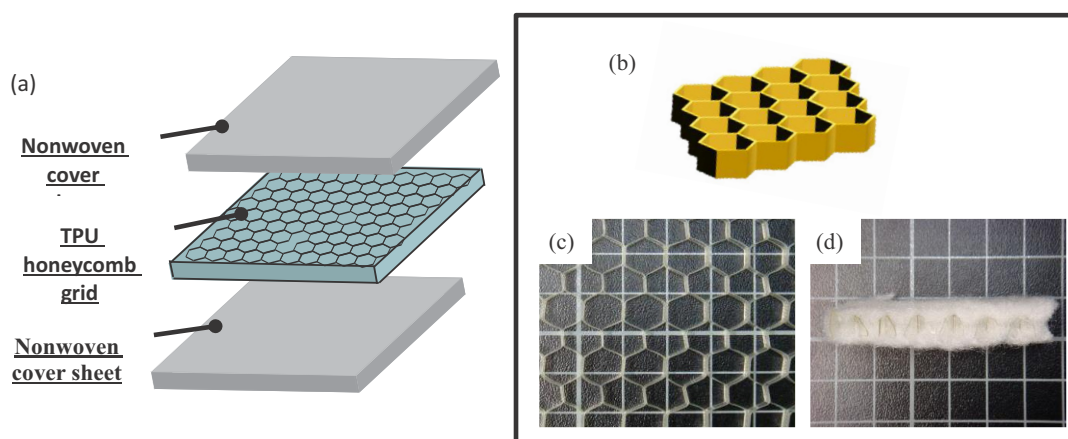


Figure 6.1 a) The composition of PET/TPU buffering sandwiches. b) and c) are the diagrams of a TPU honeycomb grid, and d) is the lateral view of the PET/TPU buffering sandwiches.

6.2.3 Test methods and standards

6.2.3.1 Bursting strength

The bursting force of the PET nonwoven fabrics and TPU/PET buffering sandwiches is evaluated according to ASTM D3787-16. The samples have a size of 100 mm × 100 mm. The speed of bursting test is 100 mm/min. The number of sample for each specification is 10.

6.2.3.2 Air permeability

A TEXTEST FX3300 (TEXTEST AG, Switzerland) is used to measure the air permeability of the samples as specified in ASTM D737-04. In the meanwhile the air flow is adjusted via a valve in order to have the correct measure. The number of sample for each specification is 12, and samples have a size of 25 cmx 25 cm. during the test. The air permeability is defined as the air volume (cm³) that passes through per 1 cm² of a sample, and is represented as cm³/cm²/s.

6.2.3.3 Resilience rate

A rebound resilience tester (Hung Ta Instrument Co., Ltd., Taiwan) is used to measure the resilience rate of the samples as specified in ASTM D2632-15 (standard test method for rubber property—resilience by vertical rebound). The testing set is firmly fixed in order to ensure the quality of the test. The drop hammer is lifted to a height of 400 mm, and then released to hit the point which is at least 14 mm away from the edge of the sample. The values obtained from the first three rounds are not recorded, and then the resilience measured from the 4th, 5th and 6th rounds are recorded and averaged to yield the resilience. The number of sample for each specification is 10.

6.2.3.4 Drop-weight impact test

The drop-weight impact strength of the samples is evaluated as specified in EN 14120 : 2003 (Protective clothing - Wrist, palm, knee and elbow protectors for users of

roller sports equipment - Requirements and test methods). The PET/TPU buffering sandwiches are trimmed into 100 mm×100 mm. The number of sample for each specification is 10. The impactor weighing 8.5 Kg is released from the top (i.e. 40 mm above) and vertically hit the samples (as show in Figure 6.2). The residual impact stress was used to characterize the cushion property of composite foam board.

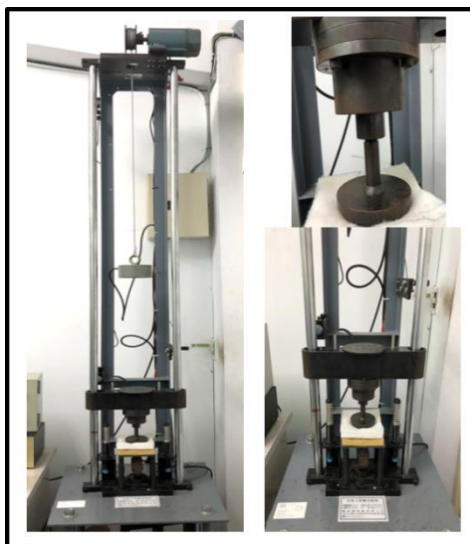


Figure 6.2 Images of the assembly of a drop-weight impact instrument.

6.3 results and discussion

6.3.1 Effects of basic weight of nonwoven cover sheets on bursting strength of PET/TPU buffering sandwiches

Figure 6.3 shows the bursting strength of the pure PET nonwoven fabrics (i.e. control group) and PET/TPU buffering sandwiches (i.e. experimental group) as related to the basic weights of 150, 200, and 250 g/m² of the cover sheets that are composed of 2-layered PET nonwoven fabrics. The control group is the pure 2-layered PET nonwoven fabrics, which is processed with needle punching. The bursting strength of the buffering sandwiches is in proportion to the basic weight of the cover sheets. A high basic weight of the nonwoven fabrics means more fibers per unit area, which can strengthen the buffering sandwiches to withstand a greater

bursting force. Comparing to the control group, using TPU honeycomb grids has a positive influence on the bursting strength of the buffering sandwiches. The bursting force is exerted along a direction that is perpendicular to the surface of nonwoven fabrics. Therefore, when the bursting force damages the nonwoven fabrics to a depth that is greater than the length of fibers, it causes breakages of the nonwoven surface. In contrast, the buffering sandwiches are not damaged until an exerted bursting force exceeds the resistance limit of the TPU core where the fibers of the cover sheets are entangled. As a result, the PET/TPU buffering sandwiches outperform PET nonwoven fabrics in terms of the bursting strength. Specifically, the optimal bursting strength of the buffering sandwiches is 1336 N when the nonwoven cover sheets have a basic weight of 250 g/m², which is 334 % greater than that of the 2-layered pure nonwoven fabrics with a basic weight of 200 g/m².

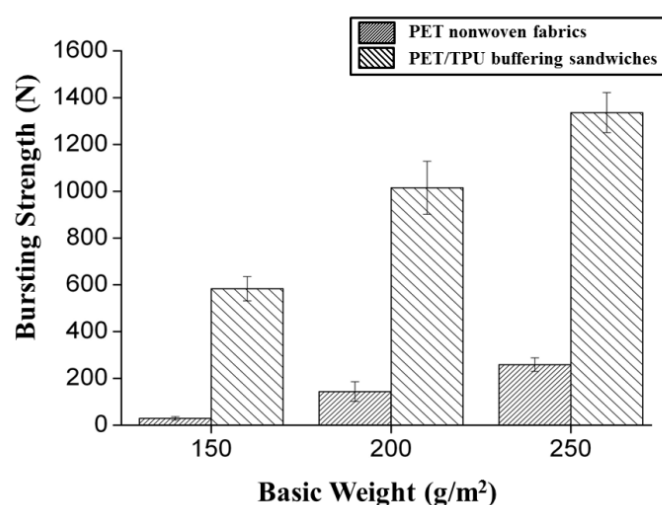


Figure 6.3 The bursting strength of the PET/TPU buffering sandwiches as related to different basic weights. The needle punching density is 240 needles/cm². The control group is 2-layered nonwoven fabrics.

6.3.2 Effects of basic weight and number of nonwoven cover sheets on air permeability of PET/TPU buffering sandwiches

Figure 6.4 shows the air permeability of the pure PET nonwoven fabrics (i.e. control group) as related to the basic weight (150, 200, and 250 g/m²) and the number of lamination layers (1-, 2-, and 3-layered). The air permeability of the pure PET nonwoven fabrics decreases when the basic weight increases from 150 g/m² to 250 g/m². A high basic weight means more constituent fiber per unit area. Namely, fibers are arranged at a greater density, which hinders the air flow from passing through. As a result, the air permeability of PET nonwoven fabrics is inversely proportional to basic weight. Figure 6.5 shows the air permeability of the PET/TPU buffering sandwiches as related to the basic weight (150, 200, and 250 g/m²) and the number (1- and 2-layered) of nonwoven cover sheets. The air permeability of sandwiches is also dependent on the basic weight of the nonwoven cover sheets.

Regardless of whether it is PET nonwoven fabrics or PET/TPU buffering sandwiches, in addition to a high basic weight, a greater number of lamination PET nonwoven layers also results in a greater amount of fibers per unit area and thus has a negative influence on the air permeability. Moreover, the PET/TPU buffering sandwiches have lower air permeability than that of the pure PET nonwoven fabrics. This is ascribed to the addition of TPU honeycomb grids, whose inner walls increases the friction against the air flow. In particular, the optimal air permeability is 366.4 cm³/cm²/s when the pure PET nonwoven fabrics are one layered and the basic weight is 150 g/m². Similarly, the optimal air permeability of 175.7 cm³/cm²/s occurs when the buffering sandwiches have a basic weight of 150 g/m² and 1-layered nonwoven cover sheets.

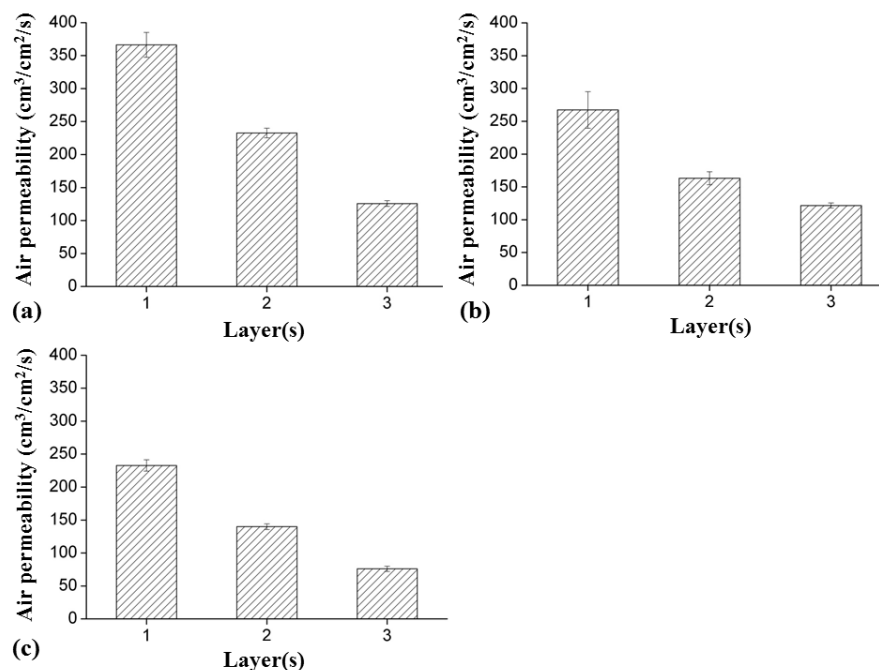


Figure 6.4 The air permeability of with a basic weight of a) 150, b) 200, and c) 250 g/m² as related to the number of lamination layers. The needle punching density is 240 needles/cm².

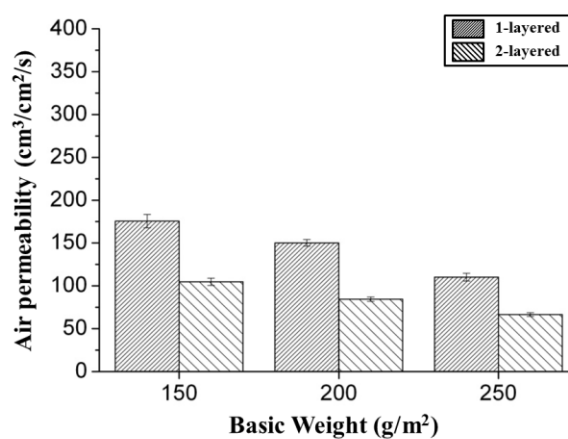


Figure 6.5 The air permeability of PET/TPU buffering sandwiches as related to the basic weight (150, 200, and 250 g/m²) and the number of the nonwoven cover sheets (1- and 2-layered). The needle punching density is 240 needles/cm².

6.3.3 Effects of basic weight and number of nonwoven cover sheets on resilience rate of PET/TPU buffering sandwiches

Figure 6.6 shows the resilience rate of the pure PET nonwoven fabrics (i.e. control group) as related to the basic weight (150, 200, and 250 g/m²) and the number of lamination layers (1-, 2-, 3-, 4-, and 5-layered). The resilience rate is not correlated with the basic weight. Because a high basic weight does not increase the thickness of the pure PET nonwoven fabrics, the resilience rate does not significantly fluctuate. Moreover, the resilience rate increases when the number of lamination layers increases from 1 to 4 layers, and then it decreases when the number of lamination layers is 5 layers. Increasing the number of lamination layers helps to increase the thickness, which is beneficial for the resilience rate. However, excessive lamination layers allow fibers to absorb a portion of the force, and the remaining force that is reflected by the resilience rate is thus lower.

Figure 6.7 shows the resilience rate of the PET/TPU buffering sandwiches as related to the basic weight (150, 200, and 250 g/m²) and the number (1-, 2-, 3-, 4-, and 5-layered) of nonwoven cover sheets on both upper and lower sides. Increasing the basic weight marginally increases the resilience rate. This result may be ascribed to the relatively increasing amount of fibers through the TPU honeycomb grids. The exerted force is distributed via both the grids and the fibers within them. Hence, the basic weight of the nonwoven cover sheets has a positive influence on the resilience rate of buffering sandwiches. Moreover, the resilience rate first increases when the number of nonwoven cover sheets increases from 1 to 3 layers, and then decreases when the number of layers exceeds 3 layers. More lamination layers contribute to the thickness per unit area, thereby strengthening the resilience rate; however, the 4- and 5-layered nonwoven cover sheets may absorb a certain portion of the force and the remaining force that is reflected by the resilience rate is thus decreased.

Specifically, the optimal resilient rate of 33.8 % occurs when the pure PET nonwoven fabrics are 5-layered and have a basic weight of 250 g/m², while the optimal resilient rate of 41.8 % occurs when the PET/TPU buffering sandwiches are composed of 3-layered nonwoven cover sheets that are at a basic weight of 250 g/m².

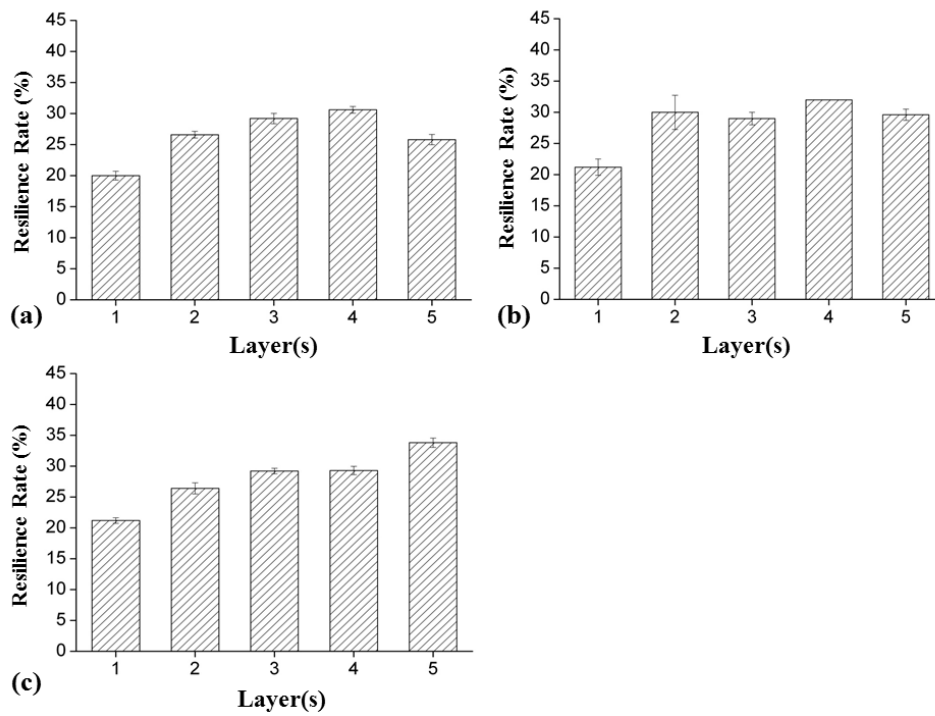


Figure 6.6 The resilience rate of PET nonwoven fabrics with a basic weight of a) 150, b) 200, and c) 250 g/m² as related to the number of lamination layers (1-, 2-, 3-, 4-, and 5-layered). The needle punching density is 240 needles/cm².

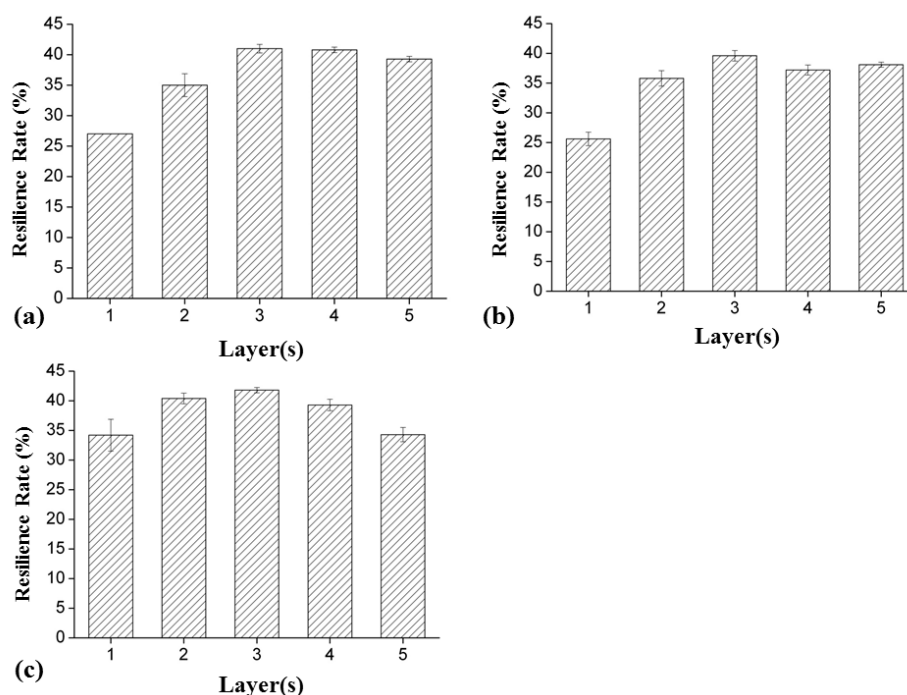


Figure 6.7 The resilience rate of PET/TPU buffering sandwiches with a basic weight of a) 150, b) 200, and c) 250 g/m² as related to the number of nonwoven cover sheets (1- 2-, 3-, 4-, and 5-layered). The needle punching density is 240 needles/cm².

6.3.4 Effects of basic weight and number of nonwoven cover sheets on drop-weight impact test of PET/TPU buffering sandwiches

Figure 6.8 shows the residual impact residual stress of the pure PET nonwoven fabrics (i.e. control group) as related to the basic weight (150, 200, and 250 g/m²) and the number of lamination layers (1-, 2-, 4-, and 6-layered). The residual stress decreases as a result of increasing the basic weight from 150 to 250 g/m². A high basic weight contributes to a greater amount of fibers per unit area, which are then needle punched to form fiber tows. A higher level of entangled fibers then improves the ability of the pure PET nonwoven fabrics to absorb a greater impact stress, and thus causes a lower residual stress. Moreover, the control group are specially designed with the particular number of lamination layers (i.e. 1-, 2-, 4- and 4-layered) in order

to compare with the experimental group (PET/TPU buffering sandwiches) that is composed of 1-, 2-, 3-layered nonwoven cover sheets on both upper and lower sides as follows.

Figure 6.9 shows the residual impact stress of the PET/TPU buffering sandwiches as related to the number (1-, 2-, and 3-layered) and the basic weight (150, 200, and 250 g/m²) of the nonwoven cover sheets. Incorporating a TPU honeycomb grid with the buffering sandwiches positively increases the residual impact stress because the grids have a three-dimensional structure that has an adverse effect against an impact force. After the drop-weight impact test, PET fabric and TPU honeycomb grids do not experience delamination. However, the test renders damage to the bonded structure of TPU honeycomb grids, which in turn leads to the decrease in the drop-weight impact resistance. Therefore, the residual impact stress of the experimental group is 23.2 % lower than that of the control group.

On the other hand, increasing the basic weight of the nonwoven cover sheets helps to improve the residual impact stress of the PET/TPU buffering sandwiches. This result may be ascribed to the relatively increasing amount of fibers within the TPU honeycomb grids, which provides the buffering sandwiches with higher impact resistance. Hence, increasing basic weight of the nonwoven cover sheets has a positive influence on the residual stress of the buffering sandwiches.

Specifically, the optimal residual stress of 4229 N occurs when the pure PET nonwoven fabrics are 6-layered and have a basic weight of 250 g/m², while the optimal residual stress of 3248 N occurs when the PET/TPU buffering sandwiches are composed of 3-layered nonwoven cover sheets that are at a basic weight of 250 g/m².

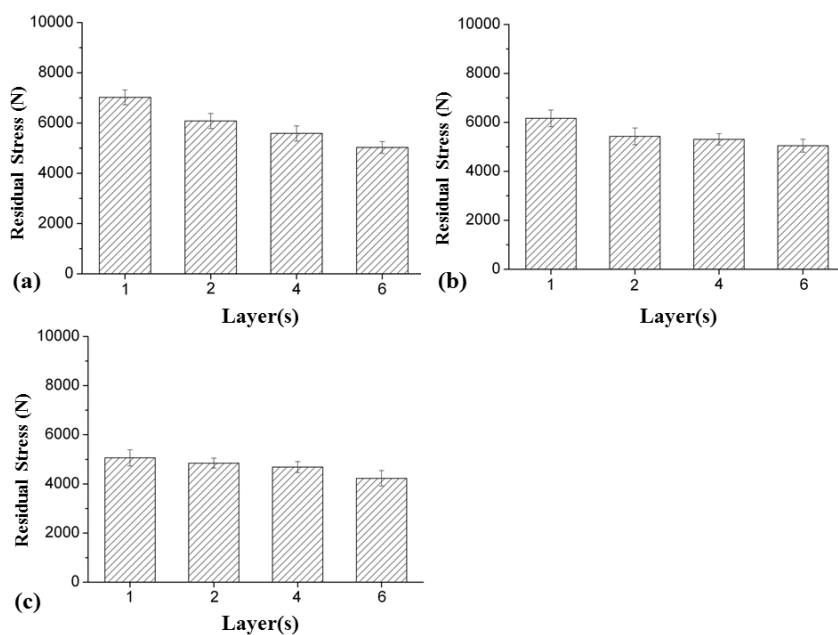


Figure 6.8 The residual stress of PET nonwoven fabrics with a basic weight of a) 150, b) 200, and c) 250 g/m² as related to the number of lamination layers (1-, 2-, 4-, and 6-layered). The needle punching density is 240 needles/cm².

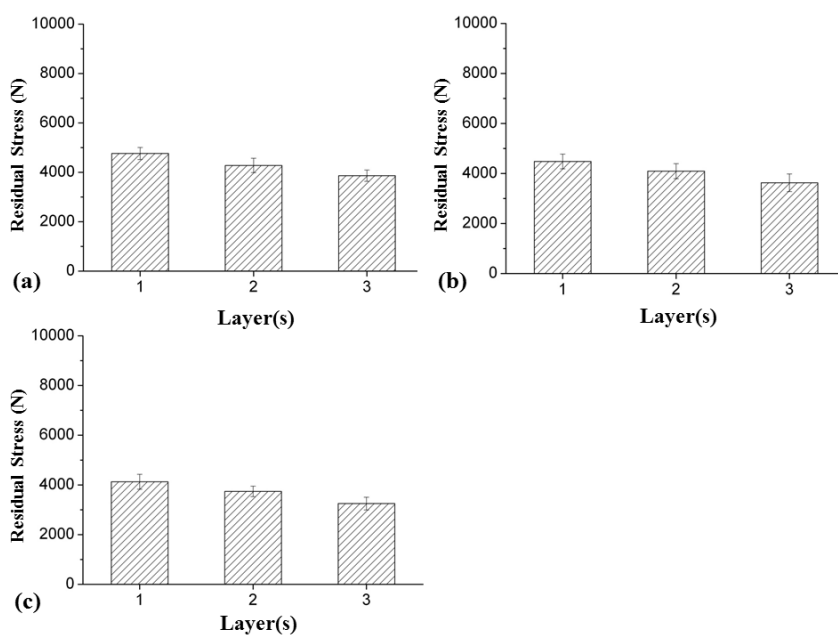


Figure 6.9 The residual stress of PET/TPU buffering sandwiches with a basic weight of a) 150, b) 200, and c) 250 g/m² as related to the number of nonwoven cover sheets on both upper and lower sides (1-, 2-, and 3-layered). The needle punching density is

240 needles/cm².

6.4 Conclusions

This study investigates the properties of the PET/TPU buffering sandwiches in terms of the basic weight and the number of nonwoven cover sheets on both upper and lower sides. The results are compared with the properties of the control group (i.e. pure PET nonwoven fabrics).

Similarly, so far as the PET/TPU buffering sandwiches are concerned, the residual impact stress is decreased when the number of the nonwoven cover sheets increases, and then reaches 3248 N when the buffering sandwiches are composed of 3-layered nonwoven cover sheets on both middles, upper and lower sides which made by the needle-punching method. Moreover, the optimal bursting strength of the experimental group is 1336 N. To sum up, compared to the control group, the experimental group has 23.2 % lower residual impact force and 5.2 times the bursting strength.

The proposed buffering sandwiches are composed environmentally friendly TPU honeycomb grids and traditional nonwoven fabrics, and are proven to have excellent buffering and protective properties. The PET/TPU buffering sandwiches are a great candidate for the use as a packaging material that decreases and minimizes the impact damage that occurs during the transportation and discharge of commodities.

References

- [1] Ruo-Si Y, Ching-Wen L and Jia-Horng L. Low-velocity impact and static behaviors of high-resilience thermal-bonding inter/intra-ply hybrid composites. *Compos. Part B Eng.* 2015; 69: 58–68.
- [2] Stelldinger E K and Kober M. Experimental evaluation of the low-velocity impact damage resistance of CFRP tubes with integrated rubber layer. *Compos. Struct.* 2016; 139:30–35.

- [3] Yang B, Wang Z, Zhou L, Zhang J, Tong L and Liang W. Study on the low-velocity impact response and CAI behavior of foam-filled sandwich panels with hybrid face sheet. *Compos. Struct.* 2015; 132:1129-1140.
- [4] Nouri MD, Hatami H. Experimental and numerical study of the effect of longitudinal reinforcements on cylindrical and conical absorbers under impact loading, *Indian Journal of Science and Technology* 2014; 7 (2) :199-210.
- [5] Experimental and numerical investigation of expanded metal tube absorber under axial impact loading, MD Nouri, H Hatami, AG Jahromi, *Struct. Eng. Mech.* 54 (6) :1245-1266.
- [6] Gui Kuna and Wang Xi. Design and Analysis of Cushioning Packaging for Home Appliances, *Procedia Engineering* 2017; 174:904–909.
- [7] Agnes H, Philipp S, Roland G and Christoph A. Effects of heel cushioning elements in safety shoes on muscle–physiological parameters, *Int. J. Ind. Ergonom.* 2015; 46:12–18
- [8] Xiang-Ming L, Guang L, Xie Y, New Cushioning Package and Its Test, *Journal of zhuzhou institute of technology* 2000; 14(6) : 6-8.
- [9] Hosur M, Abdullah M and Jeelani S. Manufacturing and low-velocity impact characterization of foam filled 3-D integrated core sandwich composites with hybrid face sheets. *Compos. Struct.* 2005; 69: pp.167-181.
- [10] Rasoul N and Ali Reza S. Study of foam density variations in composite sandwich panels under high velocity impact. *Int. J. Impact Eng.* 2014; 63:129–139.
- [11] Zhi S, Xiaozhi H, Shiyong S and Haoran C. Energy-absorption enhancement in carbon-fiber aluminum-foam sandwich structures from short aramid-fiber interfacial reinforcement. *Compos. Sci. Technol.* 2013; 77:14–21.
- [12] Fan X and Xiao-qing W. Study on impact properties of through-thickness

- stitched foam sandwich composites. *Compos Struct* 2010; 92:412-421.
- [13] Chunguang Y, Ludger F, Simon M and Jörg W. Rigid polyurethane foams incorporated with phase change materials: A state-of-the-art review and future research pathways. *Energ. Buildings* 2015; 87(1) : 25-36.
- [14] Andrea T, Antonella T, Alessandra P and Riccardo A. Thermographic analysis of polyurethane foams integrated with phase change materials designed for dynamic thermal insulation in refrigerated transport. *Appl. Therm. Eng.* 2014; 70(1) : 201-210.
- [15] Nuno P, Manuel Duarte P, José Dinis S and Jorge de B. Comparative environmental life cycle assessment of thermal insulation materials of buildings, *Energ. Buildings* 2014; 82 : 466-481.
- [16] Haruo, S, Kaku S and Kaname A. Development of an Air Cushioning Material Based on a Novel Idea. *Pack-aging Technology and Science* 1999; 12 (3) :143-150.
- [17] Dong-Mei W. Compression breakage properties research on the honeycomb paperboard. *Packaging Engineering* 2006; 27 (1) :37-39.
- [18] Kobayashi H, Daimaruya M and Kobayashi T. Dynamic and static compression tests for paper honeycomb cores and absorbed energy. *JSME International Journal Series A* 1998; 41(3) :338-344.
- [19] Karthigeyan C, Obulisamy Parthiba K and Kirsten H. Sustainable bio-plastic production through landfill methane recycling. *Renewable and Sustainable Energy Reviews* 2017; 71:555–562.
- [20] Camila S. C, Thaís F and Vânia M.D. P. Production and characterization of polyurethane foams from a simple mixture of castor oil, crude glycerol and untreated lignin as bio-based polyols. *Eur. Polym. J.* 2016; 85:53–61.
- [21] Ya-Sui Y. Dynamic axial crushing of multi-layer honeycomb panels and impact

- tensile behavior of the component members. *Int. J. Impact Eng.* 2000; 24 (6-7) :659-671.
- [22] Chun-Gon K and Eui-Jin J. Impact Resistance of Composite Laminated Sandwich Plates. *J Compos Mater* 1992; 26(15):2247-2261.
- [23] Robinson P and Davies GAO. Impactor mass and specimen geometry effects in low velocity impact of laminated composites. *Int. J. Impact Eng.* 1992; 12(2):189-207.
- [24] Werner G and Jerome L. S. An experimental study of energy absorption in impact of sandwich plates. *Int. J. Impact Eng.* 1992; 12 (2) :241- 62.
- [25] Rosenfeld MS and Gause LW. Compression fatigue behaviour of graphite/epoxy in the presence of stress raisers, Fatigue of fibrous composite materials, *ASTM STP723 1981*:174-196.
- [26] Zhao H and Gary G. Crushing behavior of aluminum honeycomb under impact loading. *Int. J. Impact Eng.* 1998; 21(10):827-836.
- [27] Yan-Feng G and Jing-Hui Z. Shock absorbing characteristics and vibration transmissibility of honeycomb paperboard. *Shock Vib.* 2004; 11(5):521- 531.
- [28] Dong-Mei W. Out-of-plane compressive properties of hexagonal paper honeycombs. *Chin. J. Mech. Eng. En.* 2007; 20 (2) :115-119.
- [29] Horrigan DPW, Aitken RR and Moltshaniwskyj G. Modelling of crushing due to impact in honeycomb sandwiches. *J Sandw Struct Mater* 2000; 2 : 131-151.
- [30] Eric J H, Anthony N. Low-velocity impact damage initiation in graphite/epoxy/Nomex® honeycomb-sandwich plates. *Compos. Sci. Technol.* 1997, 57 : 1581- 1598.
- [31] Wang D M. Comparison of the properties of paper honeycomb cores with different structures. *Packaging World* 2006; 106 (4) : 38- 40.
- [32] Wang D M, Wang Z W. Out-of-plane compressive properties of hexagonal paper

Chapter 6

honeycombs. *Chin. J. Mech. Eng.* 2007; 20 (2) : 115- 119.

CHAPTER 7

Conclusions

This thesis mainly proposes the following five aspects: 1. Recycling the waste of Nomex®, Kevlar®, and polyester fiber woven fabrics by needle rolling method and its performance evaluation; 2. Mechanical properties of hybrid composites made of recycled Nomex®, Kevlar®, and polyester selvages; 3. Mechanical and static stab resistant properties of hybrid-fabric fibrous planks: manufacturing process of nonwoven fabrics made of recycled fibers; 4. Fabric composites reinforced with thermally bonded and irregularly aligned filaments: preparation and puncture resistant performance 5. Buffering sandwiches made of thermoplastic polyurethane (TPU) honeycomb grids: manufacturing technique and property evaluations. All research conclusions are summarized in this section.

In the first chapter of this thesis, we introduce the current status of textile waste, reusing methods and current status of high modulus fibrous materials, needle-punching processing technology and mechanism, personal protective equipment (PPE), stab-proof materials and buffer resistance materials.

In chapter two of this thesis investigate the recycled fabrics in terms of characterizations and mechanical properties based on the constituent recycled staple fibers. The eco-friendly manufacturing design uses high performance of recycled Nomex®, Kevlar®, and PET selvages. The recycled fibers take up 50, 70, and 90 wt% of the hybrid composites and corresponding LMPET fibers account for 50, 30, and 10 wt%. In this study, the influence of a specified temperature of hot pressing of 130 °C on different properties is discussed. When base weight is excluded from consideration, the sample in which contents 90 wt% recycled Kevlar® has the optimal mechanical properties before hot-press treatment, and after hot-press treatment the sample in which contents 90 wt% recycled PET has the optimal mechanical properties. The satisfactory test results are ascribed to the high performance of the recycled staple fibers and the reinforcement of LMPET fibers. In particular, the combination of

recycled PET fibers and LMPET fibers has a synergistic effect in stabilized structure and mechanical improvement.

Secondly, in chapter three, I investigate the performance of hybrid-fiber-reinforced composite boards made of recycled aramid composite matrices, LMPET matrices, and aramid woven fabrics, which are laminated, needle punched and hot pressed. The test results show the tensile strength of hybrid-fiber-reinforced composite boards is 5 times greater than that of the control group, while its tearing strength is 8.5 times greater than that of the control group. The employment of hot pressing enhances the properties even more. And the composite boards with hot-pressed containing 90 % recycled aramid fibers as the aramid matrix has the optimal static puncture resistance, and the major factors are the compact plain woven structure and LMPET fibers. Hot pressing gives rise to the presence of thermal bonding points, which hampers the slipping of aramid and LMPET fibers, secures the structure, and increases the friction of fibers against the powerful punch. As a result, the hybrid-fiber-reinforced composite boards containing 90 % of recycled aramid fibers) have the optimal static puncture resistance.

In chapter four, I propose flexible fabric-based protective planks, which are recycled high strength PET fibers by processed with minimum damage for secondary production, thereby obtaining recycled high-performance fibers with relatively lower production cost. In this study, the different reinforcing woven fabrics are combined with matrices to form hybrid-fabric fibrous planks. Despite multiple combining and carding processes, the recycled PET staple fibers are proven to provide the fibrous planks with high tensile and tear strengths. The test results indicate that recycled PET fibers remain high strength and can be made into protective products. The combination of nonwoven and woven fabrics provides the benefits of their different stab behaviors, strengthening the puncture resistance of the hybrid-fabric fibrous

Chapter 7

planks. Most of all, an efficient recycling process and using textile and fiber waste to make protective fibrous planks decreases the production cost considerably, which makes the industrial and livelihood protective products more advantageous and acceptable.

In chapter five, In order to improve the stab resistance from the fabric structure, I study to develop sandwich-structured puncture-resistant fabric composites, and the optimal N/L/W/F/L/N has good puncture resistance at level 3 (N: Nylon/aramid recycled nonwoven fabrics ; L: Low-melting PET fabrics ; W: reinforced woven fabric ; F: PET filament). The proposed fabric composites are characterized in terms of tearing strength, static puncture resistance, and dynamic puncture resistance. The test results indicate that thermally treated N/L/W/F/L/N has a 63.3 % greater tearing strength at CD orientation, 63.9 % greater static puncture resistance, and 32.5 % greater bursting strength than N/L/L/N. Compared to other studies, using the LMPET adhesive layer had a positive influence, preventing the slide of the filaments, but the poor interfacial combination only contributes limited reinforcement. Hence, improving the interfacial affinity between laminates is suggested to be conducted in future studies.

In chapter six, I study investigate the properties of the PET/TPU buffering sandwiches in terms of the different basic weights and the number of nonwoven cover sheets on both middles, upper and lower sides which made by the needle-punching method. The results are compared with the properties of the control group (i.e. pure PET nonwoven fabrics). Similarly, so far as the PET/TPU buffering sandwiches are concerned, the residual impact stress is decreased when the number of the nonwoven cover sheets increases, and then reaches 3248 N when the buffering sandwiches are composed of 3-layered nonwoven cover sheets on both upper and lower sides. Moreover, the optimal bursting strength of the experimental group is 1336 N. To sum

Chapter 7

up, compared to the control group, the experimental group has 23.2 % lower residual impact force and 5.2 times the bursting strength, but slightly lower LOI. The proposed buffering sandwiches are composed of environmentally friendly TPU honeycomb grids and traditional nonwoven fabrics and are proven to have excellent buffering and protective properties.

List of publications

1 · Yu-Chun Chuang, Limin Bao, Ching-Wen Lou & Jia-Horng Lin. High-performance hybrid composites made of recycled Nomex®, Kevlar®, and polyester selvages: mechanical property evaluations. Yu-Chun Chuang, Limin Bao, Ching-Wen Lou & Jia-Horng Lin. The Journal of The Textile Institute 2019 May, doi.org/10.1080/00405000.2019.1619303 (Accepted)

2 · Yu-Chun Chuang, Limin Bao, Ching-Wen Lou, Jia-Horng Lin. Hybrid-Fiber Reinforced Composite Boards Made of Recycled aramid Fibers: Preparation and Puncture Properties. Fibers and Polymers, 2019, Vol.20, No.2, 398-405. DOI: 10.1007/s12221-019-8868-1 (Accepted)

3 · Yu-Chun Chuang, Limin Bao, Mei-Chen Lin, Ting An Lin, and Ching-Wen Lou. Fabric Composites Reinforced with Thermally Bonded and Irregularly Aligned Filaments: Preparation and Puncture Resistant Performance. Polymers (Basel), 2019 Apr; 11(4): 706. DOI: 10.3390/polym11040706 (Accepted)

4 · Yu-Chun Chuang, Limin Bao, Mei-Chen Lin, Ching-Wen Lou and TingAn Lin. Mechanical and Static Stab Resistant Properties of Hybrid-Fabric Fibrous Planks: Manufacturing Process of Nonwoven Fabrics Made of Recycled Fibers. Polymers (Basel), 2019, 11(7), 1140 DOI: 10.3390/polym11071140 (Accepted)

5 · Yu-Chun Chuang, Limin Bao, Pey Yu Chen, Ching-Wen Lou, Jia-Horng Lin. Buffering sandwiches made of thermoplastic polyurethane honeycomb grids: Manufacturing technique and property evaluations. Journal of Sandwich Structures & Materials, 2019, Vol. 21(6) 1975–1990. DOI: 10.1177/1099636217739547 (Accepted)

Scientific presentation

1. Yuchun CHUANG, Limin BAO¹, Jiahong LIN. The influence of buffer performance when vertical fiber filled in TPU honeycomb grid. 2nd Japan · China Textile Composite Symposium 2018 Sep. 06-09, Anhui Polytechnic University, Anhui, China. **(Oral Presentation Award)**

Acknowledgement

It is my pleasure to express my gratitude to all those who have contributed to my study.

First of all, I would like to thank Professor Bao Limin for his careful guidance and assistance during the research, experimentation and writing of this thesis. Professor Bao gave me a lot of support both in research and in life. At the same time, I would like to thank Professor Lin Jiahong and Professor Lou Jingwen for their support and help from Taiwan during the research, writing and experimentation of this paper, so that this paper can be successfully completed.

In addition, I would like to thank the members of the Bao Research Office for their assistance during the research, experimentation and writing.

Finally, I would like to thank my favorite parents and my sister and my brother for their patience, guidance and support during this period. I also thank the good friends around me for their concern and support.